Frauenklinik und Poliklinik der Technischen Universität München
Klinikum rechts der Isar
(Direktorin: Univ.-Prof. Dr. M. B. Kiechle)

Assessment of kallikrein-related peptidases 4 and 6 (KLK4 and KLK6) as candidate biomarkers in prostate and ovarian cancer

Lina Seiz

Vollständiger Abdruck der von der Fakultät für Medizin der Technischen Universität München zur Erlangung des akademischen Grades eines

Doktors der Medizin

genehmigten Dissertation.

Vorsitzender: Univ.-Prof. Dr. E. J. Rummeny

Prüfer der Dissertation:
1. Univ.-Prof. Dr. M. Schmitt
2. Univ.-Prof. Dr. B. Schmalfeldt
3. Univ.-Prof. Dr. J. E. Gschwend

Die Dissertation wurde am 30.01.2014 bei der Technischen Universität München eingereicht und durch die Fakultät für Medizin am 17.12.2014 angenommen.

This dissertation is dedicated to my family.

1. Introduction

1.1 Prostate cancer diagnosis, staging, and treatment

Prostate cancer is the second most common cancer in men worldwide and the most frequently diagnosed cancer among males in economically developed countries (Jemal *et al*., 2011). Incidence and mortality rates (number of cases or deaths per 100,000 persons per year) vary worldwide, with the lowest incidence rate recorded for Asia (4/100,000). For Western Europe, the incidence rate is rising (93/100,000), while the mortality rate (12/100,000) is constantly decreasing (Schmelz *et al*., 2010; Center *et al*., 2012). In 2008, prostate cancer was accounting for 766,000 new cases and 179,000 new deaths worldwide (Bray *et al*., 2012). In fact, due to increase in life expectancy and growth of the global population the worldwide prostate cancer burden is expected to grow to 1.7 million new cases and 499,000 new deaths by the year 2030 (Center *et al*., 2012).

The likelihood of developing prostate cancer increases with age: in Western Europe, 75% of men with newly diagnosed prostate cancer are older than 65 years. Additional well-established risk factors are black race/ethnicity and a family history of the disease (Almeida *et al*., 2010; Schmelz *et al*., 2010). In order to detect prostate cancer at its earliest stage, most guidelines recommend both the digital rectal examination (DRE) and the measurement of serum prostate-specific antigen (PSA) during routine annual examinations (usually starting from the age of 50 until the age of 75). Due to its mainly peripheral localization distant to the urethra, early prostate cancer rarely produces any symptoms. However, locally advanced prostate cancer sometimes gives lower urinary tract symptoms accompanied by hematuria. Occasionally, hematospermia, impotence and unilateral urinary obstruction occur in case of locally advanced prostate cancer resulting from involvement of the seminal vesicles, the neurovascular bundle, and the base of the bladder. In case of abnormal DRE or elevated age-specific PSA levels further diagnostic workup is absolutely required. For this, transrectal ultrasound (TRUS) is usually used to guide prostate core needle biopsy (Schmelz *et al*., 2010). Histologic

examination of prostate tissue obtained from systematic core needle biopsies is essential to diagnose prostate cancer, and, furthermore, it provides important information for local stage classification.

The vast majority of prostate neoplasms are hormone-dependent adenocarcinomas (Barber and Staffurth, 2008). Clinical staging of prostate cancer is based on the TNM staging system and the Gleason grading system (see appendix). Apart from DRE, PSA tests, TRUS, and systematic prostate biopsies, usually additional MRI (magnetic resonance imaging) and bone scans are performed as part of the initial staging in case of a greatly elevated PSA serum level (>20 ng/ml), which is associated with an increased probability for the presence of pelvic lymph node or bone metastases (Schmelz *et al*., 2010).

For patients with stage pT1 and pT2 tumors, *i.e.* organ confined disease (see appendix), several curative therapeutic options are available including radical prostatectomy with pelvic lymphadenectomy, interstitial brachytherapy, and external beam radiation with adjuvant hormonal therapy if indicated. Although some of the best results are reported for surgery, no definitive evidence exists that any one of these options is better in terms of cancer control (Barber and Staffurth, 2008). Furthermore, patients having a relatively high chance of not developing progressive disease throughout their lifespan due to favorable disease characteristics can only be closely monitored (active surveillance); if these patients display evidence of progressive disease, they should be subjected to curative radical treatment immediately (Barber and Staffurth, 2008). Transurethral resection of the prostate (TURP) is typically performed when a patient is experiencing difficulty urinating and is not a candidate for a radical prostatectomy (Almeida *et al*., 2010).

Patients with stage pT3 and pT4 tumors, *i.e.* non-organ confined disease, can be offered radical prostatectomy with pelvic lymphadenectomy (clinical stage T3a tumors only) or external beam radiotherapy combined with neoadjuvant hormone therapy (androgen deprivation) with or without adjuvant hormone therapy (Barber and Staffurth, 2008; Schmelz *et al*., 2010). However, watchful waiting can also be an option for elderly patients with comorbidities who are unlikely to develop symptoms from advanced prostate cancer during their lifetime; thus, these patients can be spared from morbidity caused by treatment.

Chemotherapy with docetaxel is given to patients with disease recurrence, with metastasized, or with hormone-refractory prostate cancer (Barber and Staffurth, 2008). Patients with symptoms from advanced or metastasized disease that cannot be treated by surgery, radiation, or chemotherapy are offered palliative hormone therapy (Schmelz *et al*., 2010).

The risk of prostate cancer-related death can be estimated on the basis of clinical and histomorphological parameters (see appendix). Patients with stage pT1 to pT2a tumors, low PSA serum levels (<10 ng/ml), and a Gleason score of 6 or lower have a good prognosis, meaning that their cancer-related death rate is less than 10% over 10 years. By contrast, patients with high PSA levels (>20 ng/ml) or a Gleason score of 8 and higher face a poor prognosis resulting in a 20% chance of death over 10 years (Barber and Staffurth, 2008).

1.2 Prostate-specific antigen (PSA) as a marker of prostate cancer

A tumor marker, or cancer biomarker, is a tool that enables the clinician to answer relevant questions regarding a cancer disease. Examples of established tumor markers in clinical use are: alpha-fetoprotein for tumors of the liver, testis, and other germ cell line tumors, CA125 for ovarian cancer, and steroid hormone receptors (estrogen and progesterone receptor) used in the management of breast cancer (Schrohl *et al*., 2003). The possible clinical applications of tumor markers are numerous since several categories of markers can be defined. A diagnostic marker aids in the detection of a malignant disease. The measurement of a prognostic marker helps to estimate the future course of a malignant disease (*i.e.* the risk of disease recurrence or the risk of cancer-related death) following primary surgery, but without administration of systemic adjuvant therapy. By contrast, a predictive marker can foretell how the patient is going to respond to a cancer-directed therapy. Tumor markers used for detection of disease recurrence or remission of a disease are classified as monitoring markers and determined during follow-up of the patients (Schrohl *et al*., 2003).

To date, PSA (also known as kallikrein-related peptidase 3, KLK3) is the best-established clinical marker indicating the existence and also the progression of prostate cancer. PSA is produced by glandular epithelial cells of the prostate and is responsible for liquefaction of the semen. Prostate cancer can be diagnosed up to 5.5 years earlier in men who undergo digital rectal examination (DRE) and additional measurement of serum PSA during routine annual examinations compared to men with annual DRE alone (Schmelz *et al*., 2010). However, PSA is not a specific indicator of prostate cancer, since it may also be increased in acute or chronic prostatitis, benign prostatic hyperplasia, and urinary retention (Schmelz *et al*., 2010). It follows that PSA testing generates a substantial level of false positive results leading to uncertainty for the patients and unnecessary core needle biopsies (Thorek *et al*., 2013). Therefore, additional markers for prostate cancer are needed.

Molecular profiling at the genomic, transcriptomic, or proteomic level have identified several potential markers that may distinguish between indolent and aggressive prostate cancers, including *NKX3.1*, *PTEN*, *ETS*, *MYC*, *TP53*, *AR*, *RB1*, and *APC* plus miRNAs as potential prognostic biomarkers for prostate cancer (Schmitt *et al*., 2013a). Apart from PSA/KLK3, clinical significance for prostate cancer patients has been demonstrated for other members of the kallikrein-related peptidase (KLK) family. The ratio of KLK2 to free PSA serum levels has been found to successfully discriminate the prostate cancer patients from those with benign prostatic hyperplasia (Kwiatkowski *et al*. 1998; Avgeris *et al*., 2012). In prostate cancer, increased expression of three KLKs (KLK2, 14 and 15) was found to be associated with poor prognosis (Nam *et al*., 2000; Mavridis *et al*., 2010; Schmitt *et al*., 2013a). But also decreased mRNA or protein levels of KLK2, 3, 5-7, 10, 11, 13, and 15 have been reported for prostate cancer of which KLK3 and 15 are considered as markers of poor prognosis, while decreased expression of KLK5 and 11 is associated with a favorable prognosis (Dorn *et al*., 2013).

1.3 Kallikrein-related peptidase 4 (KLK4)

KLK4 is a member of the human tissue kallikrein-related peptidase (KLK) family, constituting a group of 15 secreted serine proteases with either trypsin or chymotrypsin-like substrate specificity. KLKs are found within the glandular epithelia of many human organs, such as the colon, stomach, pancreas, breast, ovary, and prostate, and they have diverse physiological roles. *KLK1-15* genes are tightly clustered in a tandem array on chromosome 19q13.3-q13.4 spanning ~300 kb. This locus represents the largest uninterrupted cluster of protease genes within the entire human genome (Schmitt *et al*., 2013b). The *KLK* genes share remarkable homology at both the nucleotide and protein level (Diamandis *et al*., 2000; Debela *et al*., 2008; Goettig *et al*., 2010) and many of them are transcriptionally regulated by steroid hormones as well as by DNA methylation (Nelson *et al*., 1999; Yousef and Diamandis, 2001; Christophi *et al*., 2004; Pampalakis and Sotiropoulou, 2007; Lundwall and Brattsand, 2008; Lai *et al*., 2009; Bayani and Diamandis, 2011). The enzymatic activity of several KLKs is considered to be balanced by physiological inhibitors or allosterically in the presence of zinc ions (Borgoño and Diamandis, 2004; Debela *et al*., 2006a; Debela *et al*., 2006b; Luo and Jiang, 2006). Strikingly, specific members of the KLK family are known to be coexpressed in various normal and also in malignant human tissues, thus raising the possibility that KLKs may participate in proteolytic cascades and activate each other or get activated by other proteases such as the matrix metallopeptidases or proteases of the thrombosis axis, e.g. the serine proteases plasmin and urokinase-type plasminogen activator (uPA) (Borgoño and Diamandis, 2004; Pampalakis and Sotiropoulou, 2007; Lundwall and Brattsand, 2008; Beaufort *et al*., 2010; Schmitt *et al*., 2013b; Yoon *et al*., 2013). Aberrant expression profiles of KLK proteases have been linked to neurodegenerative diseases and skin disorders, but also to malignant conditions, *e.g.* ovarian, breast, and prostate cancer, or malignant melanoma (Sidiropoulos *et al*., 2005; Pampalakis *et al*., 2006; Krenzer *et al*., 2011). Unsurprisingly, KLKs came into focus as potential diagnostic, prognostic, and/or predictive tumor markers in female and male urogenital tract malignancies (Dorn *et al*., 2013; Schmitt *et al*., 2013a) and also in several other cancers, including that of the breast, brain, head and neck, gastrointestinal

tract, kidney, and lung (Emami and Diamandis, 2008; White *et al*., 2010; Avgeris *et* al., 2012).

It is believed that KLK4 could represent a candidate marker for improving diagnosis of prostate cancer or monitoring of residual prostate cancer disease (Day *et al*., 2002). KLK4 is also known by the name prostase, owing to its expression in the prostate and its presence in seminal plasma (Nelson *et al*., 1999; Obiezu *et al*., 2002; Obiezu *et al*., 2005). Indeed, under physiological conditions, KLK4, together with PSA/KLK3 and other prostatic KLKs, is part of a highly regulated proteolytic cascade, which upon ejaculation leads to activation of pro-KLK3 and subsequent semen liquefaction (Pampalakis and Sotiropoulou, 2007). Interestingly, KLK4 was independently identified as enamel matrix serine protease 1 (EMSP1; Simmer *et al*., 1998) and found to play an essential role in enamel biomineralization by degrading matrix proteins prior to their removal from the maturing enamel during tooth formation (Simmer *et al*., 2009).
Although KLK4 was originally described as a protease with prostate-restricted expression (Nelson *et al*., 1999), later studies suggested that it is expressed in a wide array of healthy adult tissues (Shaw and Diamandis, 2007). KLK4 displays trypsin-like activity (Debela *et al*., 2006a; Debela *et al*., 2006b) and is able to convert pro-urokinase-type plasminogen activator (pro-uPA) into active uPA, which is known to be a key player in extracellular matrix remodeling, angiogenesis, wound healing, embryogenesis, tumor invasion, and metastasis (Takayama *et al*., 2001; Beaufort *et al*., 2006). In addition, KLK4 can modulate cell surface-associated proteolytic activity and alter the adhesive properties of tumor cells by cleaving the uPA receptor (uPAR) (Beaufort *et al*., 2006).
Other relevant proteins cleaved by KLK4 are fibrinogen and collagen I and IV, which constitute basic components of the extracellular matrix with an important role in tissue remodeling and local tumor spread (Obiezu *et al*., 2006). Recently, KLK4 was shown to activate pro-HGFA (pro-hepatocyte growth factor activator), which is expressed by several human cancers and is believed to trigger a series of events leading to tumor progression (Mukai *et al*., 2008). Insulin-like growth factor-binding proteins (IGFBPs) have also been identified as targets of KLK4 (Matsumura *et al*., 2005). Degradation of IGFBPs leads to increased pericellular concentration of insulin-like growth factors (IGFs) inducing tumor growth and

invasion (Paliouras and Diamandis, 2006; Mukai *et al*., 2008). Based upon the optimal cleavage site residues, PTHrP (parathyroid hormone-related peptide), VEGFC (vascular endothelial growth factor C), and members of the BMP (bone morphogenic protein) family were predicted to be activated by KLK4 proteolysis. Whether KLK4 may influence tissue remodeling and tumor growth through these putative substrates has yet to be experimentally verified (Matsumura *et al*., 2005).

Apart from that, PAR-1 and PAR-2, members of the protease-activated receptor family of G-protein-coupled receptors, have been demonstrated to be activated by KLK4 (Mize *et al*., 2008; Ramsay *et al*., 2008). In the case of PAR-1, it has been proposed that KLK4, expressed by prostate cancer cells, activates PAR-1 in the surrounding stroma, which in turn releases interleukin-6 and other cytokines, which then stimulate proliferation of the cancer cells (Wang *et al*., 2010). PAR-2 is coexpressed with KLK4 in prostate cancer (Ramsay *et al*., 2008), therefore, KLK4-mediated modulation of the tumor-associated uPA/uPAR system and cell signaling via PARs could contribute to angiogenesis, invasiveness or progression of (prostate) cancer. Moreover, in *in vitro* expression models, KLK4 and PSA/KLK3 proved to have properties that facilitate the progression of prostate cancer cells by modulating regulators of the cytoskeleton as well as cellular adhesion and migration processes (Veveris-Lowe *et al*., 2005). Experimental evidence for overexpression of *KLK4* mRNA has been shown for both prostate and ovarian cancer (Dong *et al*., 2001; Xi *et al*., 2004), being associated with disease progression and unfavorable outcome of ovarian cancer patients (Obiezu *et al*., 2001). Significantly elevated *KLK4* mRNA levels were also found in cancerous breast tissue compared with the normal breast (Mangé *et al*., 2008).

1.4 Ovarian cancer diagnosis and treatment

Ovarian cancer is predominantly a disease of females in the Western world (Hanna and Adams, 2008). In Germany, approximately 9600 cases of newly diagnosed malignant ovarian tumors and about 5500 deaths from ovarian cancer are reported per year (Burges and Schmalfeldt, 2011). The greatest

number of ovarian neoplasms is recorded between ages of 55 and 74. However, borderline tumors or hereditary cancers, particularly those associated with the genes BRCA1 and BRCA2, occur at younger age (Hanna and Adams, 2008). While a positive family history of breast or ovarian cancer, infertility, and a high socioeconomic status constitute risk factors for ovarian cancer, breast feeding, pregnancy, the use of an oral contraceptive pill (ovulation inhibitor), tubal ligation, and hysterectomy are considered to elicit a protective effect (Hanna and Adams, 2008).

Around 90% of ovarian cancers arise from the surface epithelium of the ovary. Women with early stage ovarian cancer experience, if any, fairly nonspecific symptoms like diffuse abdominal complaints, newly occurred meteorism, changes in bowel habits, unexplained weight loss, and sometimes massive abdominal swelling. For this reason 70% of cases of ovarian cancer are not diagnosed until the disease has reached an advanced stage (FIGO stage IIB to IV; see appendix), which is associated with a five-year survival rate of less than 40% (Burges and Schmalfeldt, 2011). Ovarian cancer can spread locally to the internal genitals, the bowel, bladder, and pelvic side walls. Peritoneal spread to the omentum, paracolic gutters, bowel mesentery, and the undersurface of the diaphragm frequently occurs. Lymphogenous dissemination takes place into pelvic and para-aortic lymph nodes, while spread to liver, bone, and lung via the blood is rare (Hanna and Adams, 2008). Of all imaging procedures used to diagnose ovarian tumors, transvaginal ultrasound is the most valuable in determining whether ovarian lesions are benign or malignant. Computed tomography (CT scan) and MRI may be useful in particular cases, however, both of them tend to underestimate peritoneal and mesenteric carcinomatosis, which is common in advanced ovarian cancer (Burges and Schmalfeldt, 2011). In other words, no apparatus-based diagnostic procedure can replace the recommended surgical staging of ovarian cancer and can reliably assess the feasibility of surgery (Burges and Schmalfeldt, 2011). Accurate surgical staging according to the FIGO and TNM classification system (see appendix) requires a median laparotomy with a thorough examination of the abdominal cavity (Hanna and Adams, 2008; Aebi and Castiglione, 2009).

Operative treatment of ovarian cancer represents a cornerstone of successful management. Post-operative residual tumor mass is the strongest independent parameter in patients' prognosis after tumor stage. Furthermore, it is currently the only factor that can be effectively influenced (Burges and Schmalfeldt, 2011). Therefore, surgery should be performed by a specialist in gynecological oncology, according to published guidelines. In early stage disease (FIGO stage I to IIA) surgical treatment includes a median laparotomy with total abdominal hysterectomy, bilateral adnectomy, infragastric omentectomy, peritoneal biopsies and washings, and at least systematic pelvic and infrarenal para-aortic lymph node dissection (Aebi and Castiglione, 2009).
In early stages (FIGO stage I to IIA), there is a good chance to cure the disease (Burges and Schmalfeldt, 2011). In younger patients with localized, unilateral tumors and favorable histology (confirmed FIGO stage IA, Grade 1), who wish to retain their fertility, less radical surgery can be performed with removal of the affected ovary, leaving the contralateral ovary and the uterus (Hanna and Adams, 2008).
In advanced ovarian cancer (FIGO stage IIB to IIIC) surgery is performed in the same way as in early stage disease, except that here major surgical effort is undertaken in order to reach complete tumor resection to a maximum residual tumor size of less than 1 cm (Aebi and Castiglione, 2009; Burges and Schmalfeldt, 2011). To achieve this, the resection of infiltrated parietal peritoneum including the diaphragmatic peritoneum and sometimes even the resection of infiltrated portions of the small and large intestines is necessary. Systematic lymph node dissection should only be performed in case of residual tumor size less than 1 cm, otherwise systematic lymph node removal does not seem to be beneficial (Burges and Schmalfeldt, 2011).

The administration of adjuvant platinum-containing chemotherapy after surgery is essential to complete the standard treatment of ovarian cancer (excluding FIGO stage IA, G1 tumors). The chemotherapy regime is usually composed of carboplatin and paclitaxel for a total of six cycles. Recently, the use of bevazicumab, a humanized anti-VEGF monoclonal antibody, during and up to ten months after standard chemotherapy with carboplatin/paclitaxel was shown to prolong progression-free survival by about four months in patients with

advanced ovarian cancer (Burger *et al*., 2011; Perren *et al*., 2011). Therefore, the enlargement of standard front-line chemotherapy to additional targeted therapy with the VEGF inhibitor bevazicumab should be evaluated for patients with FIGO stage IIB to IV ovarian cancer. Younger patients presenting with FIGO stage IV disease can be considered for surgery if it is possible to reduce the total tumor burden to less than 1 cm, provided a good performance status and pleural effusion as the only site of disease outside the abdominal cavity. If surgery is not planned, the diagnosis should be confirmed by biopsy before chemotherapy is administered (Aebi and Castiglione, 2009).

Patients with long intervals (>6 months) from initial chemotherapy to recurrent disease (*i.e.* platinum-sensitive ovarian cancer) should be considered for surgical resection of recurrent tumor masses and subjected to platinum-based reinduction chemotherapy including carboplatin/paclitaxel or carboplatin/gemcitabine. For patients with short treatment-free intervals, *i.e.* platinum-resistant ovarian cancer recurring less than 6 months after initial chemotherapy, palliative treatment with pegylated liposomal doxorubicin is recommended. Topotecan is used in second-line therapy for women with platinum-resistant ovarian cancer for whom doxorubicin is considered inappropriate (Hanna and Adams, 2008). Patients with advanced or relapsed ovarian cancer may develop symptoms from recurrent ascites, pleural effusions or bowel obstruction. To provide relief, even if only temporary, paracentesis, pleural aspiration, anti-emetic and antispasmodic medication, and palliative surgical interventions can be offered.

The outcome of patients afflicted with ovarian cancer largely depends on the quality of treatment. While the achievement of a postoperative residual tumor size less than 1 cm improves patients' prognosis, no substantial effect on patients' survival can be obtained by surgery if the postoperative tumor size exceeds 1 cm. Further independent prognostic factors are tumor grade, lymph node status, ascites, age at diagnosis, and the general health condition. Patients' survival prognosis is also associated with FIGO stage: about 90% of women presenting with FIGO stage IA, but only 25% of women presenting with FIGO stage III survive five years or longer (see appendix).

1.5 Carbohydrate antigen 125 (CA125)

CA125 is presently the best-established marker in clinical application for therapy monitoring of ovarian cancer. Elevated CA125 concentrations are found in 80% of women afflicted with ovarian cancer and during chemotherapy, CA125 serum levels correlate with tumor response and survival. Moreover, during follow-up of ovarian cancer patients, CA125 can accurately predict disease recurrence (Schrohl *et al*., 2003; Aebi and Castiglione, 2009). However, in a randomized controlled trial of over 78,000 women aged 55 to 74 years, annual screening with CA125 and transvaginal ultrasound compared with usual care did not reduce disease-specific mortality in women at average risk for ovarian cancer, but rather increased invasive medical procedures and associated harms (Buys *et al*., 2011). Considering the fact that, due to the absence of early warning symptoms, 70% of cases of ovarian cancer are not diagnosed until the disease has reached an advanced stage, additional markers enabling early detection of ovarian cancer are needed.

In this respect, potential new biomarkers in the blood (*e.g.* ROMA® and OVA1®) were identified by protein expression analyses. These markers can help to distinguish benign from malignant adnexal masses, but are not suitable for ovarian cancer screening (Montagnana *et al*., 2011; Bast *et al*., 2012). Moreover, mRNA and protein expression levels of various members of the KLK family have been studied in the normal human ovary and ovarian cancer tissues. Compared to the normal ovary concomitant up regulation of twelve KLKs (KLK3-11 and 13-15) is found in ovarian cancer tissue. Regarding the clinical impact, expression of KLK4-7, 10 and 15 is linked to poor prognosis; KLK8, 9, 11, 13 and 14 are markers of favorable prognosis. Besides, KLK5-8, 10, 11 and 13 are considered to be promising predictive markers for ovarian cancer (Schmitt *et al.* 2013a).

1.6 Kallikrein-related peptidase 6 (KLK6)

KLK6 (formerly known as zyme, protease M, or neurosin) is abundantly expressed in the central nervous system (CNS), but not or only weakly in the normal ovary (Yousef and Diamandis, 2001; Petraki *et al*., 2006; Shaw and Diamandis, 2007). The regulation of KLK6 activity is mediated mainly through (auto-)proteolytic activation or inactivation, whereas the most efficient inhibition is achieved by endogenous antithrombin III (Magklara *et al*., 2003; Bayés *et al*., 2004). KLK6 displays trypsin-like specificity and, together with many other proteases, it participates in highly organized proteolytic cascades (Debela *et al*., 2006b; Yoon *et al*., 2007; Yoon *et al*., 2008; Beaufort *et al*., 2010), which have been suggested to play crucial roles in diverse (patho-)physiological processes, including semen liquefaction, skin desquamation, neurodegeneration, and cancer (Sotiropoulou *et al*., 2009). High abundance of KLK6 in CNS prompted further investigation of its functional role in the field of neurological disorders. Indeed, several studies suggest an involvement of KLK6 in the pathogenesis of Alzheimer's and Parkinson's disease because KLK6 has been shown to degrade both amyloid precursor protein and α-synuclein (Iwata *et al*., 2003; Yousef *et al*., 2003; Ashby *et al*., 2010). In patients with multiple sclerosis, elevated KLK6 serum levels are thought to drive disease progression and thus aggravate neurological disability, due to neurotoxic properties causing neuron cell death and inhibition of axon outgrowth (Scarisbrick *et al*., 2008). Still, the potential of KLK6 as a serological marker for multiple sclerosis is currently a subject of discussion (Hebb *et al*., 2010). However, in terms of intracranial neoplasms like the glioblastoma multiforme, KLK6 was recently shown to promote resistance of tumor cells to cytotoxic agents through the activation of PAR-1 (Drucker *et al*., 2013).

Regarding ovarian cancer, there is a growing number of evidence suggesting that KLK6 is involved in tumor growth and progression and represents a useful biomarker for screening, early diagnosis, prognosis, and prediction (Bayani and Diamandis, 2011; Sarojini *et al*., 2012). Overexpression of KLK6 in ovarian cancer cells, together with other KLKs, resulted in increased invasion in Matrigel® invasion assays and increased tumor burden in a nude mouse model

(Prezas *et al*., 2006). Determination of KLK6 and/or KLK13 in addition to carbohydrate antigen 125 (CA125) was shown to improve the sensitivity and specificity of CA125 as a diagnostic tool (Diamandis *et al*., 2003; White *et al*., 2009a). Otherwise, KLK6 and other KLKs were found to be up-regulated in CA125-negative ovarian cancer, implicating the possibility that KLKs could be useful biomarkers complementary to CA125 (Rosen *et al*., 2005).
Moreover, a score based on clinical factors, together with KLK6 and KLK13, can be applied to predict efficiency of surgical treatment (Dorn *et al*., 2007). Several research groups have retrospectively surveyed expression of KLK6 in relation to clinical and histomorphological factors. Elevated KLK6 protein or mRNA levels, quantitatively analyzed either by enzyme-linked immunoassay (ELISA) or quantitative polymerase chain reaction (PCR), were found to be associated with a more invasive cancer phenotype, late tumor (FIGO) stages, higher tumor grade, suboptimal debulking, as well as serous and undifferentiated histotypes (Shan *et al*., 2007; White *et al*., 2009b; Koh *et al*., 2011; Bandiera *et al*., 2013).

Most importantly, up-regulated KLK6 expression was also identified as a strong indicator of shortened overall survival (OS) and higher risk of disease recurrence in ovarian cancer patients (Hoffman *et al*., 2002; Kountourakis *et al*., 2008; Oikonomopoulou *et al*., 2008; White *et al*., 2009b). Finally, KLK6 may also serve as a predictive marker in ovarian cancer because elevated KLK6 serum levels were found to be associated with chemoresistance (Diamandis *et al*., 2003; Oikonomopoulou *et al*., 2008).

2. Aim of the study

The expression of KLK4 in the healthy human prostate and prostate cancer has been expansively investigated over the past years. Nevertheless, the role of KLK4 in the development of prostate cancer and its relevance as a tumor marker are still not sufficiently explained.
Therefore, the aim of this study was to characterize the expression pattern of KLK4 in healthy human organs and in tissues of prostate cancer patients and finally, to evaluate the potential of KLK4 as a clinically relevant marker for prostate cancer.

To date, KLK6 is believed to play a decisive role in tumor growth and disease progression in ovarian cancer patients. In addition, a growing number of evidence suggests KLK6 being a prognostic and predictive tumor marker in ovarian cancer.
Therefore, the aim of this study was to explore the expression pattern of KLK6 in tissue of ovarian cancer patients and to further examine whether KLK6 may constitute a clinically relevant marker in ovarian cancer.

3. Patients, materials and methods

3.1 Generation of polyclonal antibodies against KLK4 and KLK6

3.1.1 Recombinant kallikrein-related peptidases

The experimental procedures regarding cloning, expression, and purification of recombinant kallikrein-related peptidases (rec-KLKs) have previously been performed in our laboratory (Debela *et al*., 2006a, b). Based on the known nucleotide sequence of the human KLK5, individual cDNAs encoding the mature forms of KLK4 and KLK6 (excluding the signal-sequence and the pro-peptides) were generated from respective mRNAs originating from ovarian cancer tissue. Individual cDNAs were used as templates for the amplification of corresponding DNAs by polymerase chain reaction (PCR). Subsequently, the DNA constructs coding for a MRGSHHHHHHGS sequence at the N-terminus followed by an DDDDK enterokinase (EK) recognition site as a linker to the respective mature KLK were cloned into the bacterial expression vector pQE-30 (Qiagen, Hilden, Germany).

After transfecting *Escherichia coli* cells with the expression vectors, recombinant KLK4 and KLK6, all harboring an N-terminal $(His)_6$-tag followed by an EK cleavage-site, were expressed in *Escherichia coli* and purified as follows (Debela *et al*., 2006a, b): expressed (non-glycosylated) protein was purified via its histidine-tag by nickel-nitrilotriacetic acid agarose affinity chromatography (Qiagen) under denaturing/slightly reducing conditions. Subsequently, refolding procedures were employed, using reduced and oxidized glutathione as redox reagents (Sigma, Deisenhofen, Germany) to promote protein renaturation. In addition to recombinant KLK4 and KLK6, recombinant KLK7 and recombinant pro-forms of KLK proteases (rec-proKLK2 to rec-proKLK15) plus an N-terminally located $(His)_6$-tag and a C-terminal Tag100 epitope were produced and purified in a similar manner.

3.1.2 Immunization of chickens and rabbits with rec-KLK4 and rec-KLK6

At the Department of Laboratory Medicine of the Radboud University Nijmegen Medical Centre (Nijmegen, The Netherlands) chickens and rabbits were

immunized by injection of purified, refolded human rec-KLK4 and rec-KLK6, respectively, both carrying the N-terminal extension of 17 amino acids encompassing a $(His)_6$-tag and an EK cleavage site (MRGSHHHHHHGS DDDDK). Immunizations were performed according to the protocol by McKiernan *et al*. (2008). Chickens were immunized intramuscularly (pectoral muscle) with 20 µg of rec-KLK4 per injection. Antibodies (IgY, avian analog of IgG) were isolated from egg yolk by a standard step precipitation procedure utilizing increasing concentrations of polyethyleneglycol (PEG precipitation) as described previously (Grebenschikov *et al*., 1997). This procedure yielded IgY fractions with a protein purity of approximately 95% as analyzed by SDS-PAGE and subsequent Coomassie Blue staining.

Rabbits were immunized by injection of rec-KLK6, first into the popliteal lymph gland and then subcutaneously in form of booster injections with two weeks interval. After twelve booster vaccinations the rabbits were sacrificed. Citrated plasma was generated by centrifugation of the collected blood in citrate tubes and finally stored at -80°C.

3.1.3 Peptides $KLK4_{109–122}$ and $KLK6_{109–119}$

The peptide $KLK4_{109–122}$ encompassing amino acids 109 to 122 of the mature KLK4 as well as the peptide $KLK6_{109–119}$ covering amino acids 109 to 119 of the mature KLK6 (for the sequences see Figures 5A and 5B) constitute surface-exposed, flexible loops, which are not involved in secondary structures such as α-helices or β-sheets. These peptides were used for affinity chromatography to select monospecific polyclonal antibodies directed against the linear epitope 109-122 of KLK4 and 109-119 of KLK6, respectively.

The peptides $KLK4_{109–122}$ and $KLK6_{109–119}$ as well as the peptides GSHHHHHHGS and HHHGSDDDDK (corresponding to $(His)_6$-tag and the EK cleavage site of rec-KLK4 and rec-KLK6) were synthesized by the Service Center of the Max-Planck-Institute of Biochemistry, Martinsried, Germany.

3.1.4 Affinity purification of polyclonal antibodies directed against KLK4 and KLK6

Polyclonal chicken antibodies against KLK4 were purified from the IgY fraction isolated from egg yolk, while polyclonal rabbit antibodies (isotype IgG) directed to KLK6 were selected from the animal's citrated plasma.

The purification of antibodies by affinity chromatography comprised three consecutive steps as displayed in Figure 1: (a) affinity column with covalently linked peptide $KLK4_{109–122}$ or $KLK6_{109–119}$; (b) affinity column with immobilized peptides covering the tag of the recombinant proteins (GSHHHHHHGS and HHHGSDDDDK corresponding to $(His)_6$-tag and the EK cleavage site of rec-KLK4 and rec-KLK6); and (c) affinity column coupled with the immunogen, *i.e.* either rec-KLK4 or rec-KLK6. The coupling of recombinant proteins and peptides to the affinity columns was performed according to the standard BioRad procedure. After coupling, the gel slurry was packed into disposable plastic columns (Pierce, Rockford, IL, USA). For each particular column, approximately 2 ml of a 1:1 mixture of AffiGel®10 and AffiGel®15 (BioRad Laboratories, Hercules, CA, USA) was used. After filtration, at first, nearly 8 ml of the antibody solution containing IgY from egg yolk directed against KLK4 were passed through the corresponding affinity column coupled with the peptide $KLK4_{109–122}$. Analogously, approximately 4 ml of antibody solution containing IgG from citrated plasma directed against KLK6 were passed through the corresponding primary affinity column coupled with the peptide $KLK6_{109–119}$. The obtained effluent of each column was then passed through the respective second affinity column containing the mixture of immobilized poly-His and EK peptides. Finally, each effluent of the second purification step was passed through the respective last affinity column containing immobilized rec-KLK4 or rec-KLK6.

After washing with phosphate-buffered saline (PBS), bound antibodies of all three columns were eluted with 4 ml of 0.1 M glycine/HCl buffer, pH 2.4, followed by an immediate restoring of a neutral pH using appropriate amounts of KOH solution. The purified antibodies were finally concentrated by an Amicon Ultra-15 centrifugal filter device (Millipore, Amsterdam, The Netherlands),

diluted 1:1 with glycerol, and stored at -20°C until use. The described process of affinity purification was performed by colleagues at the Department of Laboratory Medicine of the Radboud University Nijmegen Medical Centre (Nijmegen, The Netherlands).

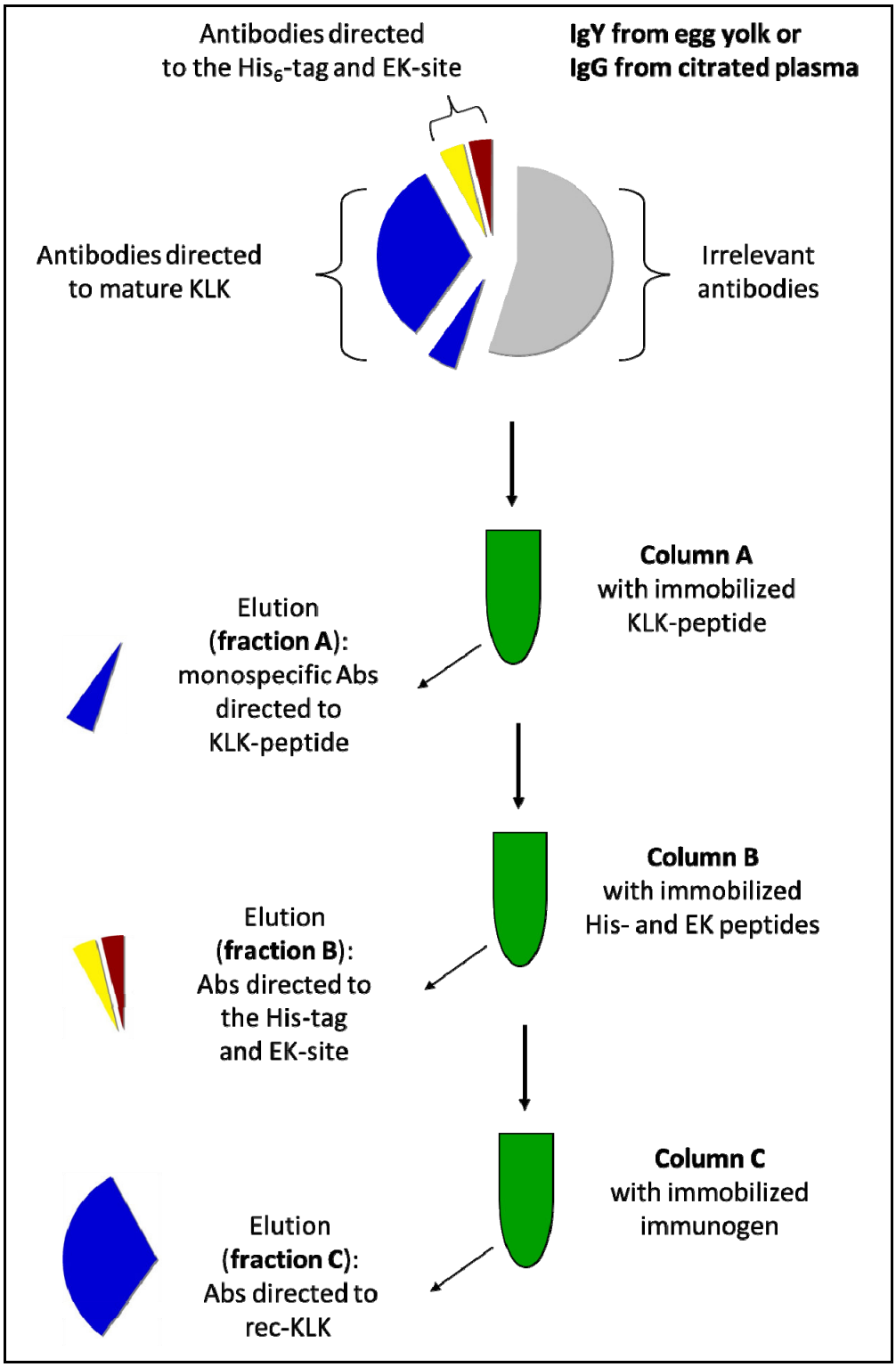

Figure 1: Scheme of the affinity purification of polyclonal antibodies directed against KLK4 and KLK6. First, the IgY fraction from egg yolk of chicken #617, immunized with rec-KLK4, and the citrated plasma of rabbit #623, immunized with rec-KLK6, were passed over column A with immobilized $KLK4_{109–122}$ or $KLK6_{109–119}$, respectively. The elution contained monospecific, polyclonal antibodies (pAbs) directed against the linear epitope 109-122 of KLK4 or 109-119 of KLK6 (**fraction A**: pAb 617A or pAb 623A).
The effluent of column A was then applied to column B with the immobilized peptides GSHHHHHHGS (His-peptide) plus HHHGSDDDDK (EK-peptide). The elution (**fraction B**) contained antibodies directed to the N-terminal extension of rec-KLK4 and rec-KLK6, *i.e.* the $(His)_6$-tag and the EK site (pAb 617B or pAb 623B).
Finally, the effluent of column B was passed over column C with immobilized rec-KLK4 or rec-KLK6, respectively. The elution contained polyclonal antibodies directed against rec-KLK4 or rec-KLK6 (**fraction C**: pAb 617C or pAb 623C).

3.2 'One-side' ELISA (Enzyme-linked immunosorbent assay)

Purified antibody fractions (pAb 617A, B, C and pAb 623A, B, C) were characterized using microtiter plate-based 'one-side' or 'indirect' ELISA assays. Briefly, Nunc MaxiSorp™ flat-bottomed immunoplates (Life Technologies, Breda, The Netherlands) were coated overnight at 4 °C with the testing proteins (rec-KLK4 and rec-KLK6) as well as testing peptides ($KLK4_{109–122}$, $KLK6_{109–119}$, $(His)_6$-tag, and EK site) diluted in coating buffer (15 mM Na_2CO_3 and 35 mM $NaHCO_3$, pH 9.6) at a concentration of 0.1 µg/ml. Afterwards, plates were washed twice (microplate washer; Tecan, Männedorf, Switzerland) and blocked with blocking buffer (1% BSA dissolved in PBS) for 2 h at 37 °C, followed by washing each of the wells four times with 300 µl washing buffer per well (0.1% Tween-20 in PBS). The last mentioned washing procedure was repeated after each single incubation step.

Next, the wells were incubated with the antibody samples (*i.e.* the purified antibody fractions pAb 617A, B, C and pAb 623A, B, C), appropriately diluted in dilution buffer (1% BSA in washing buffer), for 2 h at room temperature. Subsequently, incubation with horseradish peroxidase (HRP)-labeled detection antibodies (*i.e.* rabbit anti-chicken IgY for pAb 617A, B, C or goat anti-rabbit IgG for pAb 623A, B, C; Sigma, Deisenhofen, Germany) was performed for 2 h at

room temperature. After that incubation step, the chromogenic substrate solution consisting of ortho-phenylenediamine (OPD; Dako, Glostrup, Denmark) in color-developing buffer (phosphate-citrate buffer with sodium perborate; Sigma) was added and plates were incubated in the dark for 30 min at room temperature. After development of the golden brown color, 100 µl of 1 M H_2SO_4 were added to each well to stop the reaction. Optical density was determined at 492 nm using an automated ELISA reader (Lab Systems, Oy, Helsinki, Finland). The described 'one-side' ELISA assays were performed by colleagues at the Department of Laboratory Medicine of the Radboud University Nijmegen Medical Centre (Nijmegen, The Netherlands).

3.3 Western blot analysis

Recombinant KLK pro-forms (rec-proKLK3 to rec-proKLK15), recombinant mature KLK6 as well as brain and skeletal muscle protein extracts were denatured in the presence of 2% (w/v) sodium dodecyl sulfate (SDS) and 5% (v/v) 2-mercaptoethanol for 5 min at 95 °C. Thereafter, denatured proteins were subjected to 12% SDS-PAGE (SDS-polyacrylamide gel electrophoresis).

Separated proteins were transferred onto polyvinylidene fluoride (PVDF) membranes (PALL, Dreieich, Germany) using a semidry transfer device. Subsequently, the PVDF membranes were blocked with 5% (v/v) skim milk in PBS-0.1% Tween-20 buffer (pH 7.4) for 1 h at room temperature. Then, the membranes were incubated overnight at 4 °C with the respective primary antibodies (*i.e.* pAb 617A, pAb 617C, pAb 623A, and pAb 623C; for antibody dilutions see appendix), followed by three washes, 10 min each, in PBS-0.1% Tween-20 buffer at room temperature. Bound primary antibodies were detected by incubation of the membranes with a HRP-conjugated, secondary antibody (goat anti-chicken IgY for pAb 617A and pAb 617C; Sigma, Deisenhofen, Germany; goat anti-rabbit IgG for pAb 623A and pAb 623C; Jackson ImmunoResearch Lab, West Grove, PA, USA; both diluted 1:10,000 in PBS-0.1% Tween-20 buffer containing 5% (v/v) skim milk).

Finally, binding of antibodies to target proteins on the PVDF membranes was visualized by an enhanced chemiluminescence reaction (ECL, Pierce,

Rockford, IL, USA). The resulting light emissions were recorded on an X-ray film. To define the molecular mass of positive bands, the prestained Protein-Marker IV (peqlab, Erlangen, Germany) was employed.

3.4 Prostate cancer patients and tissues

In this retrospective study, tissue samples of eighty-four patients with primary adenocarcinoma of the prostate were evaluated. All patients underwent a radical prostatectomy at the Department of Urology of the Dresden University Medical Center. Tissue samples were obtained from the archives of the Center's Institute of Pathology. The study adhered to national regulations on ethical issues and was approved by the local Ethics Committee.

Patients' age at diagnosis ranged from 50 to 76 years (median age 64 years). Matched pairs of malignant and non-malignant tissue portions of each prostate cancer sample were used for the generation of a tissue microarray (as specified below). Some prostate cancer samples were not adequately represented on the stained tissue microarray (TMA), due to detachment or damage of tissue cores during immunohistochemical procedures. However, since we took into account only these cases for which both the tumor and the tumor-free tissue cores were evaluable on the TMA, forty-four prostate cancer patients were finally included in the statistical evaluation. The histopathological examination of corresponding autologous tissue cores (*i.e.* tumor tissue and corresponding tumor-free tissue) was based on the TNM classification system (see appendix). Tumors were graded and scored according to Gleason and the World Health Organization (WHO) grading system as modified by the German Prostate Cancer Study Group (Helpap, 1998; see appendix). Patient and tumor characteristics are summarized in Table 4.

3.5 Ovarian cancer patients and tissues

One hundred and eighteen patients afflicted with ovarian cancer stages FIGO I-IV (Fédération Internationale de Gynécologie et d'Obstétrique), all treated at the Department of Obstetrics and Gynecology of the Technical University of Munich between 1992 and 1999, were enrolled in this retrospective study. The study adhered to national regulations on ethical issues and was approved by the Ethics Committee of the Klinikum rechts der Isar, Technical University of Munich.

Patients´ age at diagnosis ranged from 20 to 85 years (median age 57 years). According to clinical recommendations all patients initially underwent the standard primary, stage-related, radical debulking operation. This surgical treatment included median laparotomy with total hysterectomy, bilateral adnectomy, infragastric omentectomy, pelvic and para-aortic lymphadenectomy if indicated, as well as removal of all existing tumor if possible. Depending on tumor spread, several patients additionally received a partial resection of the small and large intestine, the diaphragmatic peritoneum and further peritonectomies in order to achieve the greatest possible reduction of tumor mass. In younger patients (<35 years) with tumor stage FIGO I and favorable histology, who wished to retain their fertility, less radical surgery was performed. Surgical and pathological staging as well as risk evaluation were assessed on the basis of the FIGO and TNM classification system (see appendix). Sixty-one patients (51.7%) were optimally debulked with complete removal of macroscopically visible tumor manifestations. Surgical specimens were histologically examined at the Institute of Pathology of the Technical University of Munich.

Following surgical treatment, 106 (89.8%) patients received adjuvant, platinum-containing combination chemotherapy as recommended individually for each patient by a multidisciplinary tumor board. Due to unfavorable heath conditions, 10 patients received no adjuvant therapy, whereas two women were subjected to non-platinum regiments for first-line chemotherapy. After this multimodal guideline therapy, 68 (57.6%) patients experienced disease recurrence. Median

observation time for all of the patients was 51 months (observation time ranged from 1 to 244 months). For those 36 women still alive at time of recent follow-up in March 2011, the median observation time was 173 months (observation time ranged from 14 to 244 months). Patient and tumor characteristics are listed in Table 6.

3.6 Tissue preparation and microarray construction

Patients´ tissue samples were obtained during surgery, inspected by a pathologist from the Institute of Pathology of the Dresden University Medical Center (in case of prostate cancer tissue samples) or the Institute of Pathology of the Technical University of Munich (in case of ovarian cancer tissue samples), immediately fixed in neutral buffered formalin (4% formaldehyde solution), and finally embedded in paraffin. Tissue microarrays (TMAs) were constructed employing previously established and validated techniques (Wan *et al*., 1987; Skacel *et al*., 2002). First, routine H&E (hematoxylin and eosin-) stained sections were prepared for each individual tissue sample. Morphologically representative areas were marked on the original H&E slides by the pathologist. Using these slides for orientation, cylindrical core biopsies were carefully lifted from the selected areas of each individual paraffin-embedded tumor tissue (donor block) and precisely mounted into a paraffin block (recipient block) with the help of a manual tissue microarray device (MTA-1, Beecher, WI, USA). According to their predefined coordinates the core biopsies were positioned into a grid of empty cylindrical holes prepared on the recipient paraffin block.

In terms of prostate cancer tissue samples, two core punches of 0.6 mm in diameter were taken from the morphologically most representative tumor area and one core punch was taken from the corresponding tumor-free area of each individual prostate cancer sample. Thus, matched pairs of two malignant tissue cores and one non-malignant tissue core, each pair representing one prostate cancer sample, were assembled on one TMA block. Sections from this TMA block were subjected to immunohistochemical stainings using pAbs 617A and 617C, both directed to KLK4.

In the case of ovarian cancer tissue samples, three core biopsies of 1 mm in diameter were punched out from each tumor sample. Seven TMA blocks were constructed this way with each individual tumor sample being represented by three core biopsies (Figure 18A, appendix). Sections from these TMA blocks were subjected to immunohistochemical stainings using pAb 623A directed to KLK6.

In addition, various tissues from healthy human adults were obtained from the archives of the Institute of Pathology of the Technical University of Munich. Core punches from these routinely processed, formalin-fixed, paraffin-embedded (FFPE) tissue samples were assembled on a TMA. Likewise, a variety of normal adult human tissues was also obtained from the archives of the Institute of Pathology of the Dresden University Medical Center to construct another TMA. Together with conventional tissue blocks these TMAs were used to evaluate the expression patterns of KLK4 and KLK6 in normal adult human tissues by immunohistochemistry.

Using a standard routine microtome (Microm HM335E; Thermo Scientific, Germany), 2 µm-thick sections and 4-5 µm-thick sections (in case of the prostate cancer TMA) were cut from the tissue microarray blocks as well as the conventional tissue blocks and transferred to electrostatically charged glass slides. In preparation for subsequent deparaffinization, the slides were finally dried overnight at 37 °C.

3.7 Immunohistochemistry (IHC)

Sections of tissue microarrays as well as conventional tissue sections were stained using chicken pAbs 617A and 617C as well as rabbit pAbs 623A and 623C along with the Vectastain® Elite ABC-kit (Vector Laboratories, Burlingame, CA, USA) or the EnVision™ peroxidase polymer system (Dako), respectively. Sections were dewaxed in xylene, rehydrated in a descending row of graded ethanol, and then treated for antigen retrieval by pressure cooking (4 min, 120 °C, 0.1 M citrate buffer, pH 6.0). After several washes with Tris-buffered saline (TBS, pH 7.6), a dual enzyme block containing 0.5% H_2O_2 (Dako) was

applied for 10 min at room temperature to block endogenous peroxidase and alkaline phosphatase activity.

As part of the avidin-biotin complex (ABC) staining method (Vectastain® Elite ABC-kit; Vector Laboratories) sections of the prostate cancer TMA, conventional prostate cancer sections, and sections of the TMA harboring normal adult human tissues were additionally incubated with goat serum diluted 1:100 in TBS for 45 min at room temperature to block non-specific antibody binding. Subsequently, primary antibodies (*i.e.* pAb 617A, pAb 617C, pAb 623A or pAb 623C; for antibody dilutions see appendix) were allowed to react overnight at 4 °C.

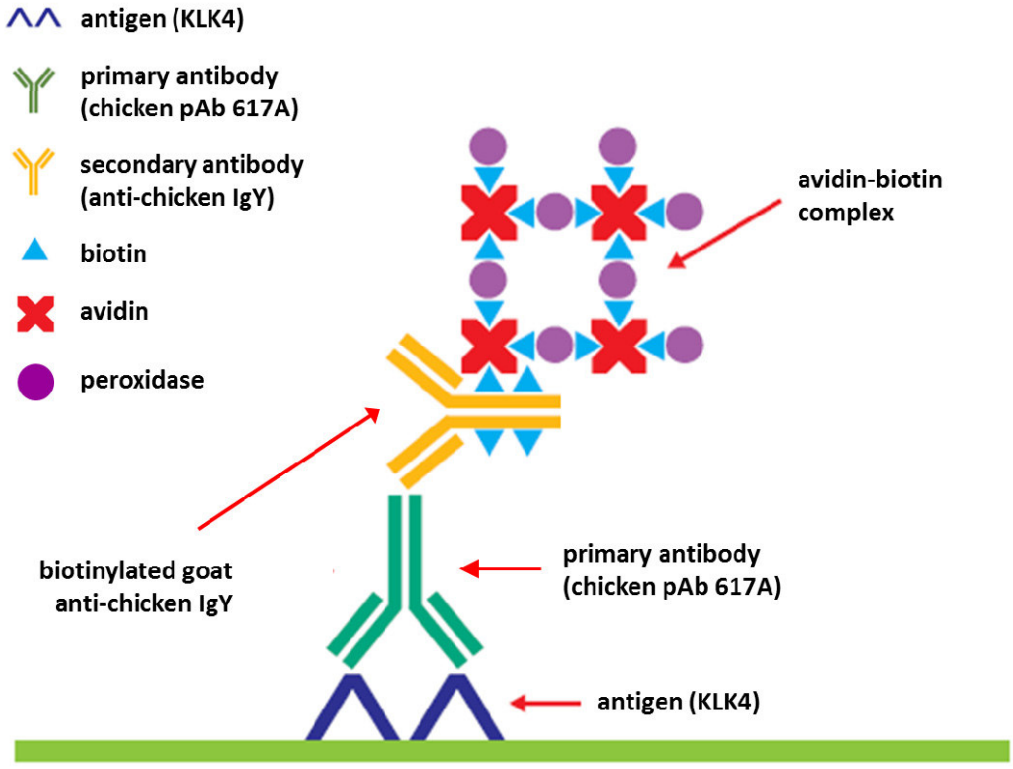

(Adapted from Kumar, G.L. and Rudbeck, L. (2009).
Education Guide – Immunohistochemical Staining Methods, 5th edition.)

Figure 2: Scheme of the avidin-biotin complex (ABC) staining method illustrated with the example of chicken pAb 617A as primary antibody. The Vectastain® Elite ABC-system (Vector Laboratories) is based on the strong affinity of avidin for the vitamin biotin.

When chicken pAbs 617A and 617C were used as primary antibodies along with the Vectastain® Elite ABC-kit (Vector Laboratories) to stain sections of the prostate cancer TMA, conventional prostate cancer tissue sections, and sections of the TMA harboring normal adult human tissues, a secondary biotinylated goat anti-chicken IgY antibody (Vector Laboratories) was applied for 50 min at room temperature. This secondary antibody functions as a link between the tissue-bound primary antibodies and the avidin-biotin-peroxidase complex (Vectastain® Elite ABC-reagent; Vector Laboratories). After several washes, finally, the Vectastain® Elite ABC-reagent was applied for 50 min at room temperature and the washing steps repeated (Figure 2).

When chicken pAbs 617A and 617C were employed as primary antibodies along with the EnVision™ peroxidase polymer system (Dako) to stain conventional sections of normal adult human tissues, a secondary rabbit anti-chicken IgY antibody (Jackson ImmunoResearch Lab, West Grove, PA, USA) was applied for 30 min at room temperature. However, only when rabbit pAbs 623A and 623C were employed as primary antibodies along with the EnVision™ peroxidase polymer system (Dako) to stain sections of the ovarian cancer TMAs, conventional sections of normal adult human tissues, and sections of the TMA harboring normal adult human tissues, no secondary antibody was needed (Figure 3). For detection of tissue-bound primary antibodies by means of the EnVision™ peroxidase polymer system (Dako) a horseradish peroxidase-labeled polymer comprising antibodies with anti-rabbit IgG and anti-mouse IgG specificity was applied to the slides for 30 min at room temperature (Figure 3).

For both the avidin-biotin complex (ABC) staining method (Vectastain® Elite ABC-kit; Vector Laboratories) and the polymer-based staining method (EnVision™; Dako) the peroxidase reaction was developed with 3,3'-diaminobenzidine (DAB$^+$; Dako) for 7.5 min at room temperature. Finally, counterstaining of sections was performed with Mayer's hematoxylin (hospital pharmacy, Technical University of Munich), resulting in a sharp blue staining of nuclei. Subsequent to counterstaining, the sections were dehydrated in an ascending row of graded ethanol and cover glasses were glued to the slides using a soluble mounting medium (Histokitt; Assistent, Sondheim, Germany) in

order to seal off the sections from contamination and decay. As a negative control, the primary antibody was omitted and replaced by green antibody diluent (Dako) or by irrelevant antibodies.

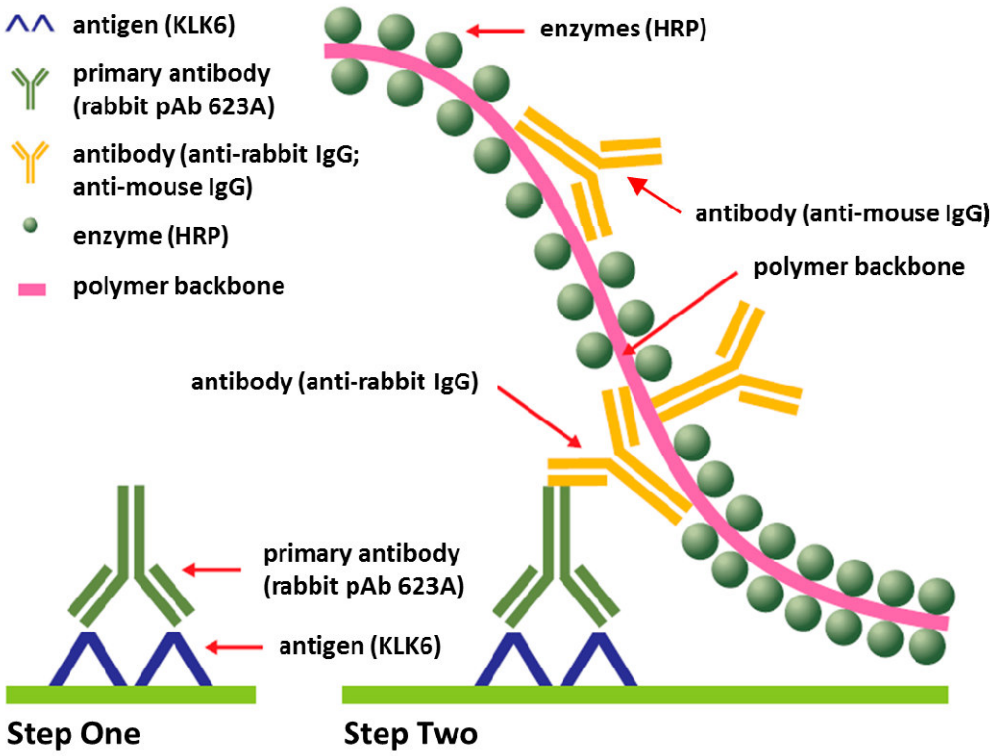

(Adapted from Kumar, G.L. and Rudbeck, L. (2009). Education Guide – Immunohistochemical Staining Methods, 5th edition.)

Figure 3: Scheme of the polymer-based staining method illustrated with the example of rabbit pAb 623A as primary antibody. The EnVision™ polymer system (Dako) contains a dextran backbone to which multiple HRP molecules as well as antibodies with anti-rabbit IgG and anti-mouse IgG specificity are attached.

Subsequent to the immunohistochemical staining, the slides were scanned by a digital slide scanner (NanoZoomer-RS; Hamamatsu Photonics, Japan) using the NDP.scan software 2.2.60. Thus, stained glass slides were digitized and converted into high-definition, high-quality digital images enabling high power magnification, copying, and editing of the entire digital image.

3.8 Quantification of KLK4 immunostaining on the prostate cancer tissue microarray

For the evaluation of KLK4 immunostaining a semiquantitative score following the Remmele score guidelines (Remmele and Stegner, 1987), which is based on staining intensity and the percentage of positively stained cells, was created. Staining intensity was classified on a scale of 0 to 3 (Table 1). Differing from the Remmele score, the percentage of positively stained cells was scored on a scale of 1 to 3 (1: staining of < 10% of cells; 2: 11–50%; 3: > 50%; compare Table 1). Based on these scores, a final immunoreactivity score (IRS) was created by multiplication of the intensity score values with the positivity score values, thus obtaining a maximum IRS of 9. For each individual prostate cancer sample a matched pair of two malignant tissue cores and one non-malignant tissue core (*i.e.* tumor tissue and corresponding tumor-free tissue) was assembled on the TMA. Therefore, in case of the malignant tissue cores, the mean score values of the two readings were used for statistical analyses. Immunostainings were evaluated under a Zeiss AxioSkop microscope (Carl Zeiss, Göttingen, Germany) with the assistance of a trained pathologist from the Institute of Pathology of the Dresden University Medical Center.

3.9 Quantification of KLK6 immunostaining on ovarian cancer tissue microarrays

For the evaluation of KLK6 immunostaining the Remmele score (Remmele and Stegner, 1987), which is a semiquantitative score based on staining intensity and the percentage of positively stained cells, was applied to patients´ tissue samples represented on seven tissue microarrays (Figure 18B, appendix). For this, staining intensity was classified on a scale of 0 to 3. The percentage of positively stained cells was scored by cell counts and graded from 0 to 4. The final immunoreactivity score (IRS) was calculated by multiplication of the intensity score values with the positivity score values, thus obtaining a final IRS between 0 and 12 (Table 1). As for each individual ovarian cancer sample three tissue cores were evaluated, the mean IRS values of the three readings were used for statistical calculations. Immunostainings were evaluated under a Zeiss

AxioSkop microscope (Carl Zeiss, Göttingen, Germany) with the assistance of a trained pathologist from the Institute of Pathology of the Helmholtz Zentrum in Munich.

Table 1: Remmele score.

Remmele Score (adapted from Remmele and Stegner, 1987)			
SI × P = IRS [0-12]			
Scale	**SI (Staining intensity)**	**P (Positivity)**	**Scale**
0	no staining	no staining	0
1	weak staining	1-10%	1
2	moderate staining	11-50%	2
3	strong staining	51-80%	3
–	–	>80%	4
IRS = Immunoreactivity Score, range from 0 (= negative) to 12 (= strongly positive)			

3.10 Statistical analyses on the basis of KLK4 score values and clinicopathological factors of prostate cancer patients

The correlation between KLK4 score values (immunoreactivity scores in tumor tissue and corresponding tumor-free tissue) obtained with either pAb 617A or pAb 617C was analyzed using the Spearman rank correlation (r_s). The relation of KLK4 immunoexpression values with patients' clinicopathological parameters was determined using nonparametric Mann-Whitney or Kruskal-Wallis tests. The statistical analyses were two-sided, *p*-values ≤ 0.05 were determined to be statistically significant. Calculations were performed using the Stat-View 5.0 statistical package (SAS Institute, Cary, NC, USA).

3.11 Statistical analyses on the basis of KLK6 score values, clinicopathological factors, and survival in patients with ovarian cancer

The relation of KLK6 immunoexpression levels (grouped according to their median values) with clinical and histomorphological parameters was determined using the chi-squared test. For survival analyses, both progression-free survival (PFS) and overall survival (OS) of ovarian cancer patients were used as follow-up end points. The association of KLK6 immunoexpression with OS and PFS as well as the association of clinical/histomorphological factors with OS and PFS was analyzed using Cox univariate and multivariate proportional hazards regression models and finally expressed as hazard ratio (HR) with its 95% confidence interval (95% CI). The multivariate Cox regression model was adjusted for known ovarian cancer-related prognostic factors: FIGO stage, nuclear grade, residual tumor after surgery, and ascitic fluid volume. Survival curves were plotted according to Kaplan-Meier (Kaplan and Meier, 1958) using log-rank tests to recognize differences. All calculations were performed using the Stat-View 5.0 statistical package (SAS Institute, Cary, NC, USA). *p*-values ≤ 0.05 were determined to be statistically significant.

4. Results

4.1 Generation and purification of monospecific polyclonal antibodies (pAb) directed to KLK4 and KLK6

Chickens and rabbits were immunized with purified and refolded recombinant (non-glycosylated) human KLK4 (rec-KLK4) and KLK6 (rec-KLK6), respectively, both of which carrying an N-terminal extension of 17 amino acids encompassing a histidine $(His)_6$-tag and an enterokinase (EK) cleavage site (Figure 4A). Subsequently, antibodies from egg yolk as well as antibodies from rabbit´s citrated plasma were purified by affinity chromatography.

In order to select peptide epitopes suitable for the affinity purification of monospecific antibodies, we searched – based on the X-ray structures of KLK4 and KLK6 (Bernett *et al*., 2002; Debela *et al*., 2006a; Gomis-Rüth *et al*., 2002) – for regions, which are surface-exposed but not involved in secondary structures. Such surface-exposed flexible loops are generally known to possess immunogenic qualities and furthermore, they often represent linear (and not conformational) epitopes. In addition, we restricted the search for appropriate peptide epitopes to those regions within KLK4 and KLK6, which are not highly conserved among the members of the KLK protease family. Finally, the region encompassing amino acids 109–122 of KLK4 ($KLK4_{109–122}$; Goettig *et al*., 2010) as well as the region covering amino acids 109–119 of KLK6 ($KLK6_{109–119}$; Goettig *et al*., 2010) were selected for affinity purification of monospecific antibodies directed against KLK4 and KLK6 (Figure 4B, C and Figure 5).

For affinity chromatography three types of consecutive affinity columns were established. The first column contained a synthetic peptide either derived from KLK4 ($KLK4_{109–122}$) or KLK6 ($KLK6_{109–119}$) to select for monospecific polyclonal antibodies. Peptides covering the $(His)_6$-tag (GSHHHHHHGS) plus the EK site (HHHGSDDDDK) were coupled to the second column to accomplish a ‘negative’ purification step. The third column was modified by covalent coupling of the immunogen, *i.e.* either rec-KLK4 or rec-KLK6. Both the IgY fraction from egg yolks of chicken #617 and the antibody solution from citrated plasma of

rabbit #623 were separately applied to the respective sequential affinity columns (Figure 1). The elutions containing different antibody fractions (pAb 617A, B, C and pAb 623A, B, C) were then characterized by ELISA and Western blot analyses.

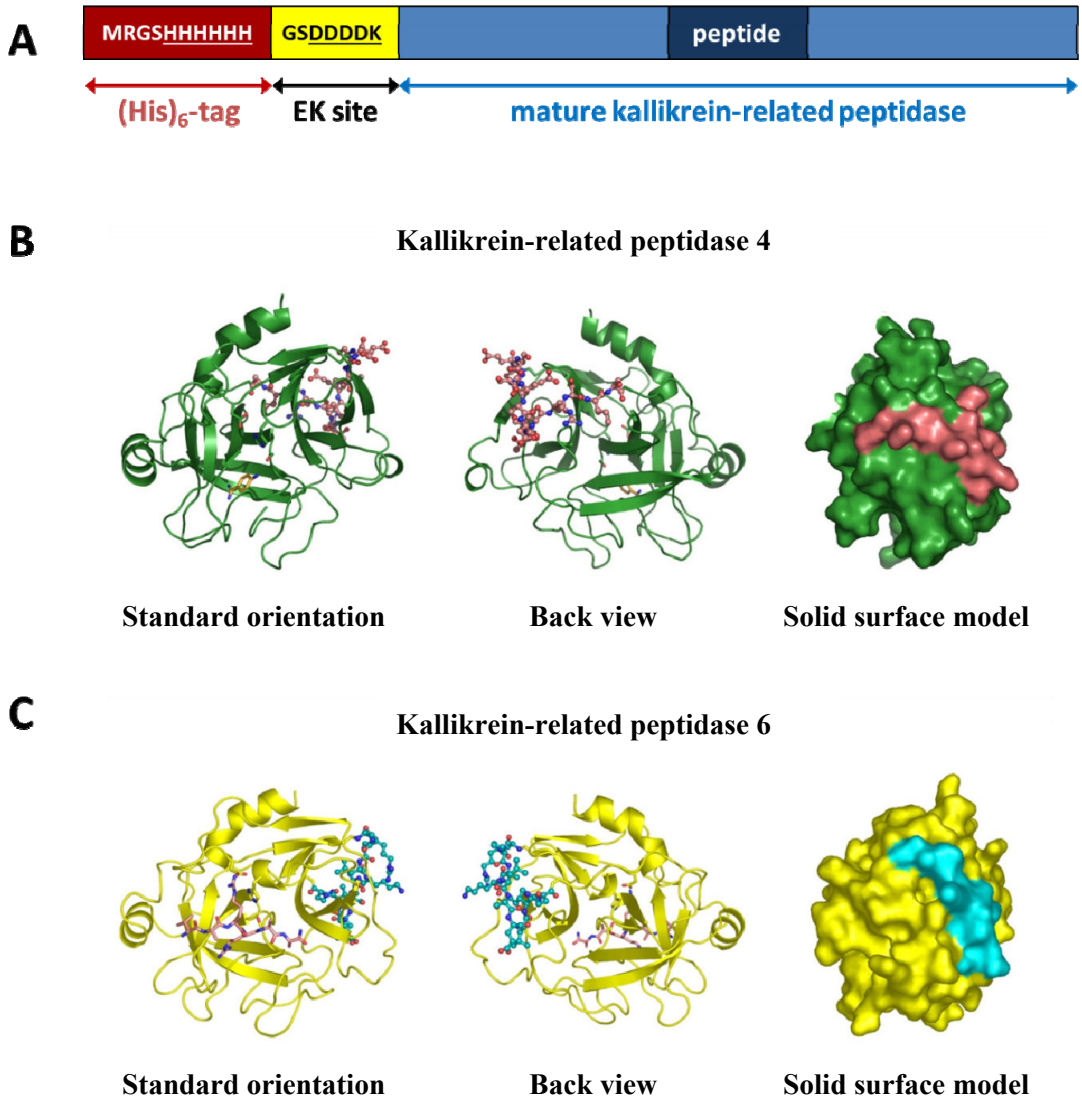

Figure 4: Peptides KLK4$_{109–122}$ and KLK6$_{109–119}$ used for the selection of monospecific polyclonal antibodies directed against KLK4 and KLK6.
(A) Simplified illustration of the primary structure of rec-KLK4 and rec-KLK6, respectively. The sequence encoding the mature human KLK (colored blue) is preceded by an N-terminal extension of 17 amino acids harboring a $(His)_6$-tag (red) and an enterokinase (EK) cleavage site (yellow). **(B, C)** Graphics illustrate the location of the peptides KLK4$_{109–122}$ and KLK6$_{109–119}$ within the structure of KLK4 and KLK6, respectively (Debela *et al*., 2006a, b). Stereo ribbon plots of KLK4 and KLK6 are shown in standard orientation (the substrate binding site from N- to C-terminus runs

horizontally from left to right) as well as from the back of the proteases. As demonstrated by solid surface representations, the selected peptides (shown in red and blue) are located on the surface of the proteases. Graphics were created with the software PyMOL (DeLano, 2002).

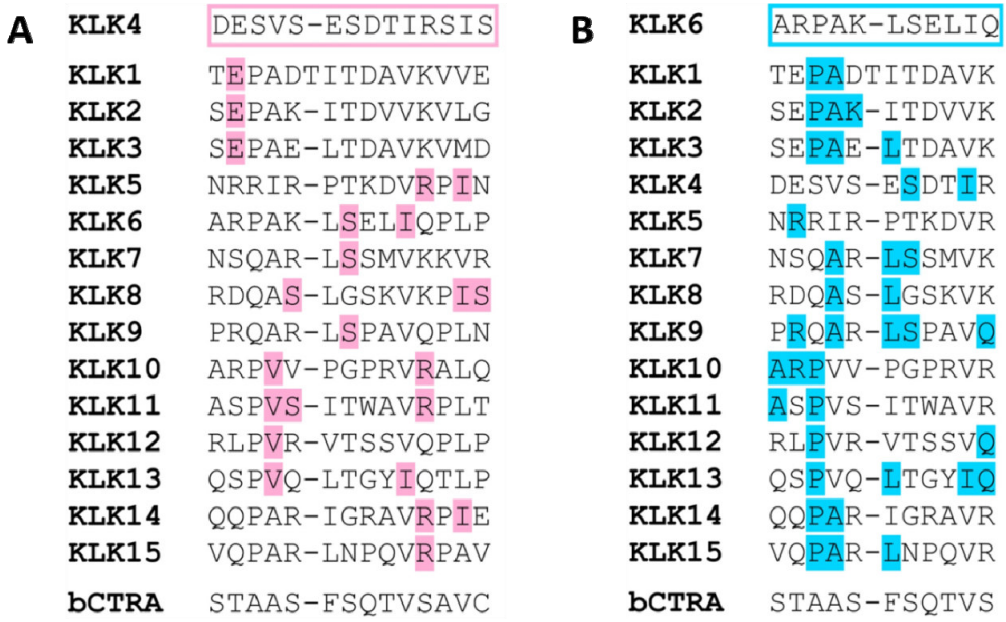

Figure 5: Multiple sequence alignment for human kallikrein-related peptidases and bovine chymotrypsin (bCTRA).
(A) The non-conserved sequence between positions 109 and 122 of KLK4 (framed in red; according to the chymotrypsin numbering) and **(B)** the non-conserved sequence between positions 109 and 119 of KLK6 (framed in blue; according to the chymotrypsin numbering) were used for affinity purification. For the amino acid single-letter code see appendix.

4.2 Characterization of polyclonal antibodies directed to KLK4 by 'one-side' ELISA

For affinity purification the IgY fraction extracted from egg yolks of chicken #617 was applied onto the first affinity column with immobilized peptide KLK4$_{109–122}$ (Figure 1). The elution of this column (elution A) contained monospecific polyclonal antibodies (pAb 617A) whose reaction pattern was characterized by 'one-side ELISA' assays. For this, microtiter plates were coated with the antigen

(KLK4-derived peptide $KLK4_{109–122}$), the immunogen (rec-KLK4), and with control proteins/peptides such as rec-KLK7 and $(His)_6$-tag/EK peptides.

Monospecific polyclonal antibody 617A strongly reacted with both the KLK4-derived peptide and the immunogen (Figure 6). The effluent was applied to the second column, loaded with $(His)_6$-tag/EK peptides. This column enabled a 'negative' purification by selection of antibodies generated against the N-terminal, non-KLK-related sequences of rec-KLK4 (elution B, pAb 617B). The effluent of the second column, now depleted from antibodies directed against the non-KLK-related sequences of rec-KLK4, was applied to the third column, loaded with the immunogen. By contrast with pAb 617A, the antibody fraction eluted from the third column (elution C, pAb 617C) distinctly reacted with the immunogen (rec-KLK4), but not with the KLK4-derived peptide $KLK4_{109–122}$ (Figure 6).

The antibody fraction 617C apparently is completely depleted from pAb 617A, which reacted with both the KLK4-derived peptide and the immunogen. Hence, pAb 617A and pAb 617C are directed against different epitopes of KLK4.

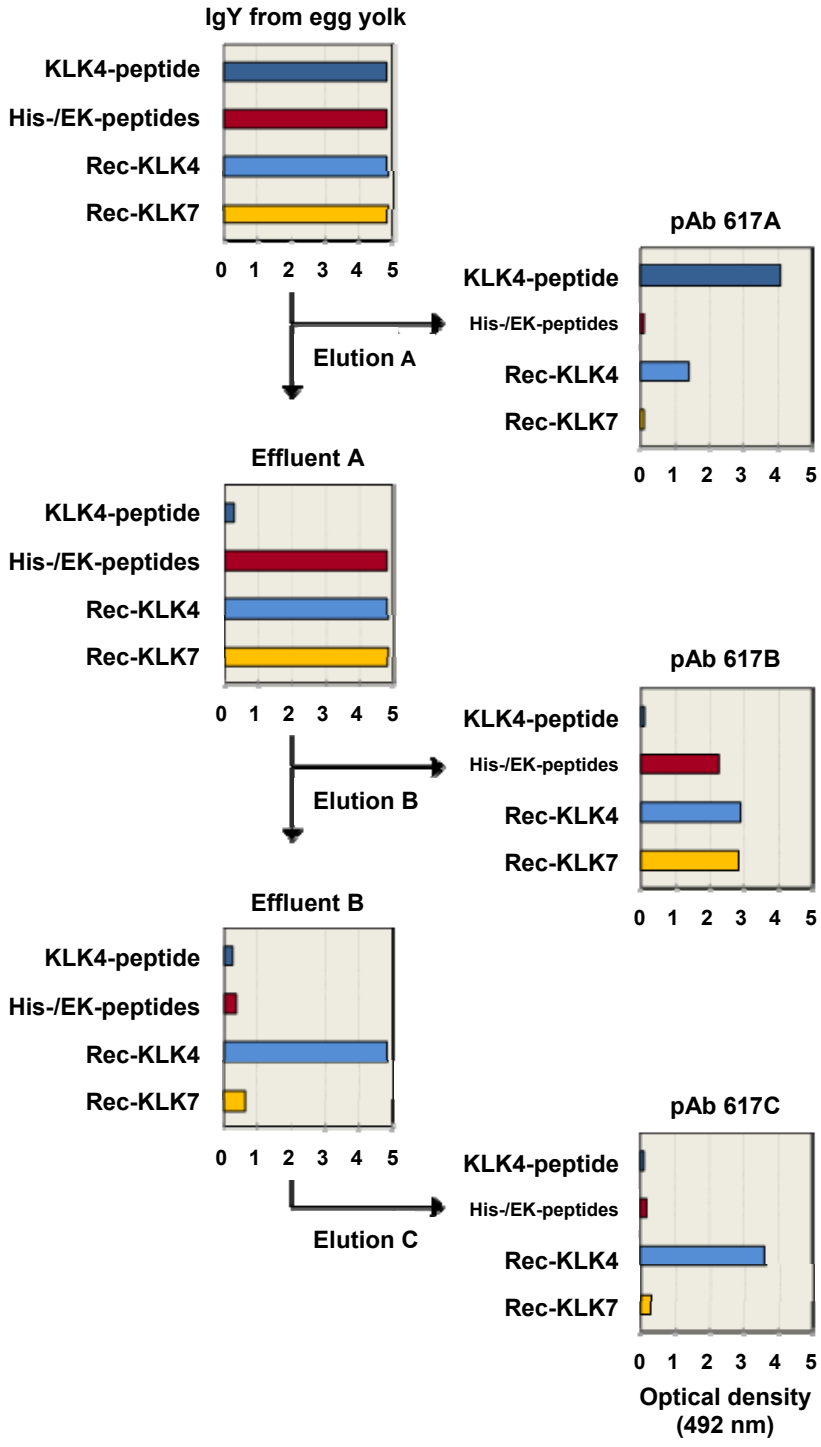

Figure 6: Characterization of purified antibody fractions 617A, B, and C by 'one-side' ELISA. Elution A (pAb 617A) reacted with both peptide $KLK4_{109–122}$ and rec-KLK4. Elution B (pAb 617B) contained antibodies reacting with rec-KLK4 and rec-KLK7 (both harboring the identical N-terminal extension of 17 amino acids), and with $(His)_6$-tag/EK peptides. Elution C (pAb 617C) only reacted with rec-KLK4 and not with the peptide $KLK4_{109–122}$, demonstrating that this fraction is completely depleted from antibodies directed against epitope 109-122 of KLK4.

4.3 Characterization of polyclonal antibodies directed to KLK6 by 'one-side' ELISA

Polyclonal antibodies directed to KLK6 were purified by affinity chromatography from citrated plasma of rabbit #623 (Figure 1). Analoguous to the testing of antibodies directed against KLK4, the reaction pattern of affinity-purified rabbit antibodies directed to KLK6 was first analyzed by 'one-side' ELISA assays. For this, microtiter plates were coated with the antigen (KLK6-derived peptide $KLK6_{109–119}$), the immunogen (rec-KLK6), and with control proteins/peptides such as rec-KLK7 and $(His)_6$-tag/EK peptides.

The eluate of the first affinity column (elution A) contained monospecific pAb 623A which strongly reacted with both the immunogen (rec-KLK6) and the peptide $KLK6_{109–119}$ used for affinity purification. No reaction was observed, neither with $(His)_6$-tag/EK peptides nor with rec-KLK7, which is carrying the identical N-terminal extension of 17 amino acids as rec-KLK6 (Figure 7). The elution of the second column, coupled with $(His)_6$-tag/EK peptides, yielded pAb 623B which was generated against the N-terminal, non-KLK-related sequences of rec-KLK6. Thus, pAb 623B did not react with the peptide epitope 109-119 located within the mature KLK6.
Finally, antibodies eluted from the third column (elution C, pAb 623C) distinctly reacted with the immunogen (rec-KLK6) but not with the KLK6-derived peptide $KLK6_{109–119}$ (Figure 7). It follows that the antibody fraction 623C is completely depleted from pAb 623A. In other words, pAb 623A and pAb 623C are directed against different epitopes of KLK6.

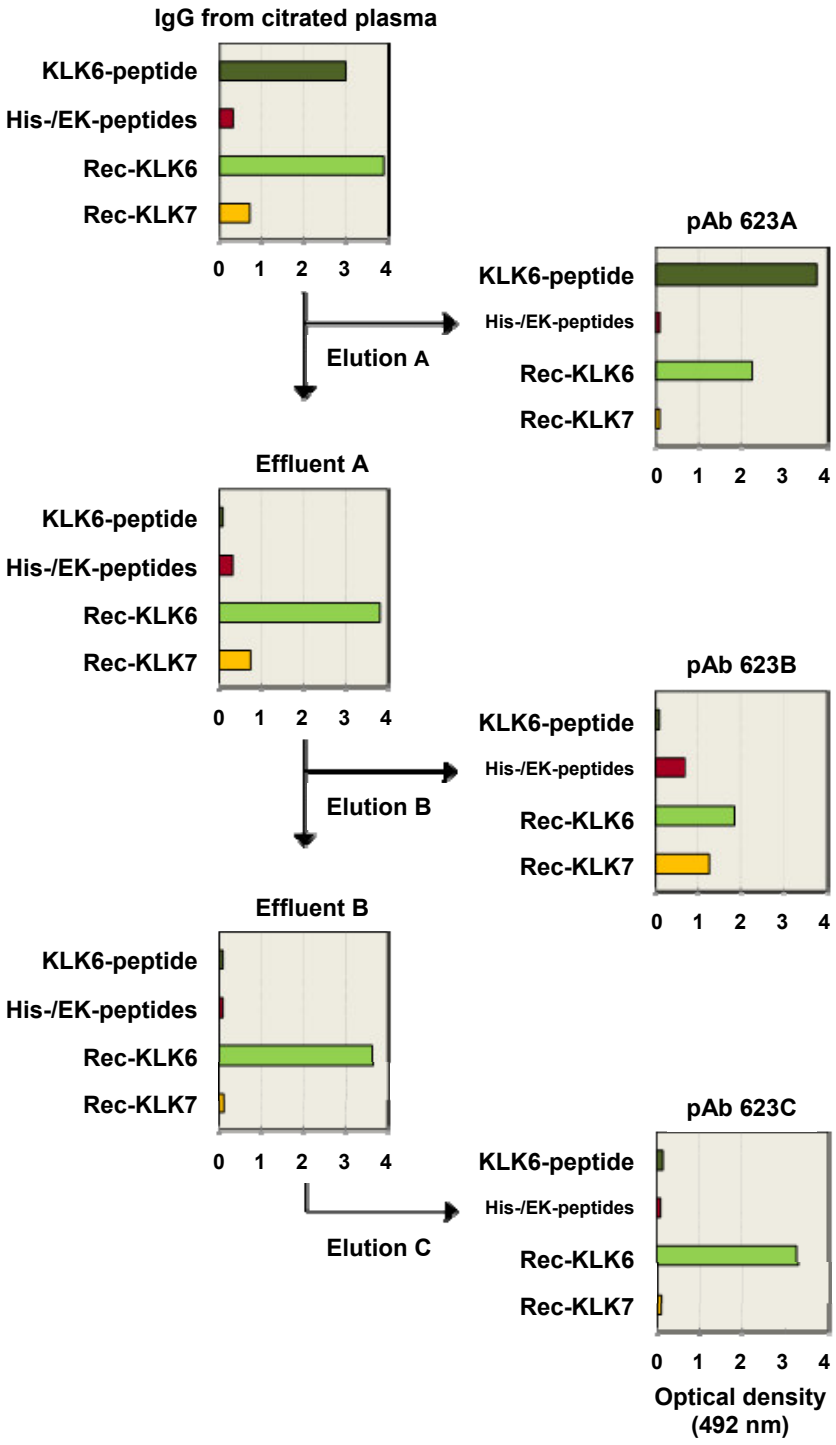

Figure 7: Characterization of purified antibody fractions 623A, B, and C by 'one-side' ELISA. Elution A (pAb 623A) reacted with both peptide $KLK6_{109–119}$ and rec-KLK6. Elution B (pAb 623B) contained antibodies reacting with rec-KLK6 and rec-KLK7 (both harboring the identical N-terminal extension of 17 amino acids), and with $(His)_6$-tag/EK peptides. Elution C (pAb 623C) only reacted with rec-KLK6 and not with the peptide $KLK6_{109–119}$, demonstrating that this fraction is completely depleted from antibodies directed against epitope 109-119 of KLK6.

4.4 Characterization of pAb 617A, C and pAb 623A, C by Western blot analyses

In Western blot analyses, pAb 617A and pAb 617C proved to be highly specific for KLK4 as there was no cross-reaction detected, neither with rec-proKLK2 (recombinant pro-form of KLK2, data not shown), rec-proKLK3, rec-proKLK5-15 nor with other His-/EK-tagged proteins (data not shown, Figure 8A). In addition, pAb 623A and pAb 623C were found to be highly specific for KLK6 since they merely reacted with rec-proKLK6 and did not react with rec-proKLK2 (data not shown), rec-proKLK3-5, or rec-proKLK7-15 (Figure 8A).

4.5 Specificity of pAb 623A analyzed by Western blot on the basis of KLK6 expression in the central nervous system

Human brain is known to express rather high amounts of KLK6 while skeletal muscle was reported to lack KLK6 expression (Shaw and Diamandis, 2007). For this reason, we used protein extracts from human brain as a positive control and extracts from skeletal muscle as a negative control to further characterize pAb 623A by Western blotting (Figure 8B).

In human brain protein extracts, we observed a strong and rather broad signal for KLK6 corresponding to a molecular weight of about 43 kDa. By contrast, the signal for (non-glycosylated) rec-KLK6 manifested at an apparent molecular weight of approximately 31 kDa. We reasoned that the higher molecular weight of KLK6 in brain protein extracts potentially results from glycosylation of the protease. In fact, previous studies investigating the structure and post-translational modifications of KLK6 in human breast and ovary as well as in ovarian cancer ascitic fluid and cerebrospinal fluid reported KLK6 to be N-glycosylated at asparagine-134 (Anisowicz *et al*., 1996; Kumanov *et al*., 2009). In skeletal muscle extracts, no KLK6 reaction was detected using pAb 623A in Western blot analysis (Figure 8B).

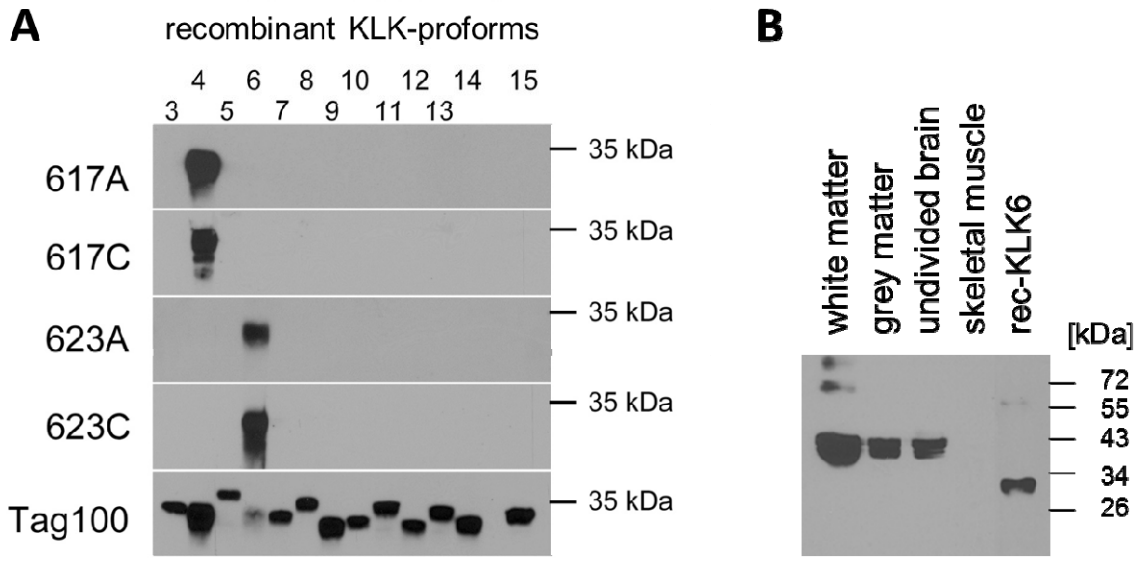

Figure 8: Specificity of polyclonal antibodies 617A, C and 623A, C as assessed by Western blot analyses.
(A) Recombinant pro-forms of KLK3-15 (~ 1 µg each) were subjected to 12% SDS-PAGE, blotted onto PVDF membranes and then probed with pAb 617A, pAb 617C, pAb 623A, or pAb 623C. Only rec-proKLK4 (with an apparent molecular weight of ~ 33 kDa) reacted with pAb 617A and pAb 617C. Polyclonal antibodies 623A and 623C only reacted with rec-proKLK6 (with an apparent molecular weight of ~ 31 kDa). Thus, no cross-reaction of the antibodies with other KLKs was observed. The transfer of the rec-proKLKs was verified by reaction with an antibody directed against the C-terminally located Tag100 epitope present in all recombinant proKLK proteins. **(B)** Glycosylated KLK6 was detected in brain protein extracts (~ 20 µg per lane) by pAb 623A. In contrast to non-glycosylated rec-KLK6, a higher molecular weight for KLK6 was found in protein extracts of the white matter, the grey matter, and the undivided brain. Skeletal muscle extract (~ 20 µg) was used as a negative control.

4.6 Immunohistochemical analyses of KLK4 expression in normal adult human tissues by pAb 617A and pAb 617C

To further analyze the specificity of antibody fractions 617A and 617C, conventional sections of various normal human tissues were investigated by immunohistochemistry using the polymer-based EnVision™ system (Dako). Using pAb 617A, a strong staining intensity was found in liver hepatocytes. By contrast, only moderate KLK4 immunoexpression in liver hepatocytes was detected by pAb 617C (Figure 9A and 10A). Distinct KLK4 immunostaining was

observed with both antibody fractions in renal tubular, but not in glomerula cells (Figure 9B and 10B). In prostate glands, moderate cytoplasmatic staining was observed with both antibodies (Figure 9C and 10C), whereas no KLK4 immunoreaction was found in intestinal crypts of the colon (Figure 9D and 10D).

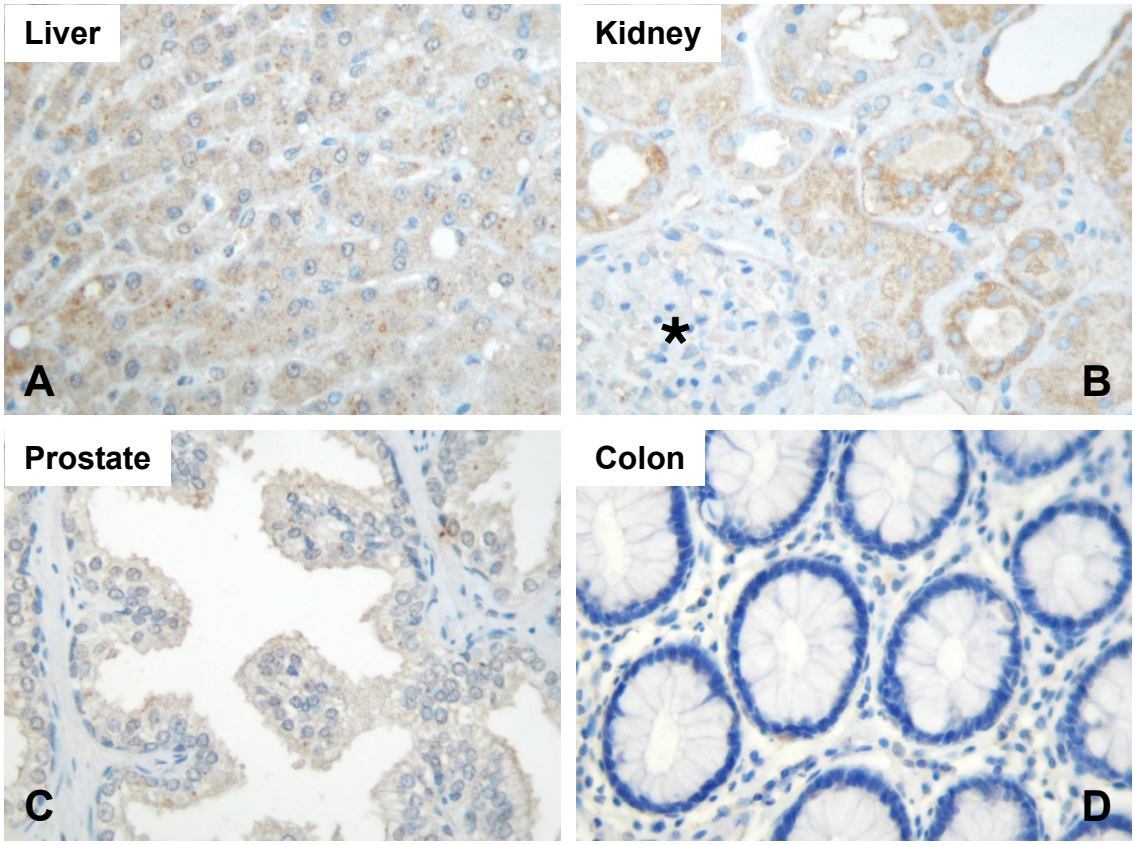

Figure 9: KLK4 immunoexpression in normal adult human tissues employing pAb 617A.
(A, B) KLK4 immunostaining is evident in both normal human liver and kidney tissue. Renal glomerula cells (marked with an asterisk) are not stained. **(C)** Moderate KLK4 expression was observed in the normal prostate tissue. **(D)** KLK4 was not detected in normal human colon tissue. Formalin-fixed, paraffin-embedded tissue sections were stained using the polymer-based EnVision™ system (Dako). Micrographs were taken with a Sony digital camera attached to a Zeiss AxioSkop microscope using the AxioVision software Release 4.6.3 (original magnification x400).

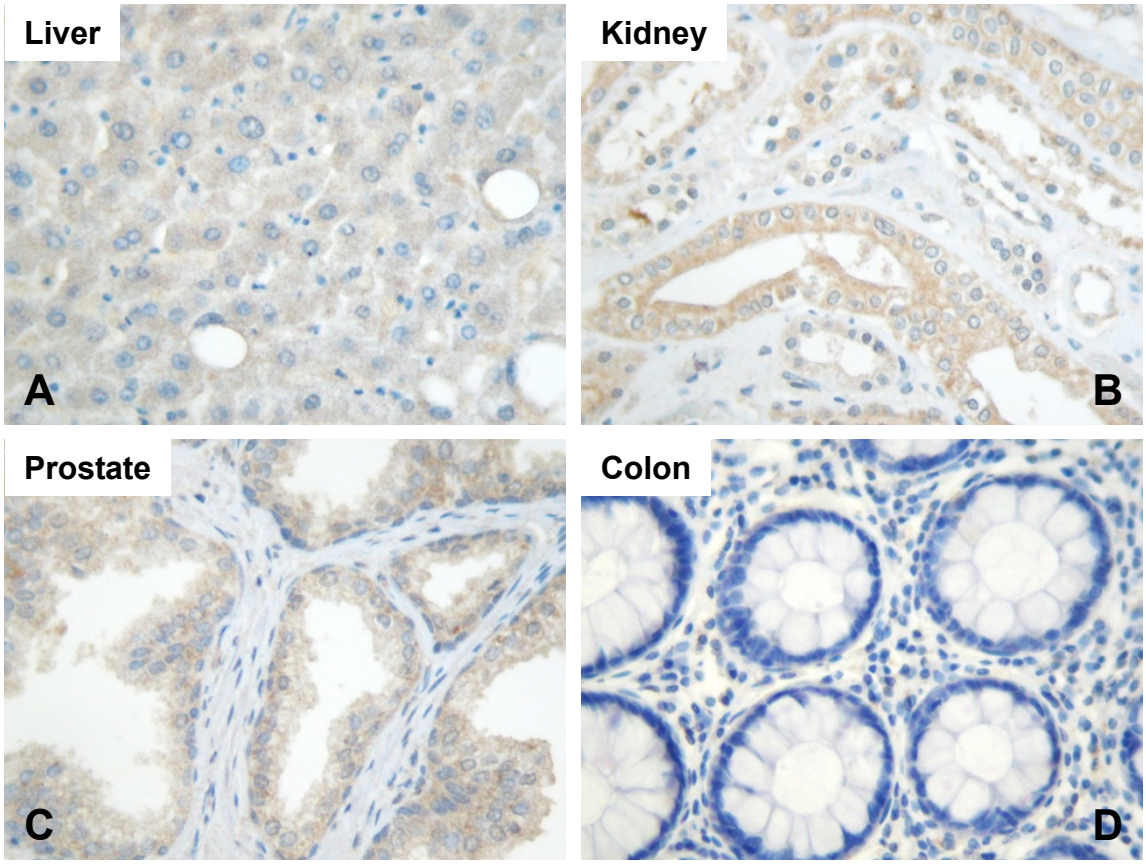

Figure 10: KLK4 immunoexpression in normal adult human tissues employing pAb 617C.
(A) Moderate KLK4 immunostaining was observed in normal adult liver tissue. **(B)** KLK4 was immunodetected with high frequency in normal kidney tubular cells. **(C)** Moderate KLK4 expression was found in normal prostate glands. **(D)** KLK4 was not detected in normal human colon tissue. Formalin-fixed, paraffin-embedded tissue sections were stained using the polymer-based EnVision™ system (Dako). Micrographs were taken with a Sony digital camera attached to a Zeiss AxioSkop microscope using the AxioVision software Release 4.6.3 (original magnification x400).

In addition to the analysis of representative conventional tissue sections using the EnVision™ peroxidase polymer system (Dako), both pAb 617A and pAb 617C were independently used along with the Vectastain® Elite ABC-kit (Vector Laboratories, Burlingame, CA, USA) to stain sections of a tissue microarray encompassing a variety of normal adult tissues. Interestingly, both antibody fractions, directed against different epitopes of KLK4, showed identical staining intensity and pattern in healthy adult tissues, irrespective of the immunohistochemical staining method applied (Figures 9, 10 and Table 2).

Table 2: Expression pattern of KLK4 in normal adult human tissues employing pAb 617A and pAb 617C. Sections of the TMA encompassing a variety of normal adult human tissues were stained using the Vectastain® Elite ABC-kit (Vector Laboratories).

	pAb 617A*	pAb 617C*
Uterus	–	–
Small intestine	–	–
Lung	–	–
Tonsil	–	–
Skeletal muscle	–	–
Cerebellum	–	–
Colon	–	–
Skin	–	–
Prostate gland	+	+
Liver	++	++
Kidney	++	++

***(* KLK4 expression**: **++**: strong; **+**: moderate; —: negative)*

4.7 Immunohistochemical analyses of KLK6 expression in normal adult human tissues by pAb 623A

In order to assess KLK6 protein expression in normal adult human tissues, representative conventional tissue sections were subjected to immunohistochemical analyses using pAb 623A along with the EnVision™ peroxidase polymer system (Dako). A strong KLK6 immunostaining was observed in the human brain (Figure 11A), whereas moderate KLK6 expression was found in the liver, kidney, and ovary (Figures 11B–D). In the normal pancreas and skeletal muscle (Figures 11E and 11F), KLK6 was not detected by pAb 623A. On top of the analysis of the above mentioned conventional tissue sections, pAb 623A was also employed to stain sections of a tissue microarray harboring additional normal adult human tissues, such as normal

breast, lung, skin, colon, and prostate (Table 3). The observed KLK6 expression pattern in normal adult human tissues proved to be perfectly in line with previous results obtained by determination of KLK6 antigen levels in adult tissue extracts applying a highly specific KLK6 ELISA (Shaw and Diamandis, 2007).

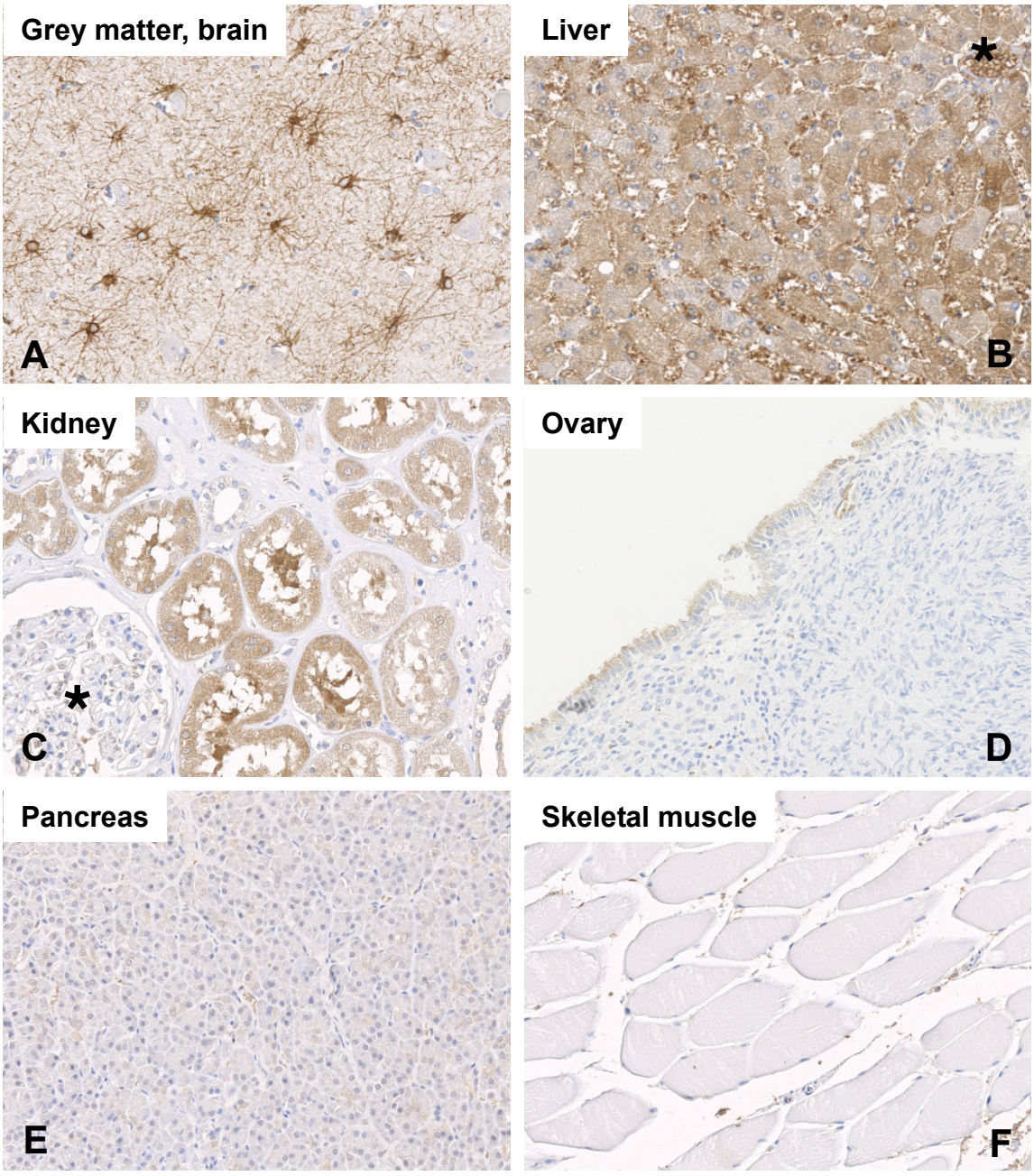

Figure 11: KLK6 immunoexpression in normal adult human tissues employing pAb 623A.
(A) In tissue of the central nervous system an intense KLK6 immunostaining was observed in astrocytes, which represent the most frequent glial cell type in grey matter. **(B)** KLK6 immunoexpression was found in normal adult liver as illustrated by a distinct, cytoplasmatic staining of hepatocytes. In addition, strong staining of erythrocytes was

observed within the hepatic venule (marked with an asterisk) as well as in the sinusoidal vasculature between the plates of hepatocytes. **(C)** Moderate KLK6 immunostaining was detected in proximal and distal convoluted tubules of the renal cortex. KLK6 expression was not observed in renal glomerula cells (marked with an asterisk). Micrograph **(D)** displays moderate, cytoplasmic KLK6 staining within the surface epithelium of the normal ovary consisting of a single layer of cuboidal to columnar cells. KLK6 was not detected in the underlying stroma harboring cells with round and spindle-shaped morphology, most of which are probably derived from cells of fibroblastic type. **(E, F)** There was no KLK6 immunoexpression in glandular cells of the exocrine pancreas or in skeletal muscle tissue. Formalin-fixed, paraffin-embedded tissue sections were stained using the polymer-based EnVision™ system (Dako). Slides were scanned with the digital slide scanner NanoZoomer-RS (Hamamatsu Photonics, Japan). Digital images were generated using the NDP.scan software 2.2.60 (original magnification x400).

Table 3: Expression pattern of KLK6 in normal adult human tissues employing pAb 623A. Sections of the TMA encompassing a variety of normal adult human tissues were stained using the polymer-based EnVision™ system (Dako).

	pAb 623A*
Skeletal muscle	–
Prostate	–
Colon	–
Pancreas	–
Kidney	+
Liver	+
Lung	+
Skin	+
Breast	+
Ovary	+
Brain	++

***(* KLK6 expression**: **++**: strong; **+**: moderate; —: negative)*

4.8 Immunohistochemical analyses of KLK6 expression in normal adult human tissues by pAb 623C

In analogy to the application of pAb 623A for immunohistochemical assessment of KLK6 expression in normal adult human tissues, pAb 623C was similarly used along with the EnVision™ peroxidase polymer system (Dako) to probe representative conventional sections of normal human tissues. However, in contrast to the immunohistochemical study using pAb 623A, KLK6 was not detected in the central nervous system or the ovary (Figures 12A and 12B) or any of the other normal adult human tissues examined (data not shown), when employing pAb 623C. Although both pAb 623A and pAb 623C were found to be highly specific for KLK6 in Western Blot analyses (Figure 8A), the antibody fraction 623C, which is completely depleted from pAb 623A (Figure 7), turned out to be not suitable for the detection of KLK6 protein expression by means of immunohistochemistry.

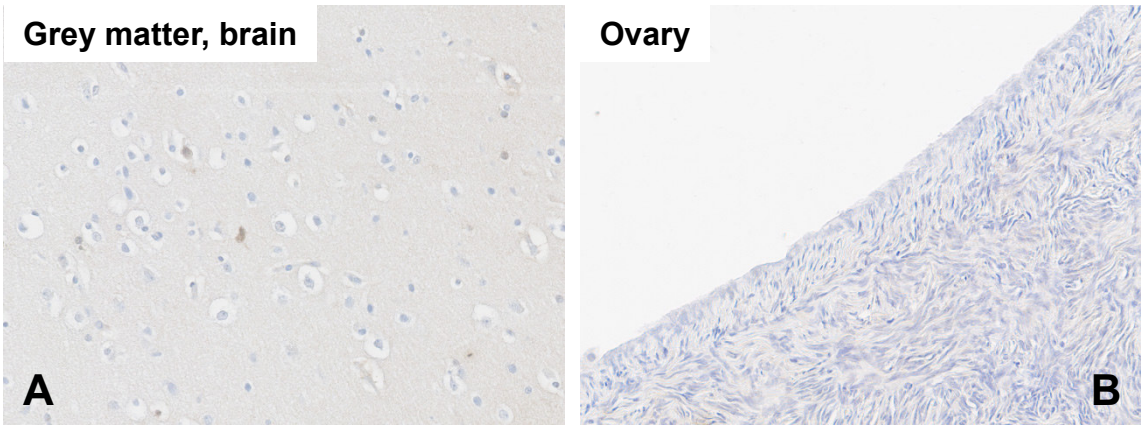

Figure 12: KLK6 immunoexpression in normal adult human tissues employing pAb 623C.
(A) In tissue of the central nervous system there was no KLK6 immunostaining in neurons or glial cells including astrocytes and oligodendrocytes (recognizable by a halo around the nucleus due to artefactual vacuolation in paraffin-embedded material). **(B)** KLK6 was not detected in the surface epithelium or the underlying stroma of the normal ovary by pAb 623C. Formalin-fixed, paraffin-embedded tissue sections were stained using the polymer-based EnVision™ system (Dako). Slides were scanned with the digital slide scanner NanoZoomer-RS (Hamamatsu Photonics, Japan). Digital images were generated using the NDP.scan software 2.2.60 (original magnification x400).

4.9 KLK4 expression in prostate cancer samples as assessed by pAb 617A and pAb 617C and its association with patients' clinicopathological parameters

In immunohistochemical analyses of normal human tissues including that of the prostate, both antibody fractions 617A and 617C were found to be suitable for the assessment of KLK4 expression by immunohistochemistry. Evidence for increased *KLK4* mRNA expression has been shown for prostate cancer suggesting that KLK4 may be involved in prostate carcinogenesis (Xi *et al*., 2004). To further elucidate the role of KLK4 in prostate cancer, conventional tissue sections of FFPE prostate cancer samples and sections of the prostate cancer TMA encompassing matched pairs of tumor tissue (Tu) and corresponding tumor-free tissue (Tf) of 44 prostate cancer patients were investigated by immunohistochemistry using both antibody fractions 617A and 617C along with the Vectastain® Elite ABC-kit (Vector Laboratories). Distinct KLK4 immunostaining was observed with both antibodies in malignant glandular epithelial cells, but not in the basal layer of surrounding normal tissue or fibromuscular stromal cells. Typically, an intense granular, cytoplasmic staining of cancer glands was observed. There was no nuclear staining detected with neither of the antibodies. Furthermore, in corresponding tumor-free areas, we found only weak KLK4 immunostaining in glandular luminal cells of non-malignant prostate glands (Figures 13 and 14). For estimation of KLK4 immunoreactivity, a semiquantitative score based on staining intensity and the percentage of KLK4-positive cancer cells (KLK4-Tu) as well as KLK4-positive glandular cells in tumor-free areas (KLK4-Tf) was applied.

When comparing KLK4 expression in tumor tissue (Tu) and tumor-free areas (Tf) by Spearman rank correlation (r_s), a strong, highly significant correlation was observed between pAb 617A and pAb 617C, both with regard to KLK4 expression in cancer cells (r_s=0.81, p<0.001) and non-malignant cells in tumor-free areas (r_s=0.83, p<0.001). For KLK4-Tu versus KLK4-Tf values, there was, however, a weaker correlation for both pAb 617A and pAb 617C (r_s=0.63, p<0.001 and r_s=0.33, p=0.026, respectively).

Furthermore, distinctly elevated KLK4 expression was observed in cancer cells compared to non-malignant cells in tumor-free areas. In the case of pAb 617A,

the mean score values were 0.43 (range 0–5.25) for KLK4-Tu versus 0.17 (range 0–2.0) for KLK4-Tf. Regarding pAb 617C, the mean values were 0.38 (range 0–6.0) for KLK4-Tu versus 0.01 (range 0–0.5) for KLK4-Tf (Figure 15).

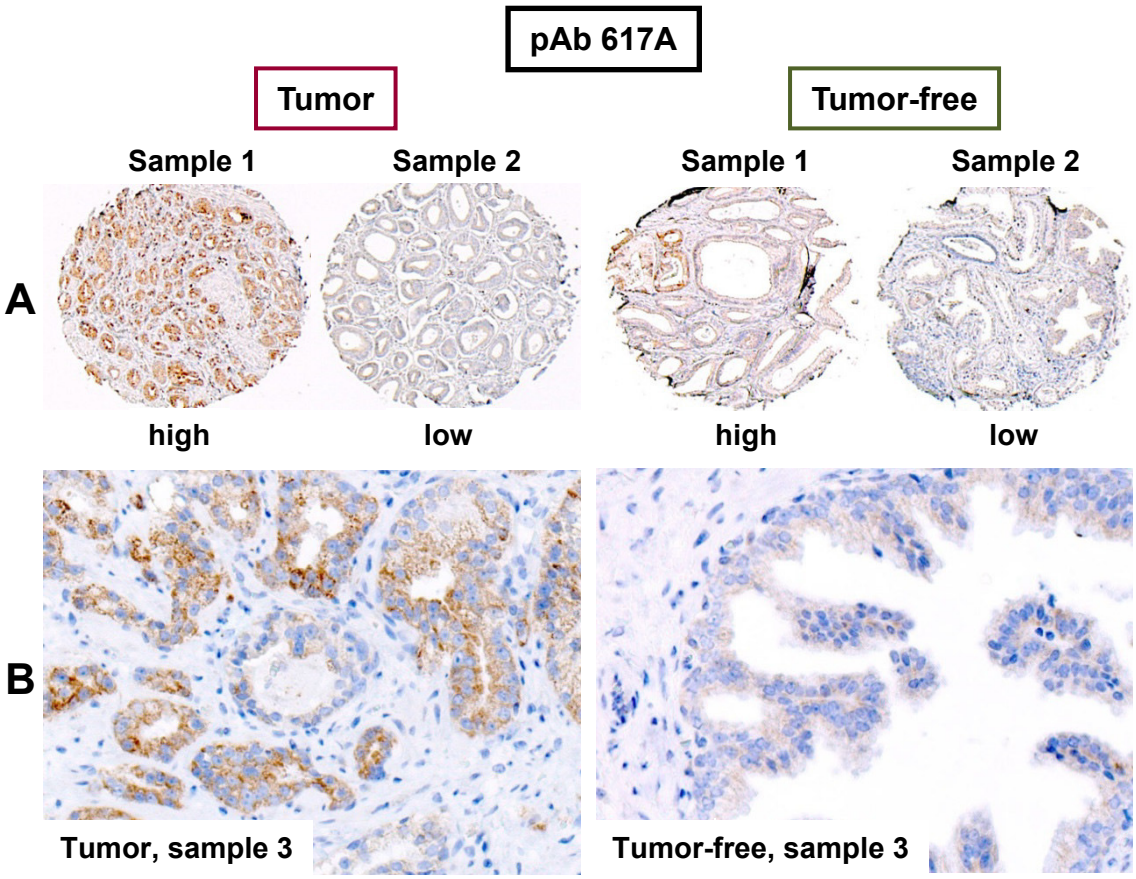

Figure 13: KLK4 expression in tumor tissues and corresponding tumor-free areas of prostate cancer specimens employing pAb 617A.
(A) Representative core punches within the prostate cancer TMA are shown illustrating different score values (original magnification x40). **(B)** Representative areas within a conventional prostate cancer tissue section at higher magnification (original magnification x200). Tissue microarray sections and conventional sections were stained using the Vectastain® Elite ABC-kit (Vector Laboratories). Micrographs were taken with a Sony digital camera attached to a Zeiss AxioSkop microscope using the AxioVision software Release 4.6.3.

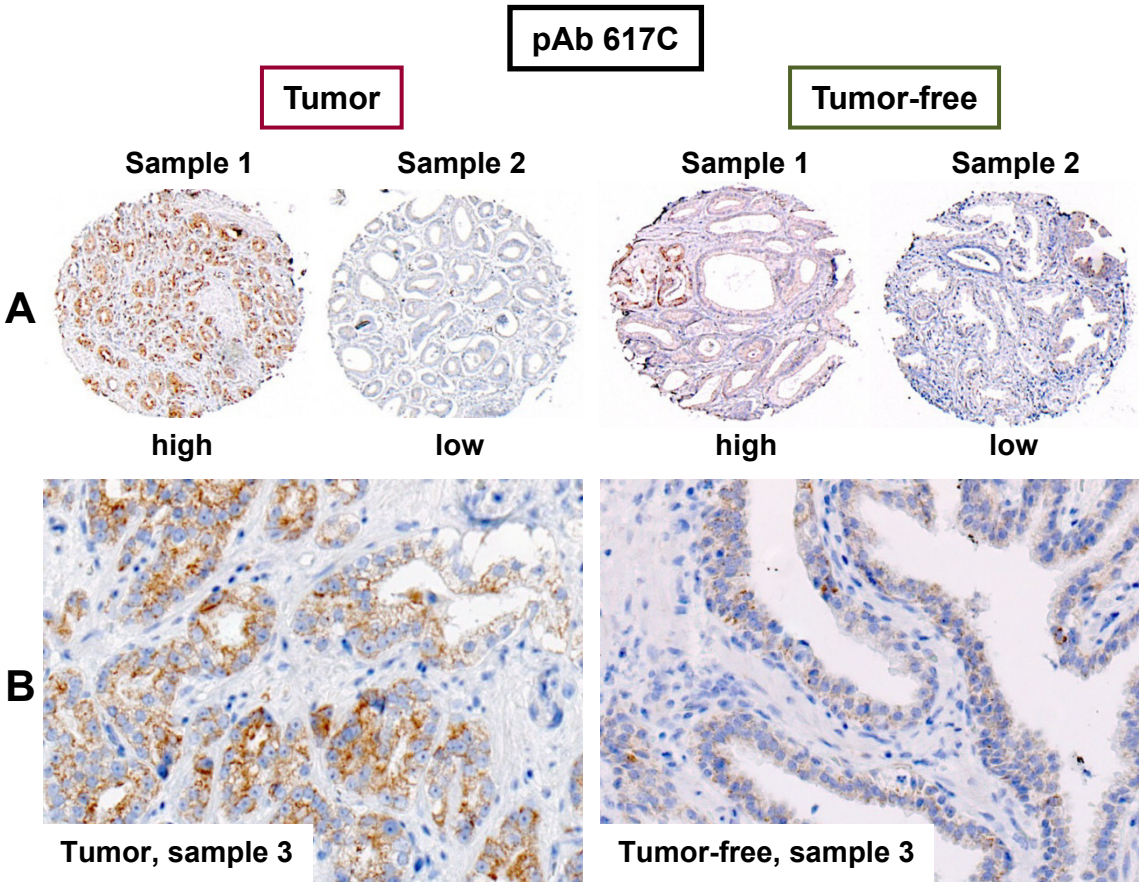

Figure 14: KLK4 expression in tumor tissues and corresponding tumor-free areas of prostate cancer specimens employing pAb 617C.
(A) Representative core punches within the prostate cancer TMA are shown illustrating different score values (original magnification x40). **(B)** Representative areas within a conventional prostate cancer tissue section at higher magnification (original magnification x200). Tissue microarray sections and conventional sections were stained using the Vectastain® Elite ABC-kit (Vector Laboratories). Micrographs were taken with a Sony digital camera attached to a Zeiss AxioSkop microscope using the AxioVision software Release 4.6.3.

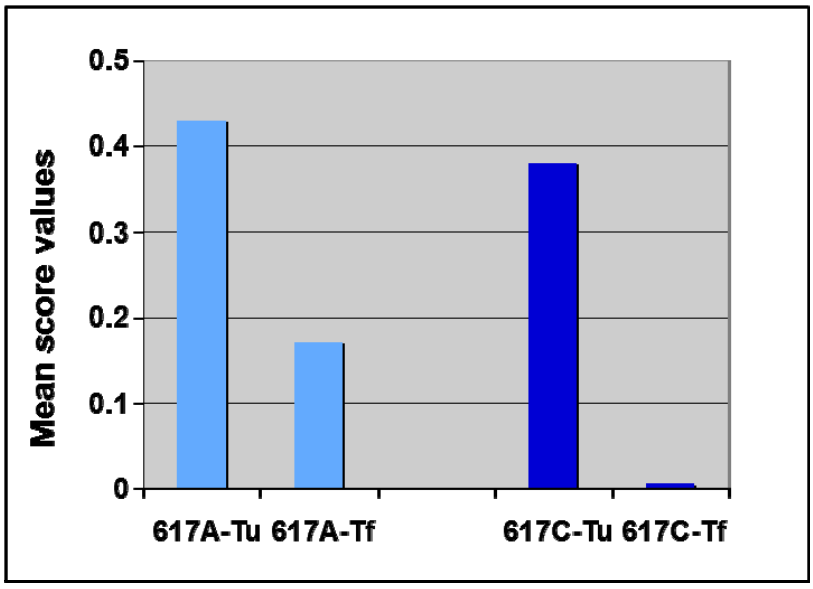

Figure 15: KLK4 expression in cancerous glandular epithelial cells (Tu) versus non-malignant cells in tumor-free areas (Tf). Mean score values for pAb 617A and pAb 617C are indicated in a bar chart. In the case of pAb 617A, the mean score values were 0.43 (617A-Tu, range 0–5.25) for cancer cells versus 0.17 (617A-Tf, range 0–2.0) for non-malignant cells in tumor-free areas. Regarding pAb 617C, the mean values were 0.38 (617C-Tu, range 0–6.0) for cancer cells versus 0.01 (617C-Tf, range 0–0.5) for non-malignant cells in tumor-free areas.

Immunohistochemical expression of KLK4 was analyzed for potential associations with patients' clinical parameters. The relationship between KLK4-Tu score values obtained with pAb 617A and pAb 617C and relevant clinicopathological characteristics of prostate cancer patients is summarized in Table 4. Interestingly, a significant association was observed between KLK4-Tu score values attained with pAb 617A and tumor stage, which is a strong prognostic indicator for prostate cancer patients. KLK4 expression was significantly lower in patients with stage pT3 and pT4 tumors, *i.e.*, non-organ confined disease, compared to patients with stage pT1 and pT2 tumors, *i.e.*, organ confined disease (Table 4 and see appendix). There was no significant relationship between KLK4-Tu score values obtained with pAb 617C and tumor stage. Furthermore, there was no significant association between KLK4-Tu and KLK4-Tf score values with any of the other clinicopathological parameters including preoperative PSA serum levels (Table 4 and data not shown).

Table 4: Association of KLK4-Tu score values obtained with pAb 617A and pAb 617C with clinicopathological parameters of prostate cancer patients (n=44).

Clinical/histomorpho-logical parameters	Patient numbers	KLK4-Tu pAb 617A[a]	KLK4-Tu pAb 617C[a]
Total	44	0.43	0.38
Nodal status [b]		*p* = 0.683	*p* = 0.120
Negative	37	0.48	0.45
Positive	5	0.20	0
Grading [c]		*p*=0.572	*p*=0.912
Grade I	8	0.34	0.34
Grade II	17	0.65	0.57
Grade III	9	0.31	0.22
Gleason score [c]		*p*=0.455	*p*=0.459
Low (2-6)	15	0.42	0.33
Intermediate (7)	17	0.56	0.57
High (8+9)	12	0.25	0.17
Tumor stage [b]		***p = 0.005***	*p* = 0.139
T1+2	25	0.68	0.54
T3+4	19	0.09	0.17

[a] Mean score values. [b] Mann-Whitney test. [c] Kruskal-Wallis test.
The number of cases does not always add up to 44 due to missing clinical data.
Statistically significant data ($p \leq 0.05$) are indicated in boldface.

4.10 Expression pattern of KLK6 in ovarian cancer tissue and its association with clinical and histomorphological parameters

There is a growing number of evidence suggesting that KLK6 is playing a crucial role in tumor growth and disease progression in ovarian cancer patients (Bayani and Diamandis, 2011). In order to assess KLK6 protein expression in ovarian cancer by immunohistochemistry and to evaluate its impact on patients' disease-free survival, tumor tissue specimens of 118 ovarian cancer patients, represented on seven tissue microarrays, were investigated using pAb 623A along with the EnVision™ peroxidase polymer system (Dako). In the majority of cases, distinct cytoplasmic KLK6 immunostaining was observed in malignant epithelial cancer cells and also, with lower frequency, in surrounding stromal cells. Based on classical morphological features, these cells most probably

represent (myo-)fibroblasts and tissue macrophages (Figure 16). For estimation of KLK6 immunoreactivity, the Remmele score (Table 1), which is a semiquantitative score ranging from 0 (negative) to 12 (strongly positive), based on KLK6 staining intensity and the percentage of KLK6-positive cancer cells (KLK6-Tc) and KLK6-positive stromal cells (KLK6-Sc), respectively, was applied.

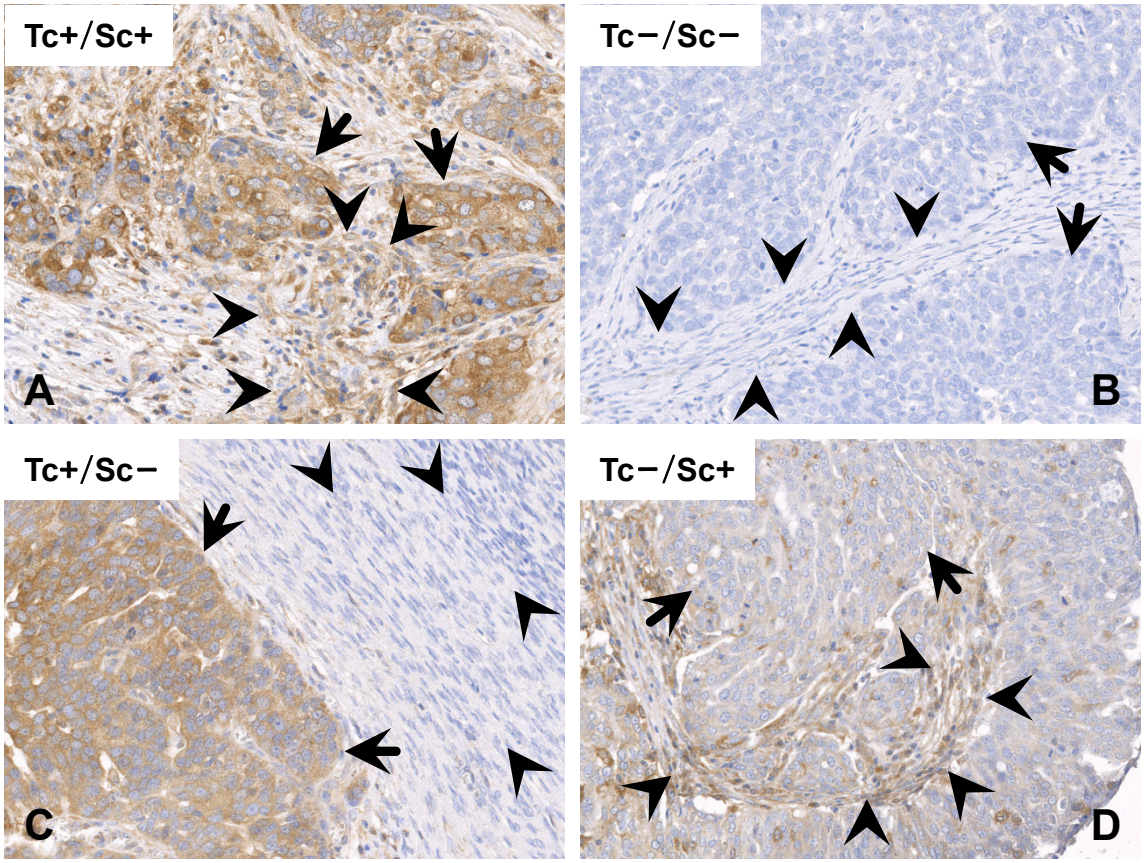

Figure 16: KLK6 expression in tumor tissue of ovarian cancer tissue specimens employing pAb 623A.
Micrographs **(A–D)** illustrate representative core punches corresponding to high (+) or low (-) KLK6 immunoexpression levels in tumor cells (Tc) and stromal cells (Sc), respectively. Arrows indicate staining of tumor cells, stromal cells are marked by arrowheads. Sections of seven ovarian cancer tissue microarrays were stained using the polymer-based EnVision™ system (Dako). Slides were scanned with the digital slide scanner NanoZoomer-RS (Hamamatsu Photonics, Japan). Digital images were generated using the NDP.scan software 2.2.60 (original magnification x400).

Using Spearman rank correlation analysis (r_s), we found a moderate, but significant correlation between KLK6-Tc and KLK6-Sc score values (r_s=0.53, p<0.001). Distinctly elevated KLK6 expression was observed in cancer cells versus stromal cells in tumor tissue, resulting in a clearly higher mean immunoreactivity score (IRS) value for KLK6-Tc (3.81) compared to the mean IRS value for KLK6-Sc (0.79). The frequency of immunoreactivity scores greater than zero was much higher for cancer cells compared to stromal cells (KLK6-Tc > 0: 90 cases vs. KLK6-Tc = 0: 28 cases; KLK6-Sc > 0: 24 cases vs. KLK6-Sc = 0: 93 cases; Table 5). For all statistical analyses, the median IRS values for both KLK6-Tc (median IRS = 4) and KLK6-Sc (median IRS = 0) were chosen to classify immunohistochemical KLK6 expression as high or low (Table 5).

Table 5: Frequency of KLK6-positive cancer cells and KLK6-positive stromal cells among ovarian cancer specimens and subdivision of ovarian cancer specimens according to median immunoreactivity score values.

	KLK6-Tc [a] (KLK6-positive cancer cells)		KLK6-Sc [b] (KLK6-positive stromal cells)	
Mean IRS	**3.81**		**0.79**	
IRS > 0	90 cases		24 cases	
IRS = 0	28 cases		93 cases	
Median IRS	**4**		**0**	
High expression level	IRS > 4	34 cases	IRS > 0	24 cases
Low expression level	IRS ≤ 4	84 cases	IRS = 0	93 cases
	[a] No. of cases n = 118.		**[b] No. of cases n = 117.**	

The relationship of KLK6 immunoreactivity score values with relevant clinical and histomorphological parameters of ovarian cancer patients is summarized in Table 6. A significant association was observed between high KLK6-Sc score values and poorly differentiated tumors (nuclear grade G3 vs. G1/2) as well as the presence of affected lymph nodes (p=0.028 and p=0.020, respectively). Otherwise, there was no significant association of KLK6-Sc score values with

other clinical and histomorphological parameters. Regarding KLK6-Tc score values, KLK6 immunoexpression did not differ significantly between tumors in relation to any of the clinical or histomorphological parameters.

Table 6: Association of clinical and histomorphological characteristics of ovarian cancer patients (n=118) with KLK6 immunoexpression in tumor tissue-associated cancer cells versus stromal cells.

Clinical/histomorpho-logical parameters	Patient numbers	KLK6-Tc low/high	KLK6-Sc [a] low/high
Total	118	84/34	93/24
Age		$p = 0.291$	$p = 0.791$
≤ 60 years	71	48/23	57/14
> 60 years	47	36/11	36/10
FIGO stage		$p = 0.141$	$p = 0.275$
I + II	24	20/4	21/3
III + IV	94	64/30	72/21
Nuclear grade		$p = 0.966$	***p = 0.028***
G1 + G2	42	30/12	38/4
G3	76	54/22	55/20
Residual tumor mass [b]		$p = 0.113$	$p = 0.276$
0 cm	61	47/14	50/10
> 0 cm	52	33/19	39/13
Ascitic fluid volume [b]		$p = 0.423$	$p = 0.512$
≤ 500 ml	74	54/20	59/14
> 500 ml	41	27/14	31/10
Lymph nodes involved [b]		$p = 0.201$	***p = 0.020***
No	43	34/9	38/4
Yes	52	35/17	37/15
Response to CT [b]		$p = 0.945$	$p = 0.746$
No	17	12/5	13/4
Yes	76	53/23	60/15

Chi-square test (cut-off point: median score values).
[a] No. of cases n = 117.
[b] The number of cases does not add up to 118 due to missing clinical data.
CT: chemotherapy.
Statistically significant data ($p \leq 0.05$) are indicated in boldface.

4.11 Association of KLK6 expression and clinical/ histomorphological parameters with patients' survival

The association of clinical/histomorphological parameters and of KLK6 immunoexpression with patients' outcome defined by progression-free survival (PFS) and overall survival (OS) is summarized in Table 7. In univariate Cox regression analysis, all established clinical and histomorphological variables, such as age, FIGO stage, nuclear grade, residual tumor mass, and ascitic fluid volume were predictors for OS in the ovarian cancer cohort. Likewise, in univariate analysis, all of the clinical and histomorphological parameters reached statistical significance with respect to PFS (Table 7).

Moreover, in univariate Cox regression analysis, we found a significant association between high KLK6-Sc score values in tumor tissue and an increased risk of death (HR: 1.80; 95% CI, 1.08–2.99; p=0.024) and a trend toward statistical significance for the correlation of high KLK6-Sc score values with tumor progression (HR: 1.68; 95% CI, 0.97–2.92; p=0.066). In case of KLK6-positive cancer cells, high KLK6-Tc score values were marginal, but significantly related with shorter PFS, whereas there was a trend only for OS (association with PFS: HR: 1.68; 95% CI, 1.02–2.76; p=0.042; association with OS: HR: 1.51; 95% CI, 0.95–2.39; p=0.080; Table 7). These findings were confirmed by Kaplan-Meier estimation. The association of KLK6-Tc and KLK6-Sc expression levels with OS and PFS is displayed by the respective survival curves (Figure 17).

Table 7: Univariate Cox regression analysis of the association of clinical/ histomorphological parameters and KLK6 immunoexpression, respectively, with survival in ovarian cancer patients (n=118).

Factor	No. cases	Overall survival		Progression-free survival	
		HR (95% CI) [a]	*p*	HR (95% CI) [a]	*p*
Total	118				
Age					
≤ 60 years	71	1		1	
> 60 years	47	1.76 (1.14-2.72)	***0.011***	1.67 (1.03-2.69)	***0.036***
FIGO stage					
I + II	24	1		1	
III + IV	94	6.12 (2.64-14.1)	***<0.001***	10.4 (3.25-33.3)	***<0.001***
Nuclear grade					
G1 + G2	42	1		1	
G3	76	2.02 (1.24-3.28)	***0.005***	1.80 (1.06-3.07)	***0.030***
Residual tumor mass [d]					
0 mm	61	1		1	
> 0 mm	52	5.74 (3.51-9.40)	***<0.001***	5.50 (3.24-9.32)	***<0.001***
Ascitic fluid volume [d]					
≤ 500 ml	74	1		1	
> 500 ml	41	3.69 (2.35-5.80)	***<0.001***	3.29 (1.99-5.43)	***<0.001***
KLK6-Tc [b]					
Low	84	1		1	
High	34	1.51 (0.95-2.39)	0.080	1.68 (1.02-2.76)	**0.042**
KLK6-Sc [b, c]					
Low	93	1		1	
High	24	1.80 (1.08-2.99)	***0.024***	1.68 (0.97-2.92)	0.066

[a] HR: hazard ratio (95% confidence interval) of univariate Cox regression analysis.
[b] Dichotomized in high and low levels by the median immunoreactivity score values.
[c] No. of cases n=117.
[d] The number of cases does not add up to 118 due to missing clinical data.
Statistically significant data ($p \leq 0.05$) are indicated in boldface.

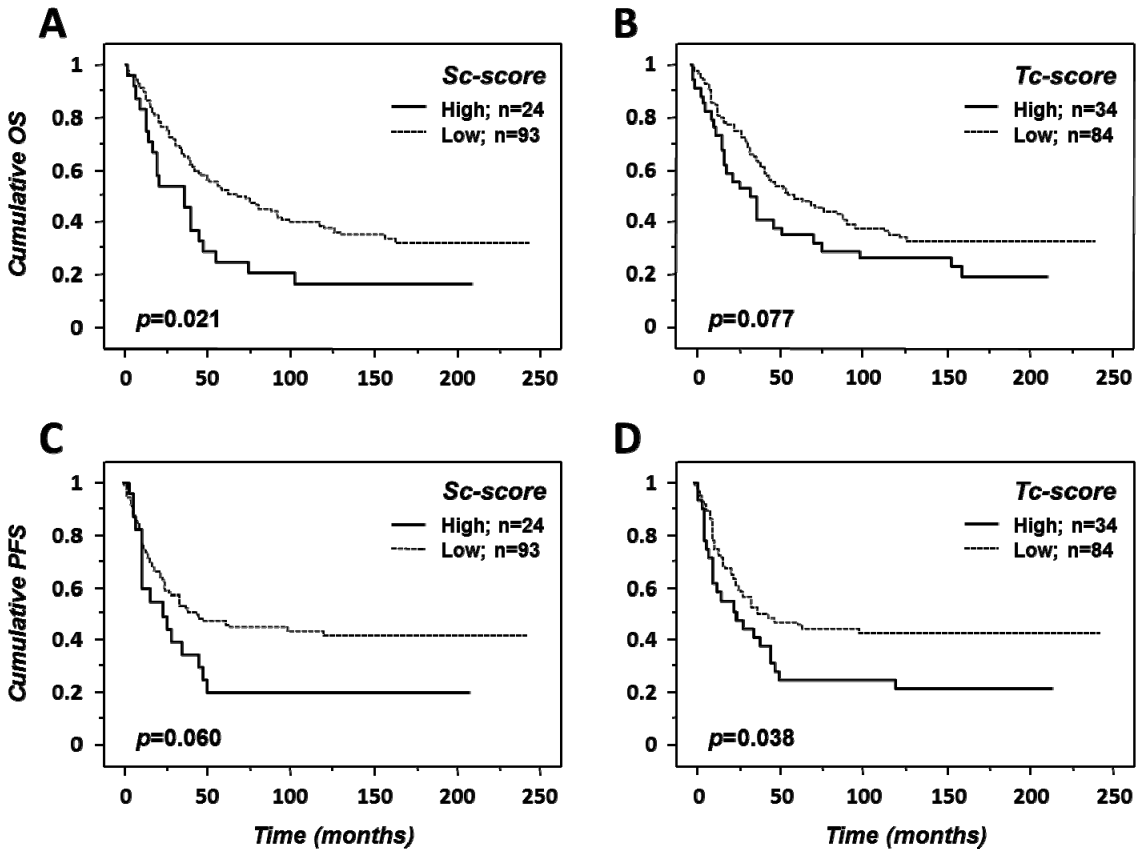

Figure 17: Probability of overall survival and progression-free survival of ovarian cancer patients with regard to KLK6 immunoexpression as assessed by pAb 623A.

(A, B) OS and **(C, D)** PFS probability curves were generated by Kaplan-Meier analysis using log-rank tests to search for differences. Patients were divided into groups with low or high KLK6 immunoexpression in **(A, C)** stromal cells and **(B, D)** cancer cells using the median immunoreactivity score values (KLK6-Sc: IRS = 0 vs. IRS > 0; KLK6-Tc: IRS ≤ 4 vs. IRS > 4).

Strikingly, in multivariate Cox regression analysis, KLK6-Sc score values were significantly associated with poor OS, *i.e.*, ovarian cancer patients with high KLK6-Sc immunoexpression in tumor tissue had a significantly, nearly twofold, higher risk of death (HR: 1.92; 95% CI, 1.12–3.27; p=0.017) as compared to patients who displayed low KLK6-Sc expression levels (Table 8).

Although displaying only a trend in univariate analysis, patients with high KLK6-Sc score values turned out to have a nearly twofold higher risk of disease progression in multivariate analysis (HR: 1.80; 95% CI, 1.02–3.19; p=0.042; Table 8).

Table 8: Multivariate Cox regression analysis of the association of clinical/ histomorphological parameters and KLK6 immunoexpression, respectively, with survival in ovarian cancer patients (n=110).

Factor	No. cases	Overall survival		Progression-free survival	
		HR (95% CI) [a]	*p*	HR (95% CI) [a]	*p*
Total	110				
FIGO stage					
I + II	21	1		1	
III + IV	89	3.13 (1.18-8.26)	***0.021***	4.96 (1.47-16.7)	***0.010***
Nuclear grade					
G1 + G2	38	1		1	
G3	72	1.28 (0.76-2.15)	0.350	0.95 (0.54-1.68)	0.868
Residual tumor mass					
0 mm	60	1		1	
> 0 mm	50	3.32 (1.73-6.39)	***<0.001***	3.21 (1.64-6.26)	***<0.001***
Ascitic fluid volume					
≤ 500 ml	73	1		1	
> 500 ml	37	1.27 (0.71-2.33)	0.406	1.31 (0.70-2.47)	0.392
KLK6-Tc [b]					
Low	77	1		1	
High	33	1.18 (0.73-1.91)	0.507	1.26 (0.75-2.10)	0.387
KLK6-Sc [b, c]					
Low	86	1		1	
High	23	1.92 (1.12-3.27)	***0.017***	1.80 (1.02-3.19)	***0.042***

[a] HR: hazard ratio (95% confidence interval) of multivariate Cox regression analysis. Biological markers were separately added to the base model of clinical parameters: FIGO stage, nuclear grade, residual tumor mass, and ascitic fluid volume.
[b] Dichotomized in high and low levels by the median immunoreactivity score values.
[c] No. of cases n=109.
Statistically significant data ($p \leq 0.05$) are indicated in boldface.

On the contrary, in multivariate analysis, KLK6 immunoexpression in cancer cells (KLK6-Tc) was not significantly related with OS or PFS of ovarian cancer patients (Table 8). Finally, concerning the clinical parameters, in multivariate Cox regression analysis, residual tumor mass and FIGO stage remained strong, statistically significant parameters for both OS and PFS. All other clinical and histomorphological markers analyzed lost significance for OS and PFS in multivariate analysis (Table 8).

5. Discussion

5.1 Concept of antibody generation and purification

In the past years, a prokaryotic expression system in *Escherichia coli* cells, allowing the recombinant expression and subsequent purification of synthetic enzyme forms of several human KLKs was established in our laboratory. After refolding and removal of the non-natural pro-peptide by enterokinase (EK), the crystal structures of mature KLKs, including KLK4 and KLK6 (Debela *et al*., 2006a, b; Debela *et al*., 2008), were resolved by us. In order to generate polyclonal antibodies in chickens and rabbits, purified and refolded human recombinant KLK4 and KLK6, both carrying an N-terminal extension of 17 amino acids encompassing a $(His)_6$-tag and an EK cleavage site (MRGSHHHHHHGSDDDDK), were employed.

The injection of a folded (native) antigen usually triggers the generation of antibodies directed against conformational epitopes, *i.e.,* the binding sites of these antibodies are defined by the three-dimensional structure of the antigen, which in turn can be formed by non-continuous peptide sequences. Such antibodies could be very useful for ELISA or FACS analyses of cell extracts and living cells, by which antigens are detected in their native (conformational) form. However, for other applications, in which the antigens are partly denatured, e.g., in immunohistochemistry or Western blot analyses, it is more favorable to employ antibodies directed against linear epitopes of the antigen. Therefore, short peptide sequences derived from the target protein are often used to generate peptide-directed antibodies (Harvey *et al*., 2003). Otherwise, it can be assumed that among the polyclonal antibodies raised against the (refolded) immunogens rec-KLK4 and rec-KLK6, there will be fractions of antibodies directed against such linear peptide sequences. Thus, based on the X-ray structures of KLK4 and KLK6 (Bernett *et al*., 2002; Debela *et al*., 2006a, b), short surface-exposed sequences that are not involved in secondary structures (α-helices or β-sheets) were searched for by us. Among the existing surface-exposed amino acid sequences the peptides $KLK4_{109–122}$ (encompassing amino acids 109–122 of KLK4) and $KLK6_{109–119}$ (encompassing amino acids 109–119

of KLK6) were selected. Importantly, these peptides constitute regions within KLK4 and KLK6 that are not highly conserved among the other members of the KLK family (Goettig *et al*., 2010), thus minimizing the risk of cross-reaction with these otherwise highly homologous proteins (Figure 5).

Using the synthetic peptide $KLK4_{109–122}$ and rec-KLK4 for affinity chromatography, we were able to isolate monospecific polyclonal antibodies, namely pAb 617A, directed against the sequence $KLK4_{109–122}$, as well as pAb 617C, directed against epitopes residing in the other parts of the mature KLK4 protein. In other words, the two antibody fractions, pAb 617A and pAb 617C, were found to be clearly directed against different epitopes of the mature KLK4 protein (Figure 6). Likewise, we isolated monospecific polyclonal antibodies directed against KLK6 by employing the peptide $KLK6_{109–119}$ as well as rec-KLK6 for affinity chromatography. The antibody fraction 623A reacted with both the peptide $KLK6_{109–119}$ and the full-length rec-KLK6, whereas pAb 623C only reacted with rec-KLK6 and was completely depleted from antibodies directed against the peptide $KLK6_{109–119}$ (Figure 7).

5.2 Validation of pAb 617A and pAb 617C regarding their suitability for the detection of KLK4 in prostate cancer

The specificity of antibody fractions 617A and 617C was first tested in Western blot analyses concerning cross-reaction with other members of the KLK family. KLK4 was reported to exhibit a minimum of 37% (versus KLK10) and a maximum of 52% (versus KLK5) identical amino acids at homologous positions within the KLK family (Lundwall and Brattsand, 2008). For the recombinant pro-forms of KLK2 to KLK15, no cross-reaction was detected with neither of the antibodies (Figure 8A).

Shortly after the *KLK4* gene had been identified as the fourth member within the human *KLK* gene family locus on chromosome 19 (Stephenson *et al*., 1999), initially, KLK4 expression was detected in hormonally responsive normal and neoplastic prostate epithelial tissues only (Nelson *et al*., 1999). Owing to this apparently prostate-restricted expression pattern, it therefore became generally known by the name prostase. However, subsequent studies could not confirm

KLK4 expression being limited to the prostate only. In independent research work on tooth formation, the enamel matrix serine protease 1 (EMSP1) was identified in the porcine enamel matrix (Simmer *et al*., 1998) and then later on it was shown to play an important role in the process of enamel maturation (Simmer *et al*., 2009). Human EMSP1 turned out to be identical with KLK4 (Simmer and Bartlett, 2004).

KLK4 has been detected in a large panel of normal adult human tissues including the prostate, liver, breast, skin, and brain (Obiezu *et al*., 2005). In our work, immunohistochemical stainings with the two antibody fractions 617A and 617C, which were independently used in comparative immunohistochemical analyses of normal adult human tissues, resulted in identical staining patterns and intensities. We observed high KLK4 immunoreactivity in liver hepatocytes and renal tubular cells as well as moderate staining intensity in the normal prostate (Figures 9 and 10, Table 2), which is in agreement with previously reported data (Shaw and Diamandis, 2007). With regard to the absence of staining in normal colon, lung, skin, and tonsil tissue (Figures 9 and 10, Table 2), our results likewise proved to be consistent with findings obtained from analyses of normal adult tissue extracts by ELISA (Shaw and Diamandis, 2007). These findings strongly indicate that the two antibody fractions 617A and 617C, directed against different epitopes of KLK4, specifically detect KLK4 in various normal human tissues including the normal human prostate and that these antibodies are suitable for the detection of KLK4 in prostate cancer samples.

5.3 Validation of pAb 623A and pAb 623C regarding their suitability for the detection of KLK6 in ovarian cancer

KLK6 is known to possess a minimum of 41% (versus KLK10) and a maximum of 53% (versus KLK13) identical amino acids at homologous positions within the KLK family (Lundwall and Brattsand, 2008). In analogy to the testing of antibody fractions 617A and 617C against KLK4, both pAb 623A and pAb 623C were first examined by Western blot analyses. In fact, for all of the recombinant pro-forms of KLK2 to KLK15, no cross-reaction was observed with neither of the antibodies (Figure 8A). In previous studies, KLK6 expression has been

investigated in normal human tissues at the mRNA and the protein level by highly specific PCR and ELISA assays (Harvey *et al*., 2000; Shaw and Diamandis, 2007). The highest KLK6 expression was reported for the CNS, followed by kidney, breast, ovary, and skin tissue. By comparison, normal adult human tissues of the liver, lung, heart, and spleen showed low KLK6 expression levels, whereas in the colon, skeletal muscle, prostate, and pancreas KLK6 expression was not detected. Using pAb 623A to assess KLK6 expression in normal human tissues by immunohistochemistry (Figure 11, Table 3), we observed a very similar staining pattern to that described by Shaw and Diamandis (2007).

However, using pAb 623C for immunohistochemical stainings of healthy adult human tissues, KLK6 expression could not be detected at all (Figure 12). Although pAb 623C appeared to be highly specific for KLK6 in Western Blot analyses, it turned out to be not suitable for the detection of KLK6 by IHC in formalin-fixed, paraffin-embedded tissue sections. One possible explanation for this is that KLK6 might be undergoing extensive conformational changes during the process of tissue preparation including formalin fixation, dehydration in ethanol, and paraffin embedding. In addition, it is also conceivable that KLK6 is completely denatured during another process of tissue pretreatment before immunohistochemical staining including dewaxing, rehydration in ethanol, and heat-induced antigen retrieval.

Formalin fixation is known to cause conformational changes of protein epitopes. Rait and coworkers (2004) observed development of extensive intra- and intermolecular cross-links (methylene bridges) under prolonged formalin treatment of bovine pancreatic ribonuclease A (RNAse A), which limited the recognition of RNAse A by a polyclonal antibody. In order to restore the immunoreactivity of RNAse A, reversal of these cross-links through high temperature treatment was necessary. The effect of formalin fixation and high-temperature incubation on the tertiary protein structure has also been investigated by Fowler *et al.* (2011). For some proteins formalin fixation left the native protein conformation unaltered, whereas for others, formalin-induced changes in secondary structures (e.g. increase in the β-sheet content) resulted in a collapse of tertiary structures coupled with the formation of a molten globule

protein. Furthermore, heating to temperatures usually suitable for antigen retrieval caused irreversible protein unfolding, thus improving accessibility to linear but not to conformational epitopes of the protein.
In summary, after formalin fixation and antigen retrieval, KLK6 may finally have lost its native conformation in the examined tissues, possibly to a greater extent than KLK4. Since the antibody fraction 623C is completely depleted from antibodies directed against the linear peptide epitope $KLK6_{109–119}$, it probably failed to detect the unfolded, denatured KLK6, even if more concentrated antibody titers were administered (see appendix).

In Western blot analysis, in brain tissue extracts, pAb 623A strongly reacted with a protein of about 43 kDa, whereas tissue extracts of skeletal muscle, known not to express KLK6 (Shaw and Diamandis, 2007), were negative (Figure 8B). The higher molecular weight of KLK6 (as well as the rather broad signal in Western blot analysis) originating from brain tissue extracts, as compared with recombinant, non-glycosylated KLK6 expressed in *E. coli*, is attributable to N-glycosylation of KLK6, as reported previously by Anisowicz *et al*. (1996) and Kuzmanov *et al*. (2009). KLK6 was detected in the white and gray matter as well as in brain tissue encompassing both white and gray matter (Figure 8B), implicating that KLK6 might be expressed by cells that are distributed throughout the entire human brain. However, by immunohistochemistry, we localized KLK6 expression exclusively to the astrocytes (Figure 11A), which represent the most numerous glial cells in the gray matter. These findings are in line with comprehensive immunohistochemical studies describing weak immunoreactivity of neural cells, but moderate to distinct staining of glial cells using polyclonal and monoclonal antibodies directed to KLK6 (Little *et* al, 1997; Petraki *et al*., 2001, Strojnik *et al*, 2009, Scarisbrick *et al*., 2012a).
In general, glial cells, including the astrocytes, are nonneural highly branched cells providing both mechanical and metabolic support to neurons. Particularly, the astrocytes, which are found not only in the gray, but also in the white matter, exhibit intimate functional relationships with neurons because they mediate the exchange of metabolites between neurons and the vascular system and are also partly forming the blood-brain barrier. Nevertheless, what seems even

more interesting is the fact that astrocytes are known to participate in the repair of CNS tissue after injury or damage by disease. Therefore, KLK6 expression restricted to astrocytes as detected by pAb 623A is supporting previous findings postulating contribution of KLK6 to the process of axon outgrowth following spinal cord injury, involvement of KLK6 in the progression of demyelinating diseases like multiple sclerosis, and a potential role of KLK6 in the pathogenesis of Alzheimer's disease and synucleinopathies like Parkinson's disease (Zarghooni *et al.*, 2002; Iwata *et al*., 2003; Yousef *et al*., 2003; Scarisbrick *et al*., 2006, 2008, 2012b; Hebb *et al*., 2010, Wennström *et al*., 2013). Furthermore, involvement of KLK6 in intracellular signaling by targeting protease-activated receptors (PARs) has also been studied. In fact, KLK6 was shown to activate astrocytic receptors PAR1 and PAR2, thus driving astrogliosis and contributing to glial scarring in the CNS (Vandell *et al*., 2008).

In view of the highly specific and convincing performance of pAb 623A in various Western blots and immunohistochemical analyses, it can reasonably be assumed that this antibody is suitable for the detection of KLK6 in ovarian cancer samples.

5.4 Evaluation of KLK4 as a potential diagnostic and prognostic marker for prostate cancer

KLK4 expression was investigated in matched pairs of tumor tissue (Tu) and corresponding tumor-free tissue (Tf) of 44 prostate cancer patients. A distinctly elevated KLK4 expression was observed in prostate cancer cells as compared to nearby non-malignant prostate epithelial cells. Contrary to previous data reporting mainly nuclear KLK4 expression in prostate cancer cells based on the proposed existence of a controversially discussed short *KLK4* gene transcript lacking the signal sequence (Simmer and Bartlett, 2004; Xi *et al*., 2004; Klokk *et al*., 2007), we exclusively observed a cytoplasmatic staining pattern in prostate cancer glands, similarly to the cytoplasmatic staining of epithelial cells in normal adult human tissues (Figures 9 and 10, Figures 13 and 14). Nuclear immunostaining did not occur with any of the two antibodies directed against KLK4, which is in line with experimental evidence, that KLKs, including KLK4,

are produced in the cytoplasm and secreted into the extracellular matrix (Simmer *et al*., 1998; Obiezu *et al*., 2005; Shaw and Diamandis, 2007). To evaluate the relevance of increased KLK4 expression in prostate cancer patients, we analyzed the relationship between KLK4-Tu score values and patients' clinicopathological parameters (Table 4). Strikingly, we found a statistically significant, inverse correlation between KLK4-Tu score values obtained with pAb 617A and tumor stage (p=0.005). Prostate cancer specimens classified as stage pT3 or pT4 tumors showed significantly lower KLK4 expression levels than stage pT1 or pT2 tumors (mean score value 0.09 vs. 0.68). That implies in particular that KLK4 expression is closely linked to tumor stage, which is a strong prognostic factor in prostate cancer patients (see appendix).

A very similar phenomenon has been observed in a study where *KLK4* mRNA levels were monitored in breast cancer patients. In parallel to the findings described above, increased KLK4 expression has been found in pT1 and pT2 tumors compared with normal breast tissues, whereas pT3 tumors displayed less elevated KLK4 expression levels (Mangé *et al*., 2008). Interestingly, another member of the KLK family, KLK5, has also been shown to be inversely associated with tumor stage as well as Gleason score in prostate cancer patients (Yousef *et al*., 2002; Korbakis *et al*., 2009). Gene expression of both KLK4 and KLK5 seems to be regulated by androgens (Korbakis *et al*., 2009; Lai *et al*., 2009) and therefore, it can be downregulated in hormone-refractory prostate cancer in comparison to androgen-sensitive tumors. Hence, decrease in KLK4 and KLK5 expression could be associated with a more advanced, potentially already castration-resistant disease. Future studies with an increased number of tissue samples could address and clarify the question whether the expression of KLK4 and KLK5 in prostate cancer is continuously and statistically significant decreasing from stage pT1 to stage pT4 tumors.

Although the expression of KLK4 in normal and neoplastic prostate epithelial tissues has been expansively investigated over the past years, the role of KLK4 in the development and progression of hormone-regulated malignancies such as prostate cancer remains to be elucidated further. In this study, highly specific antibodies directed to KLK4 allowed precise analyses and authentic monitoring

of KLK4 expression in normal human organs and in prostate cancer tissues. These analyses indicate that differential KLK4 expression levels in prostate cancer patients carry important stage-related prognostic information. However, further research is required to answer the question whether KLK4 can serve in the detection of early-stage prostate cancer as a diagnostic marker and whether on the basis of KLK4 as a prognostic marker the risk of disease recurrence or prostate cancer-related death can be reliably estimated. Clinical utility of KLK4 as a diagnostic or even prognostic marker finally depends on its potential to alter clinical decision making, which has yet to be explored.

5.5 Evaluation of KLK6 as a potential prognostic marker and therapeutic target in ovarian cancer

KLK6 expression was investigated by immunohistochemistry in tumor tissue samples of 118 ovarian cancer patients employing pAb 623A. Distinct cytoplasmic immunostaining was detected in both malignant epithelial tumor cells and, with lower frequency, in surrounding stromal cells (Figure 16). In view of their microscopic morphology and appearance, these KLK6 expressing stromal cells most probably represent fibroblasts and tissue macrophages. In the white matter of injured spinal cord, CD68-positive macrophages have been reported to abundantly express KLK6 (Scarisbrick *et al*., 2006). Strikingly, we observed a statistically significant correlation between stromal cell-associated KLK6 expression (KLK6-Sc) and survival. In multivariate analyses, ovarian cancer patients with high KLK6-Sc immunoexpression in their tumor tissue faced both a significantly shorter overall survival (OS) and progression-free survival (PFS) as compared with patients who displayed low KLK6-Sc expression levels in their tumor tissue (Table 8).

In ovarian cancer, elevated KLK6 mRNA and protein levels have repeatedly been observed and related to poor patient outcome (Hoffmann *et al*., 2002; Luo *et al*., 2006; Kountourakis *et al*., 2008; Bayani *et al*., 2011; Koh *et al*., 2011). However, this is the first study demonstrating that stromal cell-associated KLK6 expression significantly is associated with patients' prognosis. Additionally,

enhanced expression of another member of the KLK family, KLK4, has also been identified in the effusions as well as the stroma of invasive epithelial ovarian cancer (Davidson *et al*., 2005). However, no correlation was found between stromal expression of KLK4 and survival, in contrast to the data presented here for KLK6.

To date, KLK6 has shown a wide range of functional diversity with respect to carcinogenesis (Bayani and Diamandis, 2011). Yet, our understanding of its role in the reactive stroma coupled with its contribution to the tumor microenvironment is only beginning to emerge. In a recent study, the expression pattern of KLK6 was investigated in cutaneous malignant melanoma (Krenzer *et al*., 2011). Interestingly, KLK6 was not detected in tumor cells, but a strong KLK6 protein expression was found in stromal cells and keratinocytes adjacent to the tumor cells. In this context, a paracrine function of secreted KLK6 during neoplastic transformation and malignant progression was suggested. In fact, when recombinant KLK6 was added to melanoma cells *in vitro*, both cell migration and cell invasion were induced, accompanied by an activation of the signaling receptor PAR1 (Krenzer *et al*., 2011). In biochemical *in vitro* studies, KLK6 was shown to cleave prominent components of the tumor stroma, such as fibronectin and different types of collagen (Magklara *et al*., 2003; Borgoño and Diamandis, 2004; Ghosh *et al*., 2004), which does support its role in tissue remodeling, tumor invasion, and metastasis.

In conclusion, the study presented here provides evidence that, in ovarian cancer, both tumor and surrounding stromal cells frequently overexpress KLK6. Because, especially, stromal cell-associated KLK6 expression in tumor tissue was found to be significantly related to shortened OS and PFS in ovarian cancer patients, stromal cell-derived KLK6 may considerably contribute to the aggressiveness of ovarian neoplasms. Still, further studies are required to assure the prognostic value of stromal-cell derived KLK6 for patients' outcome and to provide more detailed knowledge regarding the role of KLK6 in the ovarian cancer microenvironment. A major challenge for future research will be to elucidate whether on the basis of its function in ovarian cancer microenvironment, KLK6 can serve as a potential target for therapeutic intervention.

6. Abstract

KLK4 is a member of the human kallikrein-related peptidase (KLK) family of (chymo)trypsin-like serine proteases. In this study, the expression of KLK4 was analyzed in human tissues by immunohistochemistry using highly specific antibodies, such as monospecific polyclonal antibody (pAb) 617A, which is an affinity-purified antibody fraction reacting with a linear epitope within a flexible surface-exposed loop of KLK4. The other antibody applied, antibody 617C, is a monospecific polyclonal antibody fraction which is completely depleted of pAb 617A. In normal adult tissues, KLK4 was immunodetected by both antibody fractions in the kidney, liver, and prostate, but not in other organs such as colon and lung. To examine KLK4 protein expression in prostate cancer and to evaluate the potential of KLK4 as a clinically relevant marker, samples of tumor tissue and corresponding tumor-free tissue of 44 prostate cancer patients, represented on a tissue microarray, were investigated. Distinct KLK4 immunostaining was observed with both antibodies in cancerous glandular epithelial cells, but not in the surrounding stromal cells. KLK4 expression was lower in patients with stage pT3 and pT4 tumors compared to patients with stage pT1 and pT2 tumors, which was statistically highly significant when pAb 617A was employed. Thus, our results indicate that KLK4, which is expressed in the healthy prostate, is up-regulated in early-stage but not in late-stage prostate cancer. In other words, differential expression of KLK4 in prostate cancer patients carries important stage-related prognostic information.

Several members of the human KLK family, including KLK6, are known to be up-regulated in ovarian cancer. High KLK6 mRNA and protein expression levels, measured by quantitative polymerase chain reaction and enzyme-linked immunoassay, were previously found to be associated with shorter overall survival and progression-free survival (OS and PFS) in patients afflicted with ovarian cancer. In the present study, KLK6 protein expression was analyzed in ovarian cancer tissue by immunohistochemistry. Using a newly developed monospecific polyclonal antibody, pAb 623A, KLK6 immunoexpression was first evaluated in normal tissues. Strong staining was observed in the brain and moderate staining in the kidney, liver, and ovary, whereas the pancreas and

skeletal muscle were unreactive, which is in line with previously published results. Next, both tumor cell-associated and stromal cell-associated KLK6 immunoexpression was analyzed in tumor tissue samples of 118 ovarian cancer patients. In multivariate Cox regression analysis, only stromal cell-associated KLK6 expression, besides the established clinical parameters FIGO stage and residual tumor mass, was found to be statistically significant for OS and PFS. These results indicate that KLK6 expressed by stromal cells may considerably contribute to the aggressiveness of ovarian cancer and, therefore, may have significant prognostic value in ovarian cancer patients.

7. Appendix

7.1 Definition of the TNM staging system for prostate cancer

TNM category	*Stage*	
TX **T0**		Primary tumor cannot be assessed No evidence of primary tumor
NX **N0**		Regional lymph nodes were not assessed No regional lymph node metastasis
MX **M0**		Distant metastasis cannot be assessed (not evaluated) No distant metastasis
T1	**I**	**Clinically inapparent tumor neither palpable nor visible by imaging**
T1aN0M0 ***G1***	I	Tumor, incidental histological finding in 5% or less of tissue resected by TURP
T1aN0M0 ***G2/G3***	**II**	Tumor, incidental histological finding in 5% or less of tissue resected by TURP
T1bN0M0	II	Tumor, incidental histological finding in more than 5% of tissue resected by TURP
T1cN0M0	II	Tumor identified by needle biopsy (e.g., because of elevated PSA level)
T2	**II**	**Tumor confined within the prostate**
T2aN0M0	II	Tumor involves one-half of one lobe or less
T2bN0M0	II	Tumor involves more than one-half of one lobe but not both lobes
T2cN0M0	II	Tumor involves both lobes
T3	**III**	**Tumor extends through the prostate capsule**
T3aN0M0	III	Extracapsular extension (unilateral or bilateral)
T3bN0M0	III	Tumor invades seminal vesicle(s)
T4N0M0	**IV**	**Tumor is fixed or invades bladder neck, external sphincter, rectum, levator muscles, and/or pelvic wall**
anyTN1M0	**IV**	Metastasis in regional lymph node(s)
M1 (any T, any N)	**IV**	**Distant metastasis**
M1a	IV	Metastasis in non-regional lymph node(s)
M1b	IV	Metastasis in bone(s)
M1c	IV	Metastasis in other site(s) with or without bone disease

T (primary tumor), **N** (regional lymph nodes), **M** (distant metastasis), **G** (histologic grade) **TURP** (transurethral resection of the prostate), **PSA** (prostate-specific antigen) ***Notes**:* Tumor found in one or both lobes by needle biopsy, but not palpable or reliably visible by imaging, is classified as T1c. Invasion into the prostatic apex or into (but not beyond) the prostatic capsule is classified not as T3 but as T2. When more than one site of metastasis is present, the most advanced category (*i.e.* M1c) is used.
***References**: adapted from the AJCC Cancer Staging Manual and the UICC Manual of Clinical Oncology (Pollock* et al*., 2004)*

7.2 Combined grading system for prostate tumors

Gleason score	*Study group**	*WHO*	
		GX	**Grade cannot be assessed**
2 **3,4**	**GIa** **GIb**	**G1**	**Well differentiated (slight anaplasia)**
5,6	**GIIa**	**G2**	**Moderately differentiated (moderate anaplasia)**
7 **8,9** **10**	**GIIb** **GIIIa** **GIIIb**	**G3**	**Poorly differentiated or undifferentiated (marked anaplasia)**
***Study group**: German Prostate Cancer Study Group			
***Reference**: adapted from AJCC Cancer Staging Manual and "Prognostic factors of prostatic carcinoma" (Helpap, 1998)*			

7.3 Risk stratification for localized prostate cancer

Risk group	
Low risk	**T1-2a and PSA <10 ng/ml, and Gleason 6**
Intermediate risk	**T2b-c, or PSA 10-20 ng/ml, or Gleason 7**
High risk	**T3-4, or PSA >20 ng/ml, or Gleason 8-10**
PSA (prostate-specific antigen)	
***Reference**: adapted from Oxford Handbook of Oncology (Cassidy* et al*., 2010)*	

7.4 Definition of the TNM and FIGO staging systems for ovarian cancer

TNM category	*FIGO stage*	
TX **T0**		Primary tumor cannot be assessed No evidence of primary tumor
NX **N0**		Regional lymph nodes cannot be assessed No regional lymph node metastasis
MX **M0**		Distant metastasis cannot be assessed No distant metastasis
T1	**I**	**Tumor limited to ovaries (one or both)**
T1aN0M0	IA	Tumor limited to one ovary; capsule intact, no tumor on ovarian surface No malignant cells in ascites or peritoneal washings
T1bN0M0	IB	Tumor limited to both ovaries; capsules intact, no tumor on ovarian surface No malignant cells in ascites or peritoneal washings
T1cN0M0	IC	Tumor limited to one or both ovaries with any of the following: capsule ruptured, tumor on ovarian surface, malignant cells in ascites or peritoneal washings
T2	**II**	**Tumor involves one or both ovaries with pelvic extension and/or implants**
T2aN0M0	IIA	Extension and/or implants on uterus and/or tube(s) No malignant cells in ascites or peritoneal washings
T2bN0M0	IIB	Extension to and/or implants on other pelvic tissues No malignant cells in ascites or peritoneal washings
T2cN0M0	IIC	Pelvic extension and/or implants (T2a or T2b) with malignant cells in ascites or peritoneal washings
T3 and/or N1	**III**	**Tumor involves one or both ovaries with microscopically confirmed peritoneal metastasis outside the pelvis and/or regional lymph node metastasis**
T3aN0M0	IIIA	Microscopic peritoneal metastasis beyond pelvis (no macroscopic tumor)
T3bN0M0	IIIB	Macroscopic peritoneal metastasis beyond pelvis 2 cm or less in greatest dimension
T3cN0M0 and/or anyTN1M0	IIIC	Peritoneal metastasis beyond pelvis more than 2 cm in greatest dimension and/or regional lymph node metastasis
M1 (any T, any N)	**IV**	**Distant metastasis (excludes peritoneal metastasis)**
T (primary tumor), **N** (regional lymph nodes), **M** (distant metastasis) **FIGO** (Fédération Internationale de Gynécologie et d'Obstétrique) ***Notes:*** The presence of liver capsule metastases is classified as T3/FIGO III, the presence of liver parenchymal metastases is classified as M1/FIGO IV. Pleural effusions must have positive cytology to be classified as M1/FIGO IV.		
***References**: adapted from AJCC Cancer Staging Manual and UICC Manual of Clinical Oncology (Pollock* et al.*, 2004)*		

7.5 Classification of nuclear grading of ovarian tumors

Histologic grade	
GX	**Grade cannot be assessed**
GB	**Borderline malignancy**
G1	**Well differentiated**
G2	**Moderately differentiated**
G3	**Poorly differentiated or undifferentiated**
***Reference**: adapted from AJCC Cancer Staging Manual*	

7.6 Survival in patients with epithelial ovarian cancer

FIGO stage	*Five-year survival rate*
IA	**90%**
IB	**65%**
II	**45%**
III	**25%**
IV	**5%**
***References**: adapted from Oxford Handbook of Oncology (Cassidy* et al*., 2010) and UICC Manual of Clinical Oncology (Pollock* et al*., 2004)*	

7.7 Standard amino acid abbreviations

Amino acid	*Three-letter code*	*Single-letter code*
Alanine	Ala	**A**
Arginine	Arg	**R**
Asparagine	Asn	**N**
Aspartic acid	Asp	**D**
Cysteine	Cys	**C**
Glutamic acid	Glu	**E**
Glutamine	Gln	**Q**
Glycine	Gly	**G**
Histidine	His	**H**
Isoleucine	Ile	**I**
Leucine	Leu	**L**
Lysine	Lys	**K**
Methionine	Met	**M**
Phenylalanine	Phe	**F**
Proline	Pro	**P**
Serine	Ser	**S**
Threonine	Thr	**T**
Tryptophan	Trp	**W**
Tyrosine	Tyr	**Y**
Valine	Val	**V**

7.8 Antibody characteristics and dilutions

pAb	*species*	*immunogen*	*affinity purification*	*stock concentration (mg/ml)*	*dilution*	
					WB	*IHC*
617A	chicken	rec-KLK4	$KLK4_{109–122}$	0.40	1:500	1:700
617C	chicken	rec-KLK4	rec-KLK4	0.60	1:500	1:700
623A	rabbit	rec-KLK6	$KLK6_{109–119}$	0.24	1:400	1:50
623C	rabbit	rec-KLK6	rec-KLK6	0.55	1:500	1:10
WB: Western blot, IHC: immunohistochemistry						

7.9 Ovarian cancer tissue microarrays

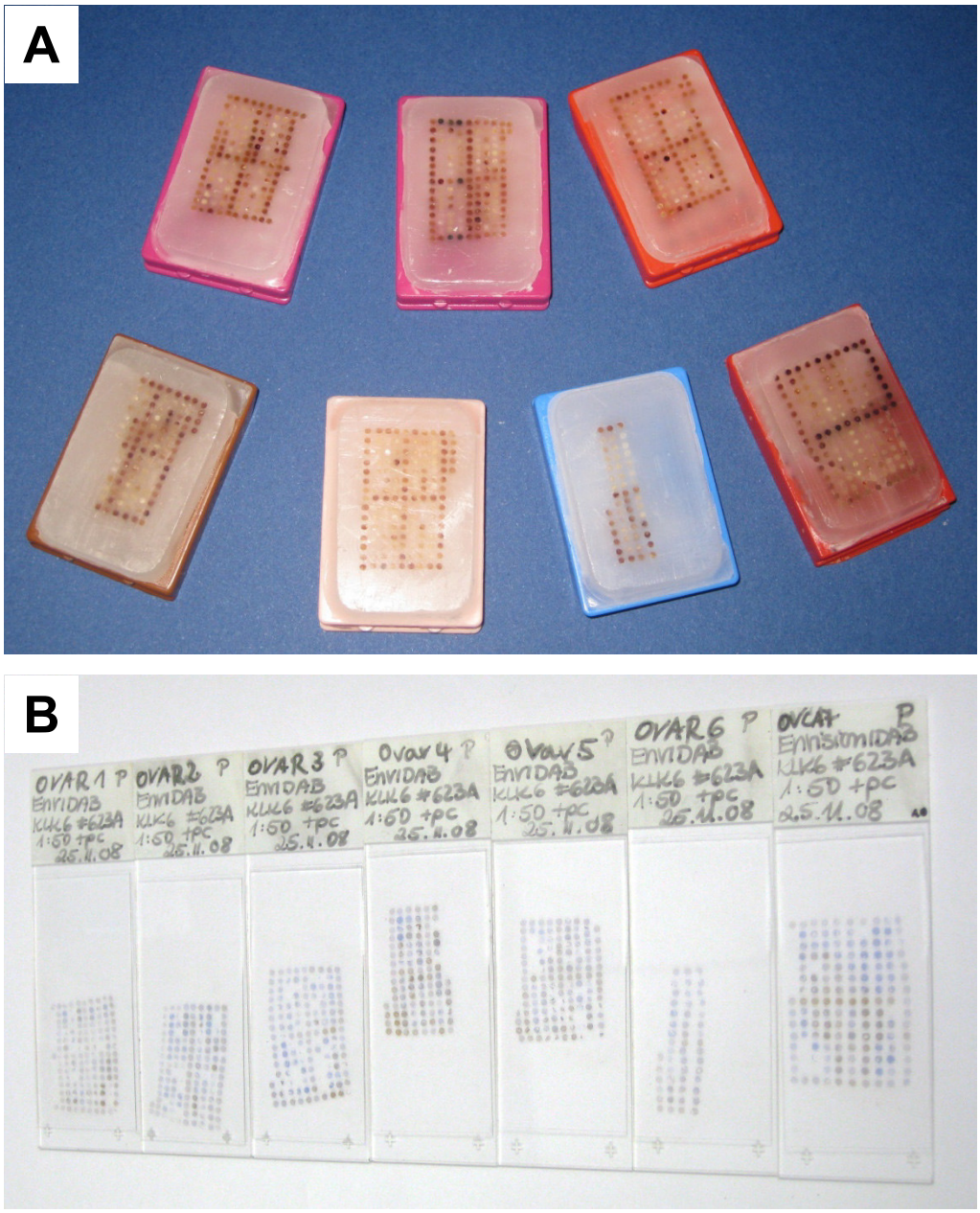

Figure 18: Ovarian cancer tissue microarrays analyzed by IHC.
(A) Photograph of seven tissue microarray blocks encompassing the tumor samples of 118 ovarian cancer patients. **(B)** Macroscopic view of seven tissue microarray sections that were cut from the respective blocks, transferred to glass slides, and subsequently, subjected to immunohistochemical staining employing pAb 623A.

7.10 Abbreviations

Ab	antibody
ABC	avidin-biotin complex
AJCC	American Joint Committee on Cancer
APC gene	encodes the tumor suppressor protein adenomatous polyposis coli (APC)
AR gene	encodes the androgen receptor (AR)
bCTRA	bovine chymotrypsin
BMP	bone morphogenic protein
BSA	bovine serum albumin
cDNA	complementary deoxyribonucleic acid
CI	confidence interval
CNS	central nervous system
CT	chemotherapy
CT scan	computed tomography
Da	alton (atomic mass unit)
DAB+	3,3'-diaminobenzidine
DNA	deoxyribonucleic acid
DRE	digital rectal examination
ECL	enhanced chemiluminescence
EK	enterokinase
ELISA	enzyme-linked immunosorbent assay
EMSP1	enamel matrix serine protease 1
ETS genes	encode transcription factors
FFPE	formalin-fixed paraffin-embedded
FIGO	Fédération Internationale de Gynécologie et d'Obstétrique
h	hour
$(His)_6$-tag	histidine tag
HR (95% CI)	hazard ratio (95% confidence interval)
HRP	horseradish peroxidase
H_2O_2	hydrogen peroxide
H_2SO_4	sulfuric acid
H&E-staining	hematoxylin and eosin-staining
i.e.	that is
IGF	insulin-like growth factor
IGFBP	insulin-like growth factor-binding protein
IgG	immunoglobulin G
IgY	immunoglobulin Y

IHC	immunohistochemistry
IRS	immunoreactivity score
kb	kilobase
kDa	kilodalton
KLK	kallikrein-related peptidase
KOH	potassium hydroxide
mg/ml	milligrams per milliliter
min	minute
miRNA	micro ribonucleic acid
MRI	magnetic resonance imaging
mRNA	messenger ribonucleic acid
MYC gene	encodes a transcription factor
$NaHCO_3$	sodium hydrogen carbonate
Na_2CO_3	sodium carbonate
ng/ml	nanograms per milliliter
NKX3.1 gene	encodes a transcription factor
nm	nanometer
No.	number
OPD	ortho-phenylenediamine
OS	overall survival
OVA1®	blood test
pAb	polyclonal antibody
PAR	protease-activated receptor
PBS	phosphate-buffered saline
PCR	polymerase chain reaction
PFS	progression-free survival
pro-HGFA	pro-hepatocyte growth factor activator
PSA	prostate-specific antigen
PTEN gene	encodes the tumor suppressor protein phosphatase and tensin homolog (PTEN)
PTHrP	parathyroid hormone-related peptide
PVDF	polyvinylidene fluoride
RB1 gene	encodes the retinoblastoma protein, a tumor suppressor
rec-KLK	recombinant KLK
rec-proKLK	recombinant pro-form of KLK
RNAse A	bovine pancreatic ribonuclease A
ROMA®	risk of ovarian malignancy algorithm, blood test
r_s	Spearman's rank correlation coefficient
SDS	sodium dodecyl sulfate

SDS-PAGE	sodium dodecyl sulfate polyacrylamide gel electrophoresis
TBS (or Tris)	Tris-buffered saline
TMA	tissue microarray
TP53 gene	encodes the tumor suppressor protein p53
TRUS	transrectal ultrasound
TURP	transurethral resection of the prostate
Tween-20	polyoxyethylene (20) sorbitan monolaurate
UICC	Union Internationale Contre le Cancer
uPA	urokinase-type plasminogen activator
uPAR	uPA receptor
VEGF	vascular endothelial growth factor
VEGFC	vascular endothelial growth factor C
WB	Western blot
WHO	World Health Organization
°C	degree Celsius
% (w/v)	weight/volume percent
% (v/v)	volume/volume percent
#	number sign

7.11 References

Aebi, S., Castiglione, M., ESMO Guidelines Working Group (2009). Newly and relapsed epithelial ovarian carcinoma: ESMO clinical recommendations for diagnosis, treatment and follow-up. Ann. Oncol. *20* (Supplement 4), 21-23.

Almeida, C.A. and Barry, S.A., Prostate cancer (chapter 11) in “Cancer: basic science and clinical aspects”, Wiley-Blackwell, West Sussex, UK, 2010, 224-246.

American Joint Committee on Cancer, AJCC Cancer Staging Manual, Springer, New York, USA, 2002, 6th edition, 275-283, 309-316.

Anisowicz, A., Sotiropoulou, G., Stenman, G., Mok, S.C., and Sager, R. (1996). A novel protease homolog differentially expressed in breast and ovarian cancer. Mol. Med. *2*, 624-636.

Ashby, E.L., Kehoe, P.G., and Love, S. (2010). Kallikrein-related peptidase 6 in Alzheimer's disease and vascular dementia. Brain Res. *1363*, 1-10.

Avgeris, M., Mavridis, K., and Scorilas, A. (2012). Kallikrein-related peptidases in prostate, breast, and ovarian cancers: from pathobiology to clinical relevance. Biol. Chem. *393*, 301-317.

Bandiera, E., Zanotti, L., Fabricio, A.S., Bucca, E., Squarcina, E., Romani, C., Tassi, R., Bignotti, E., Todeschini, P., Tognon, G., Romagnolo, C., Gion, M., Sartori, E., Maggino, T., Pecorelli, S., and Ravaggi, A. (2013). Cancer antigen 125, human epididymis 4, kallikrein 6, osteopontin and soluble mesothelin-related peptide immunocomplexed with immunoglobulin M in epithelial ovarian cancer diagnosis. Clin. Chem. Lab. Med. *51*, 1815-1824.

Barber, J. and Staffurth, J., Prostate (chapter 19) in “Practical clinical oncology”, Hanna, L., Crosby, T., and Macbeth, F., Cambridge University Press, New York, USA, 2008, 231-239.

Bast, R.C. Jr., Skates, S., Lokshin, A., and Moore, R.G. (2012). Differential diagnosis of a pelvic mass: improved algorithms and novel biomarkers. Int. J. Gynecol. Cancer *22*, 5-8.

Bayani, J. and Diamandis, E.P. (2011). The physiology and pathobiology of human kallikrein-related peptidase 6 (KLK6). Clin. Chem. Lab. Med. *50*, 211-233.

Bayani, J., Marrano, P., Graham, C., Zheng, Y., Li, L., Katsaros, D., Lassus, H., Butzow, R., Squire, J.A., and Diamandis, E.P. (2011). Genomic instability and copy-number heterogeneity of chromosome 19q, including the kallikrein locus, in ovarian carcinomas. Mol. Oncol. *5*, 48-60.

Bayés, A., Tsetsenis, T., Ventura, S., Vendrell, J., Aviles, F.X., and Sotiropoulou, G. (2004). Human kallikrein 6 activity is regulated via an autoproteolytic mechanism of activation/inactivation. Biol. Chem. *385*, 517-524.

Beaufort, N., Debela, M., Creutzburg, S., Kellermann, J., Bode, W., Schmitt, M., Pidard, D., and Magdolen, V. (2006). Interplay of human tissue kallikrein 4 (hK4) with the plasminogen activation system: hK4 regulates the structure and functions of the urokinase-type plasminogen activator receptor (uPAR). Biol. Chem. *387*, 217-222.

Beaufort, N., Plaza, K., Utzschneider, D., Schwarz, A., Burkhart, J.M., Creutzburg, S., Debela, M., Schmitt, M., Ries, C., and Magdolen, V. (2010). Interdependence of kallikrein-related peptidases in proteolytic networks. Biol. Chem. *391*, 581-587.

Bernett, M.J., Blaber, S.I., Scarisbrick, I.A., Dhanarajan, P., Thompson, S.M., and Blaber, M. (2002). Crystal structure and biochemical characterization of human kallikrein 6 reveals that a trypsin-like kallikrein is expressed in the central nervous system. J. Biol. Chem. *277*, 24562-24570.

Borgoño, C.A. and Diamandis, E.P. (2004). The emerging roles of human tissue kallikreins in cancer. Nat. Rev. Cancer *4*, 876-890.

Bray, F., Jemal, A., Grey, N., Ferlay, J., and Forman, D. (2012). Global cancer transitions according to the Human Development Index (2008-2030): a population-based study. Lancet Oncol. *13*, 790-801.

Burger, R.A., Brady, M.F., Bookman, M.A., Fleming, G.F., Monk, B.J., Huang, H., Mannel, R.S., Homesley, H.D., Fowler, J., Greer, B.E., Boente, M., Birrer, M.J., Liang, S.X.; Gynecologic Oncology Group (2011). Incorporation of bevacizumab in the primary treatment of ovarian cancer. N. Engl. J. Med. *365*, 2473-2483.

Burges, A. and Schmalfeldt, B. (2011). Ovarian cancer: diagnosis and treatment. Dtsch. Ärztebl. Int. *108*, 635-641.

Buys, S.S., Partridge, E., Black, A., Johnson, C.C., Lamerato, L., Isaacs, C., Reding, D.J., Greenlee, R.T., Yokochi, L.A., Kessel, B., Crawford, E.D., Church, T.R., Andriole, G.L., Weissfeld, J.L., Fouad, M.N., Chia, D., O'Brien, B., Ragard,

L.R., Clapp, J.D., Rathmell, J.M., Riley, T.L., Hartge, P., Pinsky, P.F., Zhu, C.S., Izmirlian, G., Kramer, B.S., Miller, A.B., Xu, J.L., Prorok, P.C., Gohagan, J.K., Berg, C.D.; PLCO Project Team (2011). Effect of screening on ovarian cancer mortality: the Prostate, Lung, Colorectal and Ovarian (PLCO) Cancer Screening Randomized Controlled Trial. JAMA *305*, 2295-2303.

Cassidy, J., Bissett, D., Spence OBE, R.A.J., and Payne, M., Oxford Handbook of Oncology, Oxford University Press, Oxford, UK, 2010, 3rd edition, 400-409, 422-425.

Center, M.M., Jemal, A., Lortet-Tieulent, J., Ward, E., Ferlay, J., Brawley, O., and Bray, F. (2012). International variation in prostate cancer incidence and mortality rates. Eur. Urol. *61*, 1079-1092.

Christophi, G.P., Isackson, P.J., Blaber, S., Blaber, M., Rodriguez, M., and Scarisbrick, I.A. (2004). Distinct promoters regulate tissue-specific and differential expression of kallikrein 6 in CNS demyelinating disease. J. Neurochem. *91*, 1439-1449.

Davidson, B., Xi, Z., Klokk, T.I., Tropé, C.G., Dørum, A., Scheistrøen, M., and Saatcioglu, F. (2005). Kallikrein 4 expression is up-regulated in epithelial ovarian carcinoma cells in effusions. Am. J. Clin. Pathol. *123*, 360-368.

Day, C.H., Fanger, G.R., Retter, M.W., Hylander, B.L., Penetrante, R.B., Houghton, R.L., Zhang, X., McNeill, P.D., Filho, A.M., Nolasco, M., Badaro, R., Cheever, M.A., Reed, S.G., Dillon, D.C., and Watanabe, Y. (2002). Characterization of KLK4 expression and detection of KLK4-specific antibody in prostate cancer patient sera. Oncogene *21*, 7114-7120.

Debela, M., Beaufort, N., Magdolen, V., Schechter, N.M., Craik, C.S., Schmitt, M., Bode, W., and Goettig, P. (2008). Structures and specificity of the human kallikrein-related peptidases KLK 4, 5, 6, and 7. Biol. Chem. *389*, 623-632.

Debela, M., Magdolen, V., Grimminger, V., Sommerhoff, C., Messerschmidt, A., Huber, R., Friedrich, R., Bode, W., and Goettig, P. (2006a). Crystal structures of human tissue kallikrein 4: activity modulation by a specific zinc binding site. J. Mol. Biol. *362*, 1094-1107.

Debela, M., Magdolen, V., Schechter, N., Valachova, M., Lottspeich, F., Craik, C.S., Choe, Y., Bode, W., and Goettig, P. (2006b). Specificity profiling of seven human tissue kallikreins reveals individual subsite preferences. J. Biol. Chem. *281*, 25678-25688.

DeLano, W.L. (2002). The PyMOL Molecular Graphics System on World Wide Web (http://www.pymol.org). Stand: 31.12.2011.

Diamandis, E.P., Scorilas, A., Fracchioli, S., Van Gramberen, M., De Bruijn, H., Henrik, A., Soosaipillai, A., Grass, L., Yousef, G.M., Stenman, U.H., Massobrio, M., Van Der Zee, A.G., Vergote, I., and Katsaros, D. (2003). Human kallikrein 6 (hK6): a new potential serum biomarker for diagnosis and prognosis of ovarian carcinoma. J. Clin. Oncol. *21*, 1035-1043.

Diamandis, E.P., Yousef, G.M., Luo, L.Y., Magklara, A., and Obiezu, C.V. (2000). The new human kallikrein gene family: implications in carcinogenesis. Trends Endocrinol. Metab. *11*, 54-60.

Dong, Y., Kaushal, A., Bui, L., Chu, S., Fuller, P.J., Nicklin, J., Samaratunga, H., and Clements, J.A. (2001). Human kallikrein 4 (KLK4) is highly expressed in serous ovarian carcinomas. Clin. Cancer Res. *7*, 2363-2371.

Dorn, J., Bayani, J., Yousef, G.M., Yang, F., Magdolen, V., Kiechle, M., Diamandis, E.P., and Schmitt, M. (2013). Clinical utility of kallikrein-related peptidases (KLK) in urogenital malignancies. Thromb. Haemost. *110*, 408-422.

Dorn, J., Schmitt, M., Kates, R., Schmalfeldt, B., Kiechle, M., Scorilas, A., Diamandis, E.P., and Harbeck, N. (2007). Primary tumor levels of human tissue kallikreins affect surgical success and survival in ovarian cancer patients. Clin. Cancer Res. *13*, 1742-1748.

Drucker, K.L., Paulsen, A.R., Giannini, C., Decker, P.A., Blaber, S.I., Blaber, M., Uhm, J.H., O'Neill, B.P., Jenkins, R.B., and Scarisbrick, I.A. (2013). Clinical significance and novel mechanism of action of kallikrein 6 in glioblastoma. Neuro-Oncol. *15*, 305-318.

Emami, N. and Diamandis, E.P. (2008). Utility of kallikrein-related peptidases (KLKs) as cancer biomarkers. Clin. Chem. *54*, 1600-1607.

Fowler, C.B., Evers, D.L., O'Leary, T.J., and Mason, J.T. (2011). Antigen retrieval causes protein unfolding: evidence for a linear epitope model of recovered immunoreactivity. J. Histochem. Cytochem. *59*, 366-381.

Ghosh, M.C., Grass, L., Soosaipillai, A., Sotiropoulou, G., and Diamandis, E.P. (2004). Human kallikrein 6 degrades extracellular matrix proteins and may enhance the metastatic potential of tumour cells. Tumour Biol. *25*, 193-199.

Goettig, P., Magdolen, V., and Brandstetter, H. (2010). Natural and synthetic inhibitors of kallikrein-related peptidases (KLKs). Biochimie *92*, 1546-1567.

Gomis-Rüth, F.X., Bayés, A., Sotiropoulou, G., Pampalakis, G., Tsetsenis, T., Villegas, V., Avilés, F.X., and Coll, M. (2002). The structure of human prokallikrein 6 reveals a novel activation mechanism for the kallikrein family. J. Biol. Chem. *277*, 27273-27281.

Grebenschikov, N., Geurts-Moespot, A., De Witte, H., Heuvel, J., Leake, R., Sweep, F., and Benraad, T. (1997). A sensitive and robust assay for urokinase and tissue-type plasminogen activators (uPA and tPA) and their inhibitor type I (PAI-1) in breast tumor cytosols. Int. J. Biol. Markers *12*, 6-14.

Hanna, L. and Crosby, T., Ovary (chapter 22) in “Practical clinical oncology”, Hanna, L., Crosby, T., and Macbeth, F., Cambridge University Press, New York, USA, 2008, 257-266.

Harvey, T.J., Dong, Y., Bui, L., Jarrott, R., Walsh, T., and Clements, J.A. (2003). Production and characterization of antipeptide kallikrein 4 antibodies. Use of computer modeling to design peptides specific to kallikrein 4. Methods Mol. Med. *81*, 241-254.

Harvey, T.J., Hooper, J.D., Myers, S.A., Stephenson, S.A., Ashworth, L.K., and Clements, J.A. (2000). Tissue-specific expression patterns and fine mapping of the human kallikrein (KLK) locus on proximal 19q13.4. J. Biol. Chem. *275*, 37397-37406.

Hebb, A.L., Bhan, V., Wishart, A.D., Moore, C.S., and Robertson, G.S. (2010). Human kallikrein 6 cerebrospinal levels are elevated in multiple sclerosis. Curr. Drug Discov. Technol. *7*, 137-140.

Helpap, B. (1998). Prognostic factors of prostatic carcinoma. Pathologe *19*, 42-52.

Hoffman, B.R., Katsaros, D., Scorilas, A., Diamandis, P., Fracchioli, S., Rigault de la Longrais, I.A., Colgan, T., Puopolo, M., Giardina, G., Massobrio, M., and Diamandis, E.P. (2002). Immunofluorometric quantitation and histochemical localisation of kallikrein 6 protein in ovarian cancer tissue: a new independent unfavourable prognostic biomarker. Br. J. Cancer, *87*, 763-771.

Iwata, A., Maruyama, M., Akagi, T., Hashikawa, T., Kanazawa, I., Tsuji, S., and Nukina, N. (2003). Alpha-synuclein degradation by serine protease neurosin: implication for pathogenesis of synucleinopathies. Hum. Mol. Genet. *12*, 2625-2635.

Jemal, A., Bray, F., Center, M.M., Ferlay, J., Ward, E., and Forman, D. (2011). Global cancer statistics. CA. Cancer J. Clin. *61*, 69-90.

Kaplan, E.L. and Meier, P. (1958). Nonparametric estimation from incomplete observations. J. Amer. Statist. Assn. *53*, 457-481.

Klokk, T.I., Kilander, A., Xi, Z., Waehre, H., Risberg, B., Danielsen, H.E., and Saatcioglu, F. (2007). Kallikrein 4 is a proliferative factor that is overexpressed in prostate cancer. Cancer Res. *67*, 5221-5230.

Koh, S.C., Razvi, K., Chan, Y.H., Narasimhan, K., Ilancheran, A., Low, J.J., Choolani, M. [Ovarian Cancer Research Consortium of SE Asia] (2011). The association with age, human tissue kallikreins 6 and 10 and hemostatic markers for survival outcome from epithelial ovarian cancer. Arch. Gynecol. Obstet. *284*, 183-190.

Korbakis, D., Gregorakis, A.K., and Scorilas, A. (2009). Quantitative analysis of human kallikrein 5 (KLK5) expression in prostate needle biopsies: an independent cancer biomarker. Clin. Chem. *55*, 904-913.

Kountourakis, P., Psyrri, A., Scorilas, A., Camp, R., Markakis, S., Kowalski, D., Diamandis, E.P., and Dimopoulos, M.A. (2008). Prognostic value of kallikrein-related peptidase 6 protein expression levels in advanced ovarian cancer evaluated by automated quantitative analysis (AQUA). Cancer Sci. *99*, 2224-2229.

Krenzer, S., Peterziel, H., Mauch, C., Blaber, S.I., Blaber, M., Angel, P., and Hess, J. (2011). Expression and function of the kallikrein-related peptidase 6 in the human melanoma microenvironment. J. Invest. Dermatol. *131*, 2281-2288.

Kumar, G.L. and Rudbeck, L. (2009). Education Guide – Immunohistochemical Staining Methods, 5th edition, (http://www.dako.com/de/08002_ihc_staining_methods_5ed.pdf). Stand: 17.12.2011.

Kuzmanov, U., Jiang, N., Smith, C.R., Soosaipillai, A., and Diamandis, E.P. (2009). Differential N-glycosylation of kallikrein 6 derived from ovarian cancer cells or the central nervous system. Mol. Cell. Proteomics *8*, 791-798.

Kwiatkowski, M.K., Recker, F., Piironen, T., Pettersson, K., Otto, T., Wernli, M., and Tscholl, R. (1998). In prostatism patients the ratio of human glandular kallikrein to free PSA improves the discrimination between prostate cancer and benign hyperplasia within the diagnostic "gray zone" of total PSA 4 to 10 ng/mL. Urology *52*, 360-365.

Lai, J., Myers, S.A., Lawrence, M.G., Odorico, D.M., and Clements, J.A. (2009). Direct progesterone receptor and indirect androgen receptor interactions with the kallikrein-related peptidase 4 gene promoter in breast and prostate cancer. Mol. Cancer Res. *7*, 129-141.

Little, S.P., Dixon, E.P., Norris, F., Buckley, W., Becker, G.W., Johnson, M., Dobbins, J.R., Wyrick, T., Miller, J.R., MacKellar, W., Hepburn, D., Corvalan, J., McClure, D., Liu, X., Stephenson, D., Clemens, J., and Johnstone, E.M. (1997). Zyme, a novel and potentially amyloidogenic enzyme cDNA isolated from Alzheimer's disease brain. J. Biol. Chem. *272*, 25135-25142.

Lundwall, A. and Brattsand, M. (2008). Kallikrein-related peptidases. Cell. Mol. Life Sci. *65*, 2019-2038.

Luo, L-Y. and Jiang, W. (2006). Inhibition profiles of human tissue kallikreins by serine protease inhibitors. Biol. Chem. *387*, 813-816.

Luo, L.Y., Soosaipillai, A., Grass, L., and Diamandis, E.P. (2006). Characterization of human kallikreins 6 and 10 in ascites fluid from ovarian cancer patients. Tumour Biol. *27*, 227-234.

Magklara, A., Mellati, A.A., Wasney, G.A., Little, S.P., Sotiropoulou, G., Becker, G.W., and Diamandis, E.P. (2003). Characterization of the enzymatic activity of human kallikrein 6: Autoactivation, substrate specificity, and regulation by inhibitors. Biochem. Biophys. Res. Commun. *307*, 948-955.

Mangé, A., Desmetz, C., Berthes, M.L., Maudelonde, T., and Solassol, J. (2008). Specific increase of human kallikrein 4 mRNA and protein levels in breast cancer stromal cells. Biochem. Biophys. Res. Commun. *375*, 107-112.

Matsumura, M., Bhatt, A.S., Andress, D., Clegg, N., Takayama, T.K., Craik, C.S., and Nelson, P.S. (2005). Substrates of the prostate-specific serine protease prostase/KLK4 defined by positional-scanning peptide libraries. Prostate *62*, 1-13.

Mavridis, K., Avgeris, M., Koutalellis, G., Stravodimos, K., and Scorilas, A. (2010). Expression analysis and study of the KLK15 mRNA splice variants in prostate cancer and benign prostatic hyperplasia. Cancer Sci. *101*, 693-699.

McKiernan, E., O'Brien, K., Grebenchtchikov, N., Geurts-Moespot, A., Sieuwerts, A.M., Martens, J.W., Magdolen, V., Evoy, D., McDermott, E., Crown, J., Sweep, F.C., and Duffy, M.J. (2008). Protein kinase Cdelta expression in breast cancer as measured by real-time PCR, western blotting and ELISA. Br. J. Cancer *99*, 1644–1650.

Mize, G.J., Wang, W., and Takayama, T.K. (2008). Prostate-specific kallikreins-2 and -4 enhance the proliferation of DU-145 prostate cancer cells through protease-activated receptors-1 and -2. Mol. Cancer Res. *6*, 1043-1051.

Montagnana, M., Danese, E., Ruzzenente, O., Bresciani, V., Nuzzo, T., Gelati, M., Salvagno, G.L., Franchi, M., Lippi, G., and Guidi, G.C. (2011). The ROMA (Risk of Ovarian Malignancy Algorithm) for estimating the risk of epithelial ovarian cancer in women presenting with pelvic mass: is it really useful? Clin. Chem. Lab. Med. *49*, 521-525.

Mukai, S., Fukushima, T., Naka, D., Tanaka, H., Osada, Y., and Kataoka, H. (2008). Activation of hepatocyte growth factor activator zymogen (pro-HGFA) by human kallikrein 1-related peptidases. FEBS J. *275*, 1003-1017.

Nam, R.K., Diamandis, E.P., Toi, A., Trachtenberg, J., Magklara, A., Scorilas, A., Papnastasiou, P.A., Jewett, M.A., and Narod, S.A. (2000). Serum human glandular kallikrein-2 protease levels predict the presence of prostate cancer among men with elevated prostate-specific antigen. J. Clin. Oncol. *18*, 1036-1042.

Nelson, P.S., Gan, L., Ferguson, C., Moss, P., Gelinas, R., Hood, L., and Wang, K. (1999). Molecular cloning and characterization of prostase, an androgen-regulated serine protease with prostate-restricted expression. Proc. Natl. Acad. Sci. USA *96*, 3114-3119.

Obiezu, C.V., Michael, I.P., Levesque, M.A., and Diamandis, E.P. (2006). Human kallikrein 4: enzymatic activity, inhibition, and degradation of extracellular matrix proteins. Biol. Chem. *387*, 749-759.

Obiezu, C.V., Scorilas, A., Katsaros, D., Massobrio, M., Yousef, G.M., Fracchioli, S., Rigault de la Longrais, I.A., Arisio, R., and Diamandis, E.P. (2001). Higher human kallikrein gene 4 (KLK4) expression indicates poor prognosis of ovarian cancer patients. Clin. Cancer Res. *7*, 2380-2386.

Obiezu, C.V., Shan, S.J., Soosaipillai, A., Luo, L.Y., Grass, L., Sotiropoulou, G., Petraki, C.D., Papanastasiou, P.A., Levesque, M.A., and Diamandis, E.P. (2005). Human kallikrein 4: quantitative study in tissues and evidence for its secretion into biological fluids. Clin. Chem. *51*, 1432-1442.

Obiezu, C.V., Soosaipillai, A., Jung, K., Stephan, C., Scorilas, A., Howarth, D.H., and Diamandis, E.P. (2002). Detection of human kallikrein 4 in healthy and cancerous prostatic tissues by immunofluorometry and immunohistochemistry. Clin. Chem. *48*, 1232-1240.

Oikonomopoulou, K., Li, L., Zheng, Y., Simon, I., Wolfert, R.L., Valik, D., Nekulova, M., Simickova, M., Frgala, T., and Diamandis, E.P. (2008). Prediction of ovarian cancer prognosis and response to chemotherapy by a serum-based multiparametric biomarker panel. Br. J. Cancer *99*, 1103-1113.

Paliouras, M. and Diamandis, E.P. (2006). The kallikrein world: an update on the human tissue kallikreins. Biol. Chem. *387*, 643-652.

Pampalakis, G. and Sotiropoulou, G. (2007). Tissue kallikrein proteolytic cascade pathways in normal physiology and cancer. Biochim. Biophys. Acta 1776, 22-31.

Pampalakis, G., Diamandis, E.P., and Sotiropoulou, G. (2006). The epigenetic basis for the aberrant expression of kallikreins in human cancers. Biol. Chem. *387*, 795-799.

Perren, T.J., Swart, A.M., Pfisterer, J., Ledermann, J.A., Pujade-Lauraine, E., Kristensen, G., Carey, M.S., Beale, P., Cervantes, A., Kurzeder, C., du Bois, A., Sehouli, J., Kimmig, R., Stähle, A., Collinson, F., Essapen, S., Gourley, C., Lortholary, A., Selle, F., Mirza, M.R., Leminen, A., Plante, M., Stark, D., Qian, W., Parmar, M.K., Oza, A.M.; ICON7 Investigators (2011). A phase 3 trial of bevacizumab in ovarian cancer. N. Engl. J. Med. *365*, 2484-2496.

Petraki, C.D., Karavana, V.N., Skoufogiannis, P.T., Little, S.P., Howarth, D.J., Yousef, G.M., and Diamandis, E.P. (2001). The spectrum of human kallikrein 6 (zyme/protease M/neurosin) expression in human tissues as assessed by immunohistochemistry. J. Histochem. Cytochem. *49*, 1431-1441.

Petraki, C.D., Papanastasiou, P.A., Karavana, V.N., and Diamandis, E.P. (2006). Cellular distribution of human tissue kallikreins: immunohistochemical localization. Biol. Chem. *387*, 653-663.

Pollock, R.E. (Ed.), Doroshow, J.H., Khayat, D., Nakao, A., and O'Sullivan, B., International Union Against Cancer, UICC Manual of Clinical Oncology, Wiley, New Jersey, USA, 2004, 8th edition, 570-577, 585-597.

Prezas, P., Arlt, M.J., Viktorov, P., Soosaipillai, A., Holzscheiter, L., Schmitt, M., Talieri, M., Diamandis, E.P., Krüger, A., and Magdolen, V. (2006). Overexpression of the human tissue kallikrein genes KLK4, 5, 6, and 7 increases the malignant phenotype of ovarian cancer cells. Biol. Chem. *387*, 807-811.

Rait, V.K., Xu, L., O'Leary, T.J., and Mason, J.T. (2004). Modeling formalin fixation and antigen retrieval with bovine pancreatic RNase A, II. Interrelationship of cross-linking, immunoreactivity, and heat treatment. Lab. Invest. *84*, 300-306.

Ramsay, A.J., Dong, Y., Hunt, M.L., Linn, M., Samaratunga, H., Clements, J.A., and Hooper, J.D. (2008). Kallikrein-related peptidase 4 (KLK4) initiates intracellular signaling via protease-activated receptors (PARs). KLK4 and PAR-2 are co-expressed during prostate cancer progression. J. Biol. Chem. *283*, 12293-12304.

Remmele, W. and Stegner H.E. (1987). Recommendation for uniform definition of an immunoreactive score (IRS) for immunohistochemical estrogen receptor detection (ER-ICA) in breast cancer tissue. Pathologe *8*, 138-140.

Rosen, D.G., Wang, L., Atkinson, J.N., Yu, Y., Lu, K.H., Diamandis, E.P., Hellstrom, I., Mok, S.C., Liu, J., and Bast, R.C. Jr. (2005). Potential markers that complement expression of CA125 in epithelial ovarian cancer. Gynecol. Oncol. *99*, 267-277.

Sarojini, S., Tamir, A., Lim, H., Li, S., Zhang, S., Goy, A., Pecora, A., and Suh, K.S. (2012). Early detection biomarkers for ovarian cancer. J. Oncol. [Epub 2012 Dec 23].

Scarisbrick, I.A., Linbo, R., Vandell, A.G., Keegan, M., Blaber, S.I., Blaber, M., Sneve, D., Lucchinetti, C.F., Rodriguez, M., and Diamandis, E.P. (2008). Kallikreins are associated with secondary progressive multiple sclerosis and promote neurodegeneration. Biol. Chem. *389*, 739-745.

Scarisbrick, I.A., Radulovic, M., Burda, J.E., Larson, N., Blaber, S.I., Giannini, C., Blaber, M., and Vandell, A.G. (2012a). Kallikrein 6 is a novel molecular trigger of reactive astrogliosis. Biol. Chem. *393*, 355-367.

Scarisbrick, I.A., Sabharwal, P., Cruz, H., Larsen, N., Vandell, A.G., Blaber, S.I., Ameenuddin, S., Papke, L.M., Fehlings, M.G., Reeves, R.K., Blaber, M., Windebank, A.J., and Rodriguez, M. (2006). Dynamic role of kallikrein 6 in traumatic spinal cord injury. Eur. J. Neurosci. *24*, 1457-1469.

Scarisbrick, I.A., Yoon, H., Panos, M., Larson, N., Blaber, S.I., Blaber, M., and Rodriguez, M. (2012b). Kallikrein 6 regulates early CNS demyelination in a viral model of multiple sclerosis. Brain Pathol. *22*, 709-722.

Schmelz, H.U., Sparwasser, C., and Weidner, W. Prostatakarzinom (chapter 23) in „Facharztwissen Urologie“, Springer, Heidelberg, Germany, 2010, 2nd edition, 316-375.

Schmitt, M., Magdolen, V., Yang, F., Kiechle, M., Bayani, J., Yousef, G.M., Scorilas, A., Diamandis, E.P., and Dorn, J. (2013a). Emerging clinical importance of the cancer biomarkers kallikrein-related peptidases (KLK) in female and male reproductive organ malignancies. Radiol. Oncol. *47*, 319-329.

Schmitt, M., Renné, T., and Scorilas, A. (2013b). The kallikreins: old proteases with new clinical potentials. Thromb. Haemost. *110*, 396-398.

Schrohl, A-S., Holten-Andersen, M., Sweep, F., Schmitt, M., Harbeck, N., Foekens, J., and Brünner, N.; European Organisation for Research and Treatment of Cancer (EORTC) Receptor and Biomarker Group (2003). Tumor markers: from laboratory to clinical utility. Mol. Cell Proteomics *2*, 378-387.

Shan, S.J., Scorilas, A., Katsaros, D., and Diamandis, E.P. (2007). Transcriptional upregulation of human tissue kallikrein 6 in ovarian cancer: clinical and mechanistic aspects. Br. J. Cancer *96*, 362-372.

Shaw, J.L. and Diamandis, E.P. (2007). Distribution of 15 human kallikreins in tissues and biological fluids. Clin. Chem. *53*, 1423-1432.

Sidiropoulos, M., Pampalakis, G., Sotiropoulou, G., Katsaros, D., and Diamandis, E.P. (2005). Downregulation of human kallikrein 10 (KLK10/NES1) by CpG island hypermethylation in breast, ovarian and prostate cancers. Tumour Biol. *26*, 324-336.

Simmer, J.P. and Bartlett, J.D. (2004). Kallikrein 4 is a secreted protein. Cancer Res. *64*, 8481–8483.

Simmer, J.P., Fukae, M., Tanabe, T., Yamakoshi, Y., Uchida, T., Xue, J., Margolis, H.C., Shimizu, M., DeHart, B.C., Hu, C.-C., and Bartlett, J.D. (1998). Purification, characterization, and cloning of enamel matrix serine proteinase 1. J. Dent. Res. *77*, 377–386.

Simmer, J.P., Hu, Y., Lertlam, R., Yamakoshi, Y., and Hu, J.C.-C. (2009). Hypomaturation enamel defects in Klk4 knockout/LacZ knockin mice. J. Biol. Chem. *284*, 19110–19121.

Skacel, M., Skilton, B., Pettay, J.D., and Tubbs, R.R. (2002). Tissue microarrays: a powerful tool for high-throughput analysis of clinical specimens:

a review of the method with validation data. Appl. Immunohistochem. Mol. Morphol. *10*, 1-6.

Sotiropoulou, G., Pampalakis, G., and Diamandis, E.P. (2009). Functional roles of human kallikrein-related peptidases. J. Biol. Chem. *284*, 32989-32994.

Stephenson, S.-A., Verity, K., Ashworth, L.K., and Clements, J.A. (1999). Localization of a new prostate-specific antigen-related serine protease gene, KLK4, is evidence for an expanded human kallikrein gene family cluster on chromosome 19q13.3-13.4. J. Biol. Chem. *274*, 23210-23214.

Strojnik, T., Kavalar, R., Zajc, I., Diamandis, E.P., Oikonomopoulou, K., and Lah, T.T. (2009). Prognostic impact of CD68 and kallikrein 6 in human glioma. Anticancer Res. *29*, 3269-3279.

Takayama, T.K., McMullen, B.A., Nelson, P.S., Matsumura, M., and Fujikawa, K. (2001). Characterization of hK4 (prostase), a prostate-specific serine protease: activation of the precursor of prostate specific antigen (pro-PSA) and single-chain urokinase-type plasminogen activator and degradation of prostatic acid phosphatase. Biochemistry *40*, 15341-15348.

Thorek, D.L., Evans, M.J., Carlsson, S.V., Ulmert, D., and Lilja, H. (2013). Prostate-specific kallikrein-related peptidases and their relation to prostate cancer biology and detection. Established relevance and emerging roles. Thromb. Haemost. *110*, 484-492.

Vandell, A.G., Larson, N., Laxmikanthan, G., Panos, M., Blaber, S.I., Blaber, M., and Scarisbrick, I.A. (2008). Protease-activated receptor dependent and independent signaling by kallikreins 1 and 6 in CNS neuron and astroglial cell lines. J. Neurochem. *107*, 855-870.

Veveris-Lowe, T.L., Lawrence, M.G., Collard, R.L., Bui, L., Herington, A.C., Nicol, D.L., and Clements, J.A. (2005). Kallikrein 4 (hK4) and prostate-specific antigen (PSA) are associated with the loss of E-cadherin and an epithelial-mesenchymal transition (EMT)-like effect in prostate cancer cells. Endocr. Relat. Cancer *12*, 631-643.

Wan, W-H., Fortuna, M.B., and Furmanski, P. (1987). A rapid and efficient method for testing immunohistochemical reactivity of monoclonal antibodies against multiple tissue samples simultaneously. J. Immunol. Methods *103*, 121-129.

Wang, W., Mize, G.J., Zhang, X., and Takayama, T.K. (2010). Kallikrein-related peptidase-4 initiates tumor-stroma interactions in prostate cancer through protease-activated receptor-1. Int. J. Cancer *126*, 599-610.

Wennström, M., Surova, Y., Hall, S., Nilsson, C., Minthon, L., Boström, F., Hansson, O., and Nielsen, H.M. (2013). Low CSF levels of both α-synuclein and the α-synuclein cleaving enzyme neurosin in patients with synucleinopathy. PLoS ONE *8*, epub, e53250.

White, N.M., Bui, A., Mejia-Guerrero, S., Chao, J., Soosaipillai, A., Youssef, Y., Mankaruos, M., Honey, R.J., Stewart, R., Pace, K.T., Sugar, L., Diamandis, E.P., Doré, J., and Yousef, G.M. (2010). Dysregulation of kallikrein-related peptidases in renal cell carcinoma: potential targets of miRNAs. Biol. Chem. *391*, 411-423.

White, N.M., Mathews, M., Yousef, G.M., Prizada, A., Fontaine, D., Ghatage, P., Popadiuk, C., Dawson, L., and Doré, J.J. (2009a). Human kallikrein related peptidases 6 and 13 in combination withCA125 is a more sensitive test for ovarian cancer than CA125 alone. Cancer Biomark. *5*, 279-287.

White, N.M., Mathews, M., Yousef, G.M., Prizada, A., Popadiuk, C., and Doré, J.J. (2009b). KLK6 and KLK13 predict tumor recurrence in epithelial ovarian carcinoma. Br. J. Cancer *101*, 1107-1113.

Xi, Z., Klokk, T.I., Korkmaz, K., Kurys, P., Elbi, C., Risberg, B., Danielsen, H., Loda, M., and Saatcioglu, F. (2004). Kallikrein 4 is a predominantly nuclear protein and is overexpressed in prostate cancer. Cancer Res. *64*, 2365-2370.

Yoon, H., Blaber, S.I., Evans, D.M., Trim, J., Juliano, M.A., Scarisbrick, I.A., and Blaber, M. (2008). Activation profiles of human kallikrein-related peptidases by proteases of the thrombostasis axis. Protein Sci. *17*, 1998-2007.

Yoon, H., Blaber, S.I., Li, W., Scarisbrick, I.A., and Blaber, M. (2013). Activation profiles of human kallikrein-related peptidases by matrix metalloproteinases. Biol. Chem. *394*, 137-147.

Yoon, H., Laxmikanthan, G., Lee, J., Blaber, S.I., Rodriguez, A., Kogot, J.M., Scarisbrick, I.A., and Blaber, M. (2007). Activation profiles and regulatory cascades of the human kallikrein-related peptidases. J. Biol. Chem. *282*, 31852-31864.

Yousef, G.M. and Diamandis, E.P. (2001). The new human tissue kallikrein gene family: structure, function, and association to disease. Endocr. Rev. *22*, 184-204.

Yousef, G.M., Kishi, T., and Diamandis, E.P. (2003). Role of kallikrein enzymes in the central nervous system. Clin. Chim. Acta *329*, 1-8.

Yousef, G.M., Scorilas, A., Chang, A., Rendl, L., Diamandis, M., Jung, K., and Diamandis, E.P. (2002). Down-regulation of the human kallikrein gene 5 (KLK5) in prostate cancer tissues. Prostate *51*, 126-132.

Zarghooni, M., Soosaipillai, A., Grass, L., Scorilas, A., Mirazimi, N., and Diamandis, E.P. (2002). Decreased concentration of human kallikrein 6 in brain extracts of Alzheimer's disease patients. Clin. Biochem. *35*, 225-231.

7.12 Own publication list

Journal publications:

Gratio, V., Beaufort, N., **Seiz, L.**, Maier, J., Virca, G.D., Debela, M., Grebenchtchikov, N., Magdolen, V., and Darmoul, D. (2010). Kallikrein-related peptidase 4: a new activator of the aberrantly expressed protease-activated receptor 1 in colon cancer cells. Am. J. Pathol. *176*, 1452-1461.

Seiz, L., Kotzsch M., Grebenchtchikov, N.I., Geurts-Moespot, A.J., Fuessel, S., Goettig, P., Gkazepis, A., Wirth, M.P., Schmitt, M., Lossnitzer, A., Sweep, F.C., and Magdolen, V. (2010). Polyclonal antibodies against kallikrein-related peptidase 4 (KLK4): immunohistochemical assessment of KLK4 expression in healthy tissues and prostate cancer. Biol. Chem. *391*, 391-401.

Seiz, L., Dorn, J., Kotzsch, M., Walch, A., Grebenchtchikov, N.I., Gkazepis, A., Schmalfeldt, B., Kiechle, M., Bayani, J., Diamandis, E.P., Langer, R., Sweep, F.C., Schmitt, M., and Magdolen, V. (2012). Stromal cell-associated expression of kallikrein-related peptidase 6 (KLK6) indicates poor prognosis of ovarian cancer patients. Biol. Chem. *393*, 391-401.

Oral presentations:

Seiz, L., Mayer, K., Gkazepis, A., Mengele, K., Magdolen, V., and Schmitt, M.: *Immunohistochemical evaluation of expression of kallikrein-related peptidases in normal organs and the malignant state* (EORTC-PBG 2007, Halle, Germany).

Seiz, L., Mengele, K., Regner, K., Gkazepis, A., Slotta-Huspenina, J., Kremer, M., and Schmitt, M.: *Clinical utility of cancer biomarkers assessed by virtual microscopy* (TIGA 2009, Heidelberg, Germany).

Seiz, L., Mengele, K., Creutzburg, S., Piontek, G., Schlegel, J., Grebenchtchikov, N.I., Sweep, F.C., Magdolen, V., and Schmitt, M.: *Expression of kallikrein-related peptidase 6 (KLK 6) in brain pathologies as assessed by immunohistochemistry* (GIF 2009, Piran, Slovenia).

Seiz, L., Kotzsch, M., Grebenchtchikov, N.I., Mengele, K., Fuessel, S., Wirth, M.P., Schmitt, M., Lossnitzer, A., Sweep, F.C., and Magdolen, V.: *Kallikrein-related peptidase 4 (KLK4) – a potential biomarker in prostate cancer* (ISOBM 2010, Munich, Germany).

Seiz, L., Dorn, J., Kotzsch, M., Walch, A., Grebenchtchikov, N.I., Mengele, K., Creutzburg, S., Schmalfeldt, B., Diamandis, E.P., Walch, A., Sweep, F.C., Schmitt, M., and Magdolen, V.: *Stromal cell-associated expression of KLK6 indicates poor prognosis of ovarian cancer patients* (ISK 2011, Rhodes Island, Greece).

Poster presentations:

Seiz, L., Gkazepis, A., Grebenchtchikov, N.I., Sweep, F.C., Beaufort, N., Porankiewicz-Asplund, J., Brattsand, M., Wojciechowski, P., Wagner, S., Creutzburg, S., Kremer, M., Magdolen, V., and Schmitt, M.: *Generation and evaluation of monospecific antibodies against kallikrein-related peptidases KLK 4, 5, 6 and 7* (IPS 2007, Patras, Greece).

Grebenchtchikov, N.I., Geurts, A., Creutzburg, S., **Seiz, L.**, Goettig, P., Kotzsch, M., Gkazepis, A., Schmitt, M., Sweep, F.C., and Magdolen, V.: *Polyclonal antibodies (pAbs) against KLK4 and 6 – isolation of monospecific pAbs directed against a linear epitope within a flexible surface-exposed loop* (IKS 2009, Munich, Germany).

Seiz, L., Kotzsch, M., Grebenchtchikov, N.I., Fuessel, S., Hofmann, J., Sweep, F.C., Schmitt, M., Lossnitzer, A., and Magdolen, V.: *Immunohistochemical assessment of KLK4 expression in prostate cancer* (IKS 2009, Munich, Germany).

7.13 Own publications underlying this dissertation

Polyclonal antibodies against kallikrein-related peptidase 4 (KLK4): immunohistochemical assessment of KLK4 expression in healthy tissues and prostate cancer.

Seiz, L., Kotzsch M., Grebenchtchikov, N.I., Geurts-Moespot, A.J., Fuessel, S., Goettig, P., Gkazepis, A., Wirth, M.P., Schmitt, M., Lossnitzer, A., Sweep, F.C., and Magdolen, V.

⇨ *Published in Biological Chemistry, Vol. 391, pp. 391-401, April 2010. Copyright © by Walter de Gruyter, Berlin, New York.*

⇨ Link to MEDLINE: *http://www.ncbi.nlm.nih.gov/pubmed/20180634*

Stromal cell-associated expression of kallikrein-related peptidase 6 (KLK6) indicates poor prognosis of ovarian cancer patients. Biol. Chem. *393*, 391-401.

Seiz, L., Dorn, J., Kotzsch, M., Walch, A., Grebenchtchikov, N.I., Gkazepis, A., Schmalfeldt, B., Kiechle, M., Bayani, J., Diamandis, E.P., Langer, R., Sweep, F.C., Schmitt, M., and Magdolen, V.

⇨ *Published in Biological Chemistry, Vol. 393, pp. 391-401, May 2012. Copyright © by Walter de Gruyter, Berlin, Boston.*

⇨ Link to MEDLINE: *http://www.ncbi.nlm.nih.gov/pubmed/22505521*

7.14 Acknowledgement

I would like to gratefully and sincerely thank Prof. Dr. rer. nat. Dr. med. habil. Manfred Schmitt for his continuous support and excellent mentoring throughout my research work. He constantly encouraged me and provided me with all the skills required for becoming an independent experimentalist and for starting an academic career. I would like to express my gratitude to Prof. Dr. rer. nat. habil. Viktor Magdolen for his valuable guidance and support during my experimental work. I have greatly benefited from his research expertise. I thank Prof. Dr. med. Marion Kiechle for the opportunity to carry out the research work at her Department.

Additionally, I want to thank all members of the Clinical Research Unit at the Department of Obstetrics and Gynecology of the Technical University of Munich. Special thanks to Daniela Hellmann und Sabine Creutzburg, who provided me with technical support and advice whenever I approached them. I am particularly grateful to Karin Mengele for her research expertise and all the valuable discussions. I owe a lot to her for the consistent and unlimited support throughout my research work, her exceptional efforts, and the close friendship we have developed. I want to thank Claudia Beutner for her help and encouragement all these years.

I acknowledge Dr. Matthias Kotzsch from the Institute of Pathology, Dresden University of Technology, for good collaborations and his help in connection with statistical analyses. I am grateful to Nikolai Grebenchtchikov from the Department of Laboratory Medicine, Radboud University Nijmegen Medical Centre, The Netherlands, who was responsible for the production and affinity purification of antibodies I was allowed to use for my research work.

This thesis would not have come to a successful completion without the help I received from experienced pathologists, who readily assisted in the evaluation of immunohistochemical stainings. I therefore thank PD Dr. Marcus Kremer from the Institute of Pathology at the Clinic in Munich Harlaching and Munich Neuperlach (formerly working at the Institute of Pathology of the Technical University of Munich), Prof. Dr. Axel Walch from the Institute of Pathology of the

Helmholtz Zentrum in Munich, Prof. Dr. Jürgen Schlegel from the Institute of Pathology of the Technical University of Munich, and Dr. Arndt Lossnitzer from the Institute of Pathology, Dresden University of Technology.

I express my deepest gratitude to my parents and my brother, who greatly supported me in every stage of my personal and academic life. Finally, I thank Roland for his patience, unending encouragement, and support.